

13628

NATIONAL LIBRARY
OTTAWA



BIBLIOTHÈQUE NATIONALE
OTTAWA

NAME OF AUTHOR..... *GRAHAME JOHN BRAMALD WILKINSON*
TITLE OF THESIS..... *Crystallographic studies of*
(1) Three Antihistaminic drugs,
(2) An Oxindole Alkaloid (3) Maleic acid
UNIVERSITY..... *University of Alberta and Malcata anions*
DEGREE FOR WHICH THESIS WAS PRESENTED..... *Ph. D*
YEAR THIS DEGREE GRANTED..... *1972*

Permission is hereby granted to THE NATIONAL LIBRARY
OF CANADA to microfilm this thesis and to lend or sell copies
of the film.

The author reserves other publication rights, and
neither the thesis nor extensive extracts from it may be
printed or otherwise reproduced without the author's
written permission.

(Signed)..... *Graham J. Wilkin*

PERMANENT ADDRESS:

Dept of Biochemistry
University of Alberta
EDMONTON

DATED..... *6th Oct/72*.....19

NL-91 (10-68)

THE UNIVERSITY OF ALBERTA

CRYSTALLOGRAPHIC STUDIES OF (1) THREE ANTIHISTAMINIC
DRUGS, (2) AN OXINDOLE ALKALOID, (3) MALEIC ACID AND
MALEATE ANIONS

by



GRAHEME JOHN BRAMALD WILLIAMS

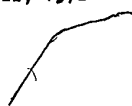
A THESIS

SUBMITTED TO THE FACULTY OF GRADUATE STUDIES AND RESEARCH
IN PARTIAL FULFILLMENT OF THE REQUIREMENTS FOR THE DEGREE
OF DOCTOR OF PHILOSOPHY

DEPARTMENT OF BIOCHEMISTRY

EDMONTON, ALBERTA

FALL, 1972

A handwritten signature or scribble located below the date.

UNIVERSITY OF ALBERTA
FACULTY OF GRADUATE STUDIES AND RESEARCH

The undersigned certify that they have read, and recommend to the Faculty of Graduate Studies and Research for acceptance, a thesis entitled, "Crystallographic Studies of (1) Three Anti-histaminic Drugs, (2) An Oxindole Alkaloid, (3) Maleic Acid and Maleate Anions", submitted by Graheme John Bramald Williams in partial fulfillment of the requirements for the degree of Doctor of Philosophy.

M. N. G. James
.....
Supervisor

H. M. [unclear]
.....

Peter G. Baxter
.....

L. B. Smiller
.....

R. [unclear]
.....

L. H. Jensen
.....
External Examiner

Date *Sept 27 1972*

ABSTRACT

PART 1 - Antihistaminic Drugs

The crystal structures of the three antihistaminic drugs *d,l*-Brompheniramine maleate, (+)-Chlorpheniramine maleate and Triprolidine hydrochloride monohydrate were investigated. All three compounds adopted a conformation with an open side which would permit both a π electron overlap linkage and a hydrogen bond to the histamine H1 receptor from the one face of the molecule. Correlations between the conformations of four antihistaminic drugs have allowed the formulation of an hypothesis for the binding of both histamine and antihistamines to the receptor site.

PART 2 - An Oxindole Alkaloid

The crystal structure of an oxindole alkaloid extracted from *Eleagnus Commutata* was undertaken to complete the structural characterization of the molecule. The material was found to be racemic and the crystal structure showed that the phenolic hydroxyl group was bonded to C(6) rather than to C(5) as previously suggested. The systematic name for the compound is 6-hydroxy-2'-(methylpropyl)-3,3'-spiro-tetrahydro-pyrrolidino-oxindole.

PART 3 - Maleic Acid and Maleate Anions

New data were collected for maleic acid and the structure refined. The internal hydrogen bond is acentric and the intermolecular hydrogen bond is not bifurcated. Disodium maleate was prepared and its structure solved. A comparison of nine available structures did not explain why some maleate mono-anions had symmetric intramolecular hydrogen bonds

ii.

whereas others were asymmetric. Based on the average molecular geometries of similar species predominating electronic distributions for the free acid, mono-anion and di-anion are given.

PART 4 - Programming

Six FORTRAN programs useful in X-ray crystallography were written. Brief descriptions and program listings are provided for each of ALPHA, CROMERCURVE, DATAMEND, FRAME, PARALISTER and PRECLP. Subroutine SIM was added to program NRC-8 and this is listed and described. Program NRC-10 was extensively re-organized to allow recycling without user intervention, and an extensive error analysis and agreement summary subroutine added. A listing of ANAL is provided.

ACKNOWLEDGEMENTS

It is a pleasure to acknowledge the role of my supervisor, Dr. M.N.G. James, in the production of this thesis. By virtue of the excellent material and intellectual resources he has provided, and through the general congeniality of the group under his direction, the past few years have been a very enjoyable and instructive experience.

The green thumb of my fellow student, Mr. W.B.T. Cruse, deserves special mention for actually growing the disodium maleate crystal used here; and for pointing the way in other instances.

Miss K. Hayakawa has provided excellent technical assistance from time to time, particularly in the drawing of diagrams, and this is gratefully acknowledged.

The semi-empirical absorption program written by Dr. M.A. Joynson was used in this work and I am thankful for this contribution.

I have been the holder of several University of Alberta Teaching Assistantships and Intersession Bursaries during the course of these studies, and am grateful for this financial support.

My wife Gail deserves special commendation for her efforts and expertise during her typing of this thesis, but as well as this the many ways she has improved my life over the last 3½ years have helped to make it all worthwhile.

TABLE OF CONTENTS

	Page
Abstract	i
List of Tables	vi
List of Figures	ix
<u>PART 1 - Antihistaminic Drugs</u>	
1.1 INTRODUCTION.....	1
1.2 dl-BROMPHENIRAMINE MALEATE.....	19
Experimental	19
Results and Discussion	22
1.3 (+)-CHLORPHENIRAMINE MALEATE.....	45
Experimental	45
Results and Discussion	54
1.4 TRIPROLIDINE HYDROCHLORIDE MONOHYDRATE.....	72
Experimental	72
Results and Discussion	76
1.5 CONCLUSIONS.....	93
<u>PART 2 - An Oxindole Alkaloid</u>	
2.1 INTRODUCTION.....	109
2.2 THE STRUCTURE ANALYSIS.....	111
Experimental	111
Results and Discussion	116
<u>PART 3 - Maleic Acid and Maleate Anions</u>	
3.1 INTRODUCTION.....	136
3.2 MALEIC ACID.....	142
Experimental	142
Results and Discussion	148

Table of Contents (Continued)

	Page
3.3 DISODIUM MALEATE.....	166
Experimental	166
Results and Discussion	180
3.4 CONCLUSIONS.....	190
<i><u>PART 4 - Computer Programs Used</u></i>	
4.1 INTRODUCTION.....	198
4.2 ALPHA.....	199
4.3 CROMERCURVE.....	201
4.4 DATAMEND.....	203
4.5 FRAME.....	206
4.6 PARALISTER.....	208
4.7 PRECLP.....	211
4.8 NRC-8.....	213
4.9 NRC-10.....	215
REFERENCES.....	218

LIST OF TABLES

Page

PART 1 - Antihistaminic Drugs

Table 1	A summary of data for d,l-Brompheniramine maleate.....	20
2	The final set of positional parameters for the non-hydrogen atoms of one d,l-Brompheniramine maleate "molecule".....	23
3	The thermal motion parameters for the atoms of Table 2.....	24
4	The positional and thermal parameters for the hydrogen atoms of d,l-Brompheniramine maleate.....	25
5	The observed structure amplitudes and the calculated structure factors for d,l-Brompheniramine maleate.....	26
6	Bond distances and interbond angles involving the hydrogen atoms of d,l-Brompheniramine maleate.....	31
7	Bromine-C _{aromatic} bond lengths: a representative survey....	35
8	Molecular bond distances and angles for some 2-pyridyl groups.....	37
9	(+)-Chlorpheniramine maleate physical data.....	47
10	Observed and calculated structure factor amplitudes for the hkl/hkl Friedel pairs used to determine the absolute configuration of (+)-Chlorpheniramine maleate.....	53
11	The observed and calculated structure factor amplitudes, x 10, and the phase angles for (+)-Chlorpheniramine maleate.....	55
12	Atomic positional parameters (x 10 ⁴) for the non-hydrogen atoms of (+)-Chlorpheniramine maleate.....	58
13	Anisotropic thermal parameters (x 10 ⁴) used to describe the atoms of Table 12.....	59
14	Atomic parameters (x 10 ³) for the hydrogen atoms of (+)-Chlorpheniramine maleate.....	60
15	Distances and angles involving the hydrogen atoms of (+)-Chlorpheniramine maleate.....	63
16	Some physical constants and other quantities relating to Triprolidine hydrochloride monohydrate.....	73

List of Tables (Continued)

	Page
Table 17 Positional parameters ($\times 10^4$) for the non-hydrogen atoms of Triprolidine hydrochloride monohydrate.....	77
18 Thermal parameters ($\times 10^4$) describing the atomic vibration of the atoms in Table 17.....	78
19 Positional and isotropic vibration parameters ($\times 10^3$) for the hydrogen atoms of Triprolidine hydrochloride monohydrate.....	79
20 The observed structure amplitudes and calculated structure factors based on the final model for Triprolidine hydrochloride monohydrate.....	80
21 A listing of the bond distances and angles involving the hydrogen atoms of Triprolidine hydrochloride monohydrate.....	84

PART 2 - An Oxindole Alkaloid

Table 22 Some physical constants and other data for oxindole alkaloid crystals.....	112
23 The set of observed structure amplitudes and calculated structure factors ($\times 10$) based on the final model for the oxindole alkaloid.....	117
24 The positional parameters for the non-hydrogen atoms of one molecule.....	119
25 The parameters describing the anisotropic vibration of the atoms contained in Table 24.....	120
26 Positional and thermal parameters ($\times 10^3$) for the hydrogen atoms.....	121
27 Bond distances and angles for the hydrogen atoms.....	124

PART 3 - Maleic Acid and Maleate Anions

Table 28 The unit cell constants and some other quantities relating to the crystal structure analysis of maleic acid.....	143
29 A listing of the observed structure amplitudes and the final calculated structure factors.....	149
30 Positional parameters for the atoms of one maleic acid molecule.....	151

List of Tables (Continued)

	Page
Table 31 Thermal motion parameters for the atoms of Table 30.....	152
32 A results summary for the least-squares planes calculations of maleic acid.....	158
33 The root-mean-square displacements and direction cosines of the principal axes of the ellipsoids used to describe the thermal motion of the maleic acid atoms.....	161
34 A data summary for the structural analysis of disodium maleate monohydrate.....	167
35 A listing of the observed structure amplitudes and final structure factors (absolute scale x 10) for disodium maleate monohydrate.....	174
36 Positional parameters for one unique portion of the disodium maleate monohydrate structure.....	178
37 The thermal vibration parameters used in the description of the final model for disodium maleate monohydrate.....	179
38 A results summary for the least-squares planes for the maleate di-anion.....	186
39 A summary of the geometry of maleic acid/maleate anion structures.....	191

LIST OF FIGURES

Page

PART 1 - Antihistaminic Drugs

Figure 1	The atomic numbering scheme used in the analysis of d,l-Brompheniramine maleate.....	29
2	Bond distances and interbond angles for the non-hydrogen atoms of d,l-Brompheniramine maleate.....	30
3	A stereoscopic pair of the d,l-Brompheniramine maleate complex showing the R absolute configuration.....	39
4	A drawing of the d,l-Brompheniramine maleate complex as viewed down the C(9)-C(8) bond direction.....	41
5	A packing diagram of several molecules viewed parallel to a.....	42
6	The $u \cdot \frac{1}{2} \cdot w$ section of the three dimensional Patterson synthesis for (+)-Chlorpheniramine maleate and the relationship of the initial model to this section.....	48
7	Bond distances and angles for the non-hydrogen atoms of (+)-Chlorpheniramine maleate.....	61
8	A stereo pair of the (+)-Chlorpheniramine maleate complex.....	67
9	A drawing of the (+)-Chlorpheniramine maleate structure viewed down the C(9)-C(8) bond direction.....	69
10	A stereoscopic packing diagram of several (+)-Chlorpheniramine maleate molecules viewed parallel to a*.....	70
11	The chain of polar and non-polar bonding interactions involving the maleate ion.....	71
12	Bond distances and angles for the non-hydrogen atoms of Triprolidine hydrochloride monohydrate.....	83
13	A view of the Triprolidine hydrochloride structure viewed in the C(9)-C(8) bond direction.....	87
14	A drawing showing the immediate environment of one class of inversion centres in the crystals of Triprolidine hydrochloride monohydrate.....	90

List of Figures (Continued)

	Page
Figure 15 A stereoscopic pair packing diagram for Triprolidine hydrochloride monohydrate.....	91
16 A composite diagram showing five antihistamine molecules viewed in the C(9)-C(8) (C _α -C _β) bond direction.....	94
17 A sketch of the proposed model for the H1 receptor showing a (+)-Chlorpheniramine molecule bound to the site.....	104
18 The binding of a histamine molecule to the proposed site.....	106

PART 2 - An Oxindole Alkaloid

Figure 19 The intensity distribution (Wilson plot) for the oxindole alkaloid.....	113
20 The numbering scheme and the bond distances involving the non-hydrogen atoms of the oxindole alkaloid.....	122
21 The interbond angles calculated on the basis of those parameters contained in Table 24.....	123
22 One molecule of the oxindole alkaloid viewed parallel to the c axis.....	126
23 A packing diagram of several molecules of the alkaloid showing the sheet structure and the intermolecular hydrogen bonding.....	130

PART 3 - Maleic Acid and Maleate Anions

Figure 24 A plot of relative intensity versus ϕ for the maleic acid crystal.....	144
25 The molecular plane section of the final difference map...147	147
26 The final difference map showing the difference electron density of one molecule's environment.....	148
27 A diagram showing the numbering scheme, the bond distances and the interbond angles for maleic acid.....	153
28 The molecular packing viewed parallel to the c* direction.....	154

List of Figures (Continued)

	Page
Figure 29 An ORTEP drawing of one molecule of maleic acid.....	159
30 A computer produced diagram of one maleate di-anion showing the conformation assumed by the species and the numbering scheme of this analysis.....	180
31 Bond distances and interbond angles for the maleate di-anion.....	181
32 A stereoscopic pair diagram showing the crystal structure of disodium maleate monohydrate.....	182
33 A diagrammatic representation of the environments of the five oxygen atoms of the disodium maleate monohydrate structure.....	184
34 A sketch showing the distances and angles of the coordination pattern for the sodium ions.....	187

1.

PART 1

Antihistaminic Drugs

1.1 INTRODUCTION

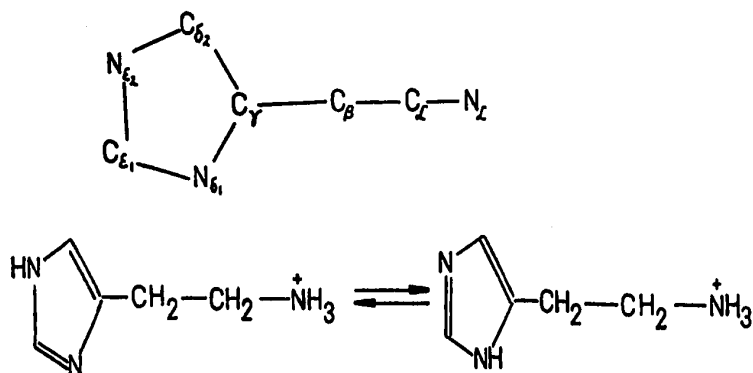
Ever since its introduction by Langley in 1878⁽¹⁾, the concept of a receptor site has been useful in the study of interactions of drugs with biological systems. The functional nature of generalized receptor sites has been enunciated by Erlich⁽²⁾ whose paraphrased statement reads "...that they were small, structurally discrete areas from which a biological response emanated following interaction with a complementary foreign molecule"⁽³⁾. Various kinetic formulations based on either "occupancy" or "rate" models have been used with some success to describe some aspects of the drug/receptor interaction, but recently theories related more to the actual molecular events of these interactions have been proposed. A "macromolecular perturbation theory" has been developed by Nachmansohn⁽⁴⁾, which although similar to, was developed independently of, Koshland's "induced fit theory"⁽⁵⁾, primarily with respect to the muscarinic cholinergic receptor and the acetylcholinesterase sites. A "dynamic receptor hypothesis" which owes much to classical enzymology was used in rationalizing studies of the adrenergic system⁽⁶⁾ in terms of enzyme activities. Work in this latter area especially has been greatly facilitated by the isolation and characterization of very highly purified receptor sites (enzymes) but unfortunately this is not true for most other systems of pharmacological interest.

If it can be shown that the agonist (response inducer) and the

2.

antagonist (response repressor) bind with and compete for the same site, then despite the above difficulties, those attributes of the receptor site which serve to define its activity and specificity can, in principle, be deduced and meaningfully mapped in space by a suitable investigation of both agonists and antagonists.

It is believed⁽⁷⁾ that histamine (1) and many of the various anti-histaminic drugs do compete for the same site and much work based on the above principle has been performed on this system.



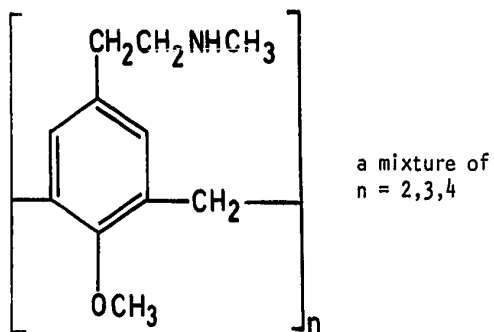
(1) The atomic nomenclature for histamine and two tautomers of the mono-cation. The imidazole ring is aromatic and it is believed that the primary amine function is protonated at physiological pH⁽⁸⁾.

Large stores of histamine are to be found in the bodies of all mammals so far investigated. Normally this histamine is kept in an inactive form, either by being bound to the heparin of mast cells or in combination with ATP and ADP in blood platelets⁽⁸⁾. The release of histamine from these storage locations may occur when the cells encounter:

(a) Physical maltreatment such as burning or mechanical damage;

3.

(b) Chemical agents of a basic nature that will displace the histamine from its heparin complex. Another type of chemical agent, and one whose mode of action is not understood, is typified by the compound known as "48/80" (11);



(11) Compound 48/80.

or

(c) The complex series of events that result from antigen/antibody interactions in allergically sensitised individuals. This condition is the most common and the most severe, but despite the large research effort which has been expended in trying to discern the mechanism of the histamine release this area remains little understood.

The physiological responses which arise from increased histamine levels are usually categorized according to their response to chemotherapy and, by inference, according to the nature of the receptor site.

Type I responses include:

(i) Smooth muscle contraction, especially that of the gut, bronchial tree and uterus. This leads to, for example, restricted

breathing.

(ii) Relaxation of arteriole smooth muscle with their consequent dilation and a fall in blood pressure.

(iii) Increased capillary wall permeability which permits escape of plasma constituents into the tissue spaces.

(iv) Increased secretion by the mucous glands of the respiratory passages and by the tear glands.

It is this set of responses which is antagonized by antihistaminic drugs⁽⁸⁾. Because of their common chemotherapeutic denominator these are said to result from interactions of histamine with the H1 receptor site.

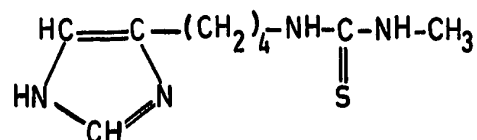
Manifestations of histamine binding to the H2 receptor include⁽⁸⁾:

(i) Increased production of hydrochloric acid by acid secreting glands in the stomach.

(ii) Stimulation of the heart rate.

(iii) Inhibition of uterine contractions in the rat.

Until very recently there were no known specific antagonists for these H2 responses but eight years of research involving the synthesis and pharmacological testing of more than 700 compounds has resulted in the demonstration that Burimamide (III) does possess this activity⁽⁹⁾.



(III) Burimamide

5.

The remainder of this discussion is concerned solely with the pharmacology of the H1 receptor, and no further reference is made to the histamine H2 receptor interaction.

A great many chemical and/or structural analogues of histamine have been tested for their ability to elicit the allergic (H1) responses^(10,11). It has been found that almost any modification to the histamine molecule results in an, often precipitous, decrease in activity.

When the alkylamine side chain of histamine is reduced by one methylene carbon a compound of only feeble activity is obtained. However, it is necessary to insert two more carbon atoms into the chain before all activity is lost. Monomethylation of the side-chain nitrogen, or of the ring carbon adjacent to the ring/side-chain junction [C_{δ_2}] yields compounds of moderate activity. Methylation at all other positions produces weak histamine agonists with equipotent molar ratios in the range 50 - 100. Substitution of the imidazole system by other small aromatic rings of similar basicity, e.g., triazole, pyrazole, thiazole, pyridine, pyridazine and pyrimidine, gave compounds of the same weak activity as those mentioned above.

It seems, therefore, that the requirements of the H1 site are optimally satisfied only by the histamine molecule and that very little structural variation is permitted if full potency is to be retained.

A logical extension of the above work, and one that has been pursued by several methods, is the study of the molecular conformations of the histamine species. It was hoped that these studies would permit the preferred molecular geometry to be defined and so allow some reasonable

speculation on the topology of the receptor site.

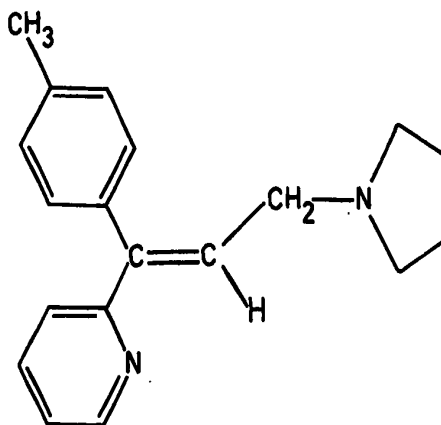
The basic centre of the ethylamine function has a pKa of 9.7 and so is largely protonated at physiological pH; the imidazole ring with its pKa of 5.9 pH units is uncharged within this context. The fact that the histamine mono-cation has both a donor and acceptor of hydrogen bonding power led Niemann and Hays⁽¹²⁾ to suggest that an intramolecular hydrogen bond could be formed with one of the aryl nitrogen atoms acting as an acceptor, and that this (the implied folded conformation) may be important in terms of the agonist binding to the receptor site. This suggestion of an internal hydrogen bond has received some support from an analysis of infra-red studies on histamine and some of its derivatives⁽¹³⁾, although spectrophotometric titration studies provided evidence that this bond was not formed⁽¹⁴⁾.

A theoretical calculation based on an Extended Hückel Theory (EHT), performed by Kier⁽¹⁵⁾ and designed to determine the total energy of the species as a function of the torsion angles around the $C_{\text{ring}}-C_{\text{alkyl}}$ and the $C_{\text{alkyl}}-C_{\text{alkyl}}$ bonds, predicted that the conformer with the torsion angles $C_{\alpha}C_{\beta}C_{\gamma}N_{\delta_1}$ and $N_{\alpha}C_{\alpha}C_{\beta}C_{\gamma}$ equal to 60° and 180° respectively is slightly preferred (energy difference = 1.6 kcal/mole) over that which has these angles equal to 60° and -60° respectively.

The nomenclature and sign convention for these torsion angles is as follows: If A-B-C-D is a set of atoms connected as shown, then the torsion angle about the bond B-C is defined as the dihedral angle between the planes defined by the atomic positions ABC and BCD. A positive angle is one which requires a clockwise rotation of atom A to achieve superposition of the AB and CD bond vectors when viewed in the

direction B \rightarrow C.

These two conformers correspond to the trans and gauche forms with respect to the $C_{\alpha}-C_{\beta}$ bond and this information in conjunction with the known constrained geometry of Triprolidine (IV) led Kier to postulate that these two conformations might be responsible for interactions at the H1 and H2 sites respectively.



(IV) Triprolidine

Only the trans 2-py/ CH_2-N isomer of Triprolidine is an effective histamine antagonist⁽¹⁶⁾ and evidence exists for the pyridyl ring being coplanar with the ethylenic bond⁽¹⁷⁾.

Kier reasoned that since both the alkylamine and the pyridyl functions are common in antihistamines (see later) and since these two groups had their counterparts in the histamine molecule, the internitrogen separation was an important parameter in describing the "binding conformations" of these species. The distance from N_{α} to N_{δ_1} for the trans conformer was measured by Kier to be 4.55\AA and for the gauche form

as 3.60Å. This latter distance is too long for any significant hydrogen bond formation, and since the geometry is unfavourable anyway, it is not now believed that an intramolecular hydrogen bond is formed.

By building a model of the Triprolidine molecule and arranging it to mimic the proposed *trans* conformation of histamine, Kier was able to measure the nitrogen/nitrogen distance in this species as 4.80Å. The difference between this and the 4.55Å quoted above is probably not great enough to preclude similar binding of the two molecules to the same site.

Nuclear magnetic resonance studies of the histamine mono-cation in D₂O⁽¹⁸⁾ support the EHT calculations in that Casy, Ison and Ham find approximately equal proportions at the *trans* and the two *gauche* conformers in their solutions.

Further evidence for a fully extended conformation of the di-cation in the solid state⁽¹⁹⁾ has been published but little weight can be given to this latter study for two reasons:

(i) The di-cation is not expected to predominate in situations where the pH is above 5.90 and so will be an unimportant species physiologically.

(ii) The main feature of the above crystal structure seems to be a ring of water and phosphate moieties which surround and are hydrogen bonded to the di-ion in five places. It is therefore probable that this arrangement is sufficiently strong to force the adoption of an unfavourable conformation.

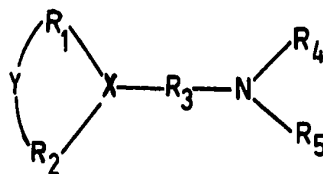
The mono-ion has been re-investigated by quantum mechanical methods, this time by French workers⁽²⁰⁾ using the "Perturbative Configuration Interaction using Localized Orbitals" (PCILO) method⁽²¹⁾ which, according

to these researchers, should yield more reliable results than are obtainable from EHT. Pullman and co-workers find two enantiomorphous conformational energy minima corresponding to torsion angles of 0° and 45° for $C_\alpha C_\beta C_\gamma N_{\delta_1}$ and $N_\alpha C_\alpha C_\beta C_\gamma$ respectively.

Despite the effort which has gone into studies designed to discern the most probable binding conformation of histamine, little by way of concrete results can be said to have ensued. The most important aspect of this work is the knowledge that the physiologically active mono-cation has considerable flexibility and so little can be hoped for by way of receptor site mapping from studies on this molecule.

On the other hand, there are many compounds, of varying degrees of structural rigidity, which are effective histamine antagonists, and so by drawing as many correlations as are possible from pharmacological and physico/chemical studies of these species, it should be possible to make some progress towards defining the receptor site.

The most generalised formulation for histamine antagonists which has appeared in print to date is given below⁽²²⁾:



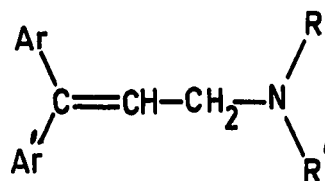
(V) A generalised antihistamine

In this symbolism R_1 and R_2 are aromatic or heteroaromatic rings one of which may be separated from X by a methylene group; X is a

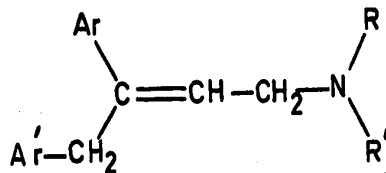
CO (ether), N or CH linkage; R_3 is most often an ethylene group or a two-carbon fragment of a nitrogen heterocycle; R_4 and R_5 are substituents of small size, usually methyl carbons but a small saturated ring may occupy both these positions. The R_1 and R_2 aryl groups may be ortho linked by Y which in turn may be a one or two atom linkage of quite variable character.

Even these generalities do not cover the gamut of compounds known as histamine antagonists. Because of this, and also because of the very large number of currently available drugs, no attempt will be made to review all of the available material. Mention will be made of selected compounds where appropriate, but the interested reader should refer to citations (8) and (22) for more exhaustive discussions.

In the case where the X- R_3 -N feature does not involve a cyclic system, the introduction of a double bond into the alkylamine chain provides a simple way of imposing some structural rigidity without grossly changing the system's character. Casy and co-workers^(23,24,25) have studied a series of isomeric diarylaminopropenes and diarylaminobutenes corresponding to the structural types (VI) and (VII) respectively.

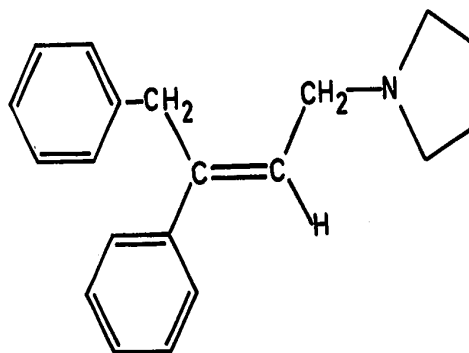


(VI) A 3-amino-1,1-diaryl-prop-1-ene derivative



(VII) A 4-amino-1,2-diaryl-but-2-ene derivative

These workers find that the greatest antihistaminic potency is obtained from the Ar = Ar' = Ph series when the alkylamine function is substituted trans to the aromatic grouping bonded directly to the ethylenic system, and they further find that greater activity is obtained when this trans aryl group is a 2-pyridyl moiety. Triprolidine and Pyrrobutamine (VIII) are both in clinical use and they both have a trans Ar/CH₂-N configuration at the ethylenic centre^(16,23).



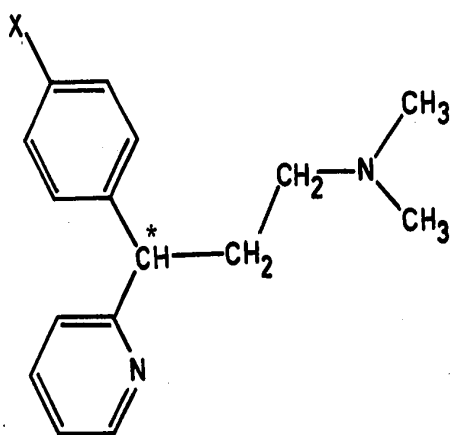
(VIII) Pyrrobutamine (Pyronil)

Evidence cited above⁽¹⁷⁾ has been presented to show that the pyridyl ring of Triprolidine is coplanar with the double bond. Unpublished evi-

dence from proton magnetic resonance (pmr) spectroscopy⁽²³⁾ also purports to show that the 2-phenyl group of Pyrrobutamine is approximately coplanar with the ethylenic linkage. If this proposed coplanarity of π molecular orbital systems is strongly preferred, then it should persist in the solid state and X-ray crystallography should reveal its presence. Triprolidine hydrochloride monohydrate was chosen for study for three reasons:

- (i) Only one of the geminal aromatic rings can be coplanar with the ethylene system, and it seemed important either to verify the results of Adamson et al.⁽¹⁷⁾ or to demonstrate that some arrangement permitting partial overlap of both extended π systems with the double bond exists.
- (ii) The compound was easily available in a good crystalline habit.
- (iii) The hydrochloride derivative is clinically administered as an antihistamine.

The Pheniramines (IX) provide a conformationally mobile but simply related variant of the 1,1-diaryl-prop-1-ene system, and some useful information should be obtainable from structural studies on these compounds.

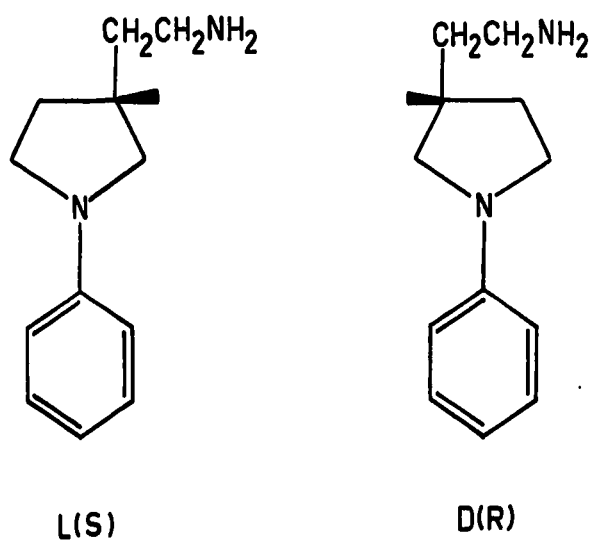


(IX)

- a X = H Pheniramine
- b X = Cl Chlorpheniramine
- c X = Br Brompheniramine

In this series the optically active carbon, C1 of the alkylamine chain, is more crowded than is the corresponding atom in Triprolidine and this fact may well impose some conformational restraints not implied by the fewer number of substituents of the ethylene bond. It has been said that in both systems the two aryl functions maintain a dihedral angle of approximately 90° ⁽²⁴⁾, and the extent to which this is true can most accurately be determined by X-ray crystallographic studies.

The question of site specificity with respect to optic hand of either the agonist or antagonist has not arisen up to this point because of the lack of optical activity in the compounds under discussion. The Pheniramines, however, are optically active and have been resolved into pure isomers⁽²⁶⁾. Pharmacological testing of these enantiomers indicates that the (+) rotamer is twelve times more effective in combating the effects of histamine than is its antipode⁽²⁷⁾. Specificity with respect to absolute configuration has also been demonstrated for the L(S) and D(R) forms of 3-ethylamino-1-phenylpyrrolidine (X).



(X) Enantiomeric 3-ethylamino-1-phenylpyrrolidine structures

These two compounds were shown to have pA_2 activity indices of 5.92 and 4.92 logarithmic units respectively⁽²⁸⁾ when tested for their antihistaminic efficacy on the isolated guinea pig ileum. The absolute configuration cryptics R and S are used here and subsequently in the sense of their definition by Cahn, Ingold and Prelog⁽²⁹⁾.

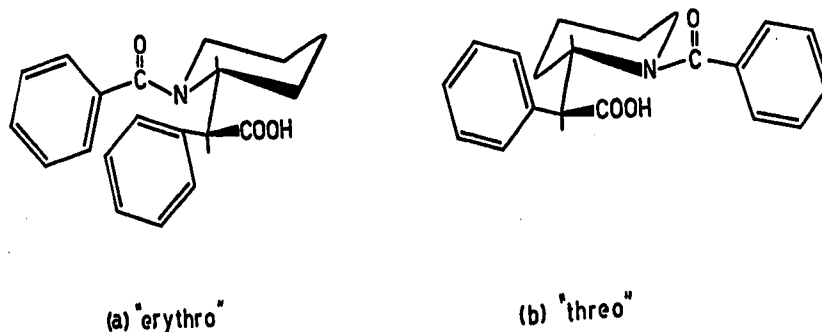
The pA_2 parameter is a common pharmacological quantity and is defined by the relation: $pA_2 \stackrel{\text{def}}{=} -\log_{10}[A]$, where [A] is the antagonist concentration (moles/litre) which necessitates a doubling of the agonist concentration to maintain a constant effect. By analogy with this the quantities pA_4 , pA_{10} , etc. may be defined.

Antihistamines in clinical use typically have pA_2 indices in the range 8 - 10⁽³⁰⁾ and so these two compounds are much less active. However, the above demonstration does reinforce the observations made on the antipodal Chlorpheniramines.

Barlow⁽³¹⁾ proposed that the more active (+) isomer of Chlorpheniramine should have the R configuration. However, Barlow's reasoning was criticised by Hite and Shafi'ee⁽³²⁾ on the grounds of arbitrariness and these latter workers went on to show, by chemical means, that (+)-Pheniramine has the S absolute configuration⁽³³⁾. No fault could be found with either the logic or the procedures of the above determination, but it was felt that the absolute configuration of the reference compound had not been determined in a completely unambiguous way. For the sake of convenience and self-sufficiency, the complete argument is summarized below.

Pure (+)-Pheniramine (XIa) was catalytically hydrogenated and a mixture of two diastereoisomeric secondary amines produced. A mixture

of solid amides was prepared from the above product by reaction with benzoyl chloride in basic solution. Hofman elimination conditions (pyrolysis of the quaternary nitrogen hydroxide) were applied and the diastereoisomers (XI) obtained.

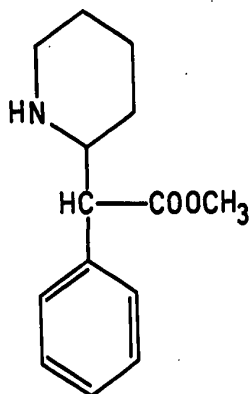


(XI) Two isomers of 2-phenyl-2-[2-(benzoyl)piperidyl]acetic acid

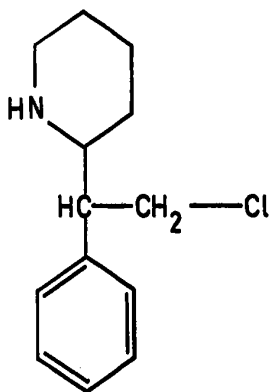
Fractional crystallization methods were used to separate these two isomers. The isomers were debenzoylated and one of these products shown (method not stated) to be identical to that compound which had previously been designated "erythro"⁽³⁴⁾. The "erythro" and "threo" labels here are used for convenience; the assignment is based on the stereochemical relationships of the two methine hydrogens and of the phenyl and methylene substituents of the asymmetric centres.

The method used by Weisz and Dudás⁽³⁴⁾ to determine the stereochemistry is as follows:

The compound methyl- α -(2-piperidyl)phenylacetate (XII) was prepared as a mixture of two racemates according to the method of Panizzon⁽³⁵⁾.

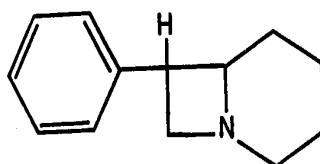
(XII) Methyl- α -(2-piperidyl)phenylacetate

Separation of the isomers was achieved by saponification of the ester followed by reliance on the different pK's of the groups to effect preferential solvent extraction⁽³⁶⁾. This procedure was developed by Rometsch who designated the two racemic mixtures "a" and "b". Reduction of the acids with LiAlH_4 followed by reaction with SOCl_2 resulted in formation of the alkyl halide(s) (XIII).



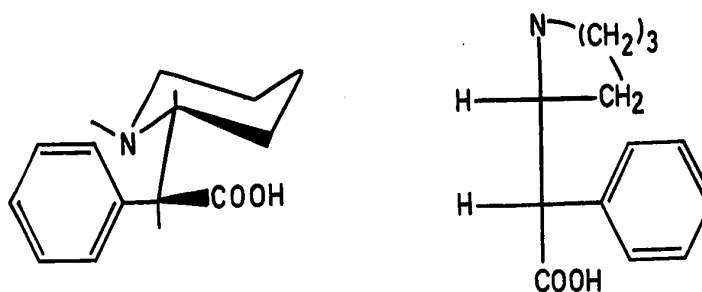
(XIII) 2-phenyl-2-(2-piperidyl)ethylchloride

The crucial step in the work of Weisz and Dudás was to then boil these two mixtures in xylene. It was found that the chloride derived from Rometsch's "b" racemate was converted to 7-phenyl-1-azabicyclo[4.2.0]octane (XIV), whereas that prepared from the "a" racemate remained unchanged.



(XIV) 7-phenyl-1-azabicyclo[4.2.0]octane

Weisz and Dudás argued on the basis of an assumed cis 6/4 ring fusion and from a consideration of non-bonded repulsive interactions that only the "erythro" configuration of the starting material was capable of yielding a stable bicyclic system. The "b" isomers can then be represented by the structural formulae (XV).



(XV) "erythro" 2-phenyl-2-(2-piperidyl)acetic acid

Unfortunately, this latter argument is seriously weakened by the knowledge that trans 6/4 ring fusion is permitted⁽³⁷⁾ and also by a detailed examination of the, supposedly forbidden, cis fused molecule derived from the "threo" form. This scrutiny indicates that any slight repulsive interactions can easily be removed by small deformations of the species.

The proof of the structure is therefore inconclusive and to resolve this problem we have undertaken an absolute configuration study of (+)-Chlorpheniramine maleate.

The three drugs, d&l-Brompheniramine maleate, (+)-Chlorpheniramine maleate and Triprolidine hydrochloride monohydrate, form the subject of this investigation into the structural features necessary for anti-histaminic action.

1.2 d,l-BROMPHENIRAMINE MALEATEExperimental

A sample of this racemate was supplied by Drs. R.R. Ison and A.F. Casey of the Faculty of Pharmacy at this University. Crystals, suitable for single crystal X-ray diffraction work, were easily grown by vapour diffusion of diethylether into an ethanolic solution of the salt. Preliminary oscillation and Weissenberg photography of a crystal exhibiting 2/m symmetry and of maximum dimensions 0.20 x 0.18 x 0.20 mm revealed the diffraction symmetry and systematic absences expected for space group $P2_1/c$.

The crystal lattice parameters, originally obtained from films, were refined by a least-squares process⁽³⁸⁾ during the alignment of the crystal on the Picker FACS-1 diffractometer; these parameters and other constants are contained in Table 1.

A total of 3374 different reciprocal lattice points within the sphere limited by $2\theta = 129^\circ$ were examined using Ni filtered Cu K radiation and the diffractometer in the coupled $\theta/2\theta$ scan mode. The 2θ scan speed was $1^\circ/\text{min}$. over a basic peak width of 1.8° , this width being increased as a function of θ ⁽⁴²⁾ to cope with the dispersion of the Cu K _{α} doublet.

Data reduction included corrections for Lorentz and polarization effects⁽⁴³⁾ and calculation of observational weights according to the expression $\sqrt{w} = 2 F_o/[T + (kl)^2 + B]^{\frac{1}{2}}$ ⁽⁴⁴⁾ where T is the total peak count, l is the net peak count, B is the peak background and k is a small constant (0.04 in this case) included to allow for minor experimental errors. A total of 3164 unique and space group permissible

TABLE I

A summary of data for d&l-Brompheniramine maleate.

empirical formula	$C_{20}H_{23}BrN_2O_4$
molecular weight	435.32 Daltons
melting point (lit.) ⁽³⁹⁾	132-4°C
space group	$P2_1/c$
a	9.863(10) Å
b	10.836(7) Å
c	21.494(10) Å
cos β	-0.4356(9)
β	115.83(5)°
V	2067.67 Å ³
Z	4
ρ_{calc}	1.42 gm/cm ³
$\rho_{obs} [(C_2H_5)_2O/CH_2Br_2]$	1.43(1) gm/cm ³
$\mu (Cu K_\alpha)$	32.6 cm ⁻¹
2 θ range explored	4°-129°
no. unique reflections	3164
no. observed reflections	2266 (71.6% of total)
no. variable parameters	336
ratio observations/parameters	6.7
final unweighted R ⁽⁴⁰⁾	4.55%
final weighted R ⁽⁴¹⁾	6.37%
mean sigma in C-C bond distance	0.006 Å
mean sigma in C-C-C angle	0.4°

reflections of which 2266 satisfied the observed/unobserved criterion that the net counts should not be less than the smaller of 75 counts or 10% of the total background for that reflection were obtained. The scattering factors used were derived from the published analytical coefficients of Cromer and Mann⁽⁴⁵⁾ except for the hydrogen curve which was that of Mason and Robertson⁽⁴⁶⁾. The data were corrected for the effects of absorption according to the method of Busing and Levy⁽⁴⁷⁾ during the latter stages of the structure refinement.

A Patterson map computed with coefficients modified to approximate those expected from "point atoms at rest"⁽⁴⁸⁾ unambiguously showed the positions of the expected three bromine-bromine vectors, and from a heavy atom phased Fourier synthesis suitable locations corresponding to the remainder of the pheniramine moiety were found. The atoms of the maleate ion were located in a subsequent electron difference synthesis. The positional parameters so defined along with individual atom isotropic temperature factors were subjected to three cycles of unit-weighted full-matrix least-squares refinement, using the locally modified version of ORFLS⁽⁴⁹⁾. During this process which reduced the conventional residual, R ⁽⁴⁰⁾, from 18.0 to 7.7%, a correction term corresponding to the real part of the anomalous scattering by bromine ($\Delta f' = -0.529$) was applied and all atoms of the pyridyl ring were treated as carbon atoms. A difference map computed at this stage made it possible to distinguish the nitrogen atom from the carbons of the pyridyl ring and showed sensible locations for the hydrogen atoms (the position of the second base dissociable proton of the maleate was deliberately bypassed here since it was desired to have as few errors as possible in

the F_c 's when this atom was being searched for).

Least-squares refinement was continued with observational weights, making the block-diagonal approximation, and with correction for the imaginary part of the anomalous scattering by the bromine ($\Delta f'' = 1.305$)⁽⁵⁰⁾. The hydrogen atom parameters were permitted to vary but were constrained to isotropic thermal motion, the remaining atoms being allowed to assume their anisotropic form. A final difference map revealed the remaining hydrogen of the maleate with a peak height of $0.3 \text{ e}/\text{\AA}^3$ and regions of electron density in the range $\pm 0.3 \text{ e}/\text{\AA}^3$ very close to the bromine. The background level of this map was $\pm 0.1 \text{ e}/\text{\AA}^3$. That the electron density near the bromine was due to the inability of the assumed temperature factor model to adequately describe the thermal motion of this atom and not to absorption effects was shown by the fact that after the data were corrected for absorption and the structure re-refined, no change resulted in either the R factor or the parameters and the "ripple" remained. The final weighted⁽⁴¹⁾ and unweighted⁽⁴⁰⁾ R factors are 6.37 and 4.55% respectively.

Results and Discussion

The atomic parameters used to describe the final model are contained in Tables 2, 3 and 4. Table 5 is a listing of the observed structure amplitudes and the calculated structure factors based on the final model. Figure 1 presents the numbering scheme adopted here, while Figure 2 displays the bond distances and interbond angles of this complex. The comparable molecular parameters for the hydrogen atoms are collected into Table 6.

TABLE 2

The final set of positional parameters for the non-hydrogen atoms of one d&l-Brompheniramine maleate "molecule". Estimated standard deviations in the last figure quoted are in parentheses.

Atom	x/a	y/b	z/c
Br	-0.03052(8)	-0.15502(5)	0.04388(3)
C(1)	-0.0557(5)	-0.0621(4)	0.1129(2)
C(2)	0.0355(5)	0.0389(4)	0.1413(2)
C(3)	0.0200(6)	0.1031(4)	0.1936(2)
C(4)	-0.0827(5)	0.0674(4)	0.2185(2)
C(5)	-0.1747(5)	-0.0334(4)	0.1884(2)
C(6)	-0.1622(5)	-0.0975(4)	0.1351(2)
C(7)	-0.0869(5)	0.1333(4)	0.2801(2)
C(1')	-0.0176(5)	0.0509(4)	0.3432(2)
C(2')	0.1382(5)	0.0533(4)	0.3835(3)
C(3')	0.2033(6)	-0.0188(4)	0.4408(2)
C(4')	0.1114(6)	-0.0925(5)	0.4579(3)
C(5')	-0.0412(6)	-0.0904(6)	0.4148(3)
N(6')	-0.1098(4)	-0.0214(4)	0.3585(2)
C(8)	-0.2470(5)	0.1803(4)	0.2670(2)
C(9)	-0.2972(5)	0.2833(4)	0.2148(2)
N(1)	-0.4419(6)	0.3450(1)	0.2078(1)
Ca	-0.4752(6)	0.4593(4)	0.1657(2)
Cb	-0.5759(5)	0.2606(4)	0.1807(2)
Cm(1)	-0.4748(5)	0.2559(4)	0.4929(2)
Cm(2)	-0.3948(6)	0.3726(4)	0.4910(2)
Cm(3)	-0.3730(6)	0.4245(4)	0.4403(2)
Cm(4)	-0.4173(5)	0.3819(4)	0.3682(2)
O(1)	-0.4976(5)	0.2354(4)	0.5429(2)
O(2)	-0.5161(4)	0.1800(3)	0.4416(2)
O(3)	-0.4758(4)	0.2764(3)	0.3496(2)
O(4)	-0.3951(4)	0.4537(3)	0.3293(2)

TABLE 3

The thermal motion parameters for the atoms of Table 2.

Atom	U_{11}^*	U_{22}	U_{33}	U_{23}	U_{13}	U_{12}
Br	0.1231 (5)	0.0722 (4)	0.0686 (4)	-0.0055 (3)	0.0491 (3)	0.0193 (4)
C (1)	0.069 (3)	0.046 (2)	0.053 (2)	0.010 (2)	0.029 (2)	0.020 (2)
C (2)	0.072 (4)	0.060 (3)	0.070 (3)	-0.003 (3)	0.045 (3)	-0.007 (3)
C (3)	0.073 (3)	0.051 (3)	0.068 (3)	-0.005 (2)	0.037 (3)	-0.009 (3)
C (4)	0.043 (3)	0.040 (2)	0.049 (2)	0.002 (2)	0.019 (2)	0.002 (2)
C (5)	0.046 (3)	0.049 (3)	0.062 (3)	0.002 (2)	0.026 (2)	0.001 (2)
C (6)	0.056 (3)	0.039 (2)	0.059 (3)	-0.004 (2)	0.016 (2)	-0.001 (2)
C (7)	0.051 (3)	0.042 (2)	0.055 (2)	-0.002 (2)	0.023 (2)	-0.002 (2)
C (1')	0.048 (3)	0.041 (2)	0.044 (2)	-0.003 (2)	0.014 (2)	0.001 (2)
C (2')	0.050 (3)	0.050 (3)	0.080 (3)	0.005 (2)	0.029 (3)	0.001 (2)
C (3')	0.050 (3)	0.067 (3)	0.079 (3)	0.010 (3)	0.011 (3)	0.009 (2)
C (4')	0.073 (4)	0.082 (4)	0.056 (3)	0.022 (3)	0.007 (3)	0.011 (3)
C (5')	0.068 (4)	0.101 (5)	0.078 (4)	0.036 (4)	0.022 (3)	-0.014 (3)
N (6')	0.052 (3)	0.078 (3)	0.058 (2)	0.023 (2)	0.010 (2)	-0.008 (2)
C (8)	0.061 (3)	0.043 (2)	0.052 (2)	0.007 (2)	0.030 (2)	0.013 (2)
C (9)	0.056 (3)	0.047 (2)	0.051 (2)	0.002 (2)	0.027 (2)	0.008 (2)
Ca	0.094 (4)	0.047 (3)	0.068 (3)	0.014 (2)	0.042 (3)	0.019 (3)
Cb	-0.062 (3)	0.056 (3)	0.064 (3)	-0.002 (2)	0.028 (3)	0.006 (2)
N (1)	0.060 (2)	0.038 (2)	0.043 (2)	0.006 (2)	0.026 (2)	0.012 (2)
O (1)	0.126 (3)	0.105 (3)	0.065 (2)	0.013 (2)	0.056 (2)	-0.016 (3)
O (2)	0.078 (2)	0.054 (2)	0.059 (2)	-0.001 (1)	0.027 (2)	-0.016 (2)
O (3)	0.109 (3)	0.054 (2)	0.052 (2)	-0.015 (1)	0.043 (2)	-0.018 (2)
O (4)	0.106 (3)	0.057 (2)	0.061 (2)	0.033 (2)	0.051 (2)	-0.002 (2)
Cm (1)	0.050 (3)	0.063 (3)	0.052 (2)	0.009 (2)	0.020 (2)	0.006 (2)
Cm (2)	0.074 (3)	0.063 (3)	0.050 (3)	-0.011 (2)	0.029 (3)	-0.010 (3)
Cm (3)	0.083 (4)	0.052 (3)	0.055 (3)	-0.018 (2)	0.036 (3)	-0.021 (3)
Cm (4)	0.064 (3)	0.049 (3)	0.054 (3)	0.001 (2)	0.033 (2)	0.007 (2)

* These U_{ij} values are coefficients in the expression

$$\exp[-2\pi^2(a^*2U_{11}h^2 + b^*2U_{22}k^2 + c^*2U_{33}l^2 + 2a^*b^*U_{12}hk + 2a^*c^*U_{13}hl + 2b^*c^*U_{23}kl)]$$

TABLE 4

The positional and thermal parameters for the hydrogen atoms of d,l-Brompheniramine maleate.

Atom	x/a	y/b	z/c	$U_{iso} (\text{\AA}^2)$
H(2)	0.113(5)	0.054(4)	0.128(2)	0.08(1)
H(3)	0.067(6)	0.171(5)	0.220(3)	0.08(2)
H(5)	-0.243(4)	-0.058(4)	0.202(2)	0.07(1)
H(6)	-0.209(4)	-0.161(4)	0.114(2)	0.06(1)
H(7)	-0.012(5)	0.210(4)	0.286(2)	0.07(1)
H(2')	0.190(5)	0.109(5)	0.372(2)	0.09(2)
H(3')	0.296(5)	-0.020(4)	0.471(2)	0.09(1)
H(4')	0.161(5)	-0.134(5)	0.502(3)	0.08(2)
H(5')	-0.105(5)	-0.122(4)	0.431(2)	0.11(1)
H(81)	-0.243(4)	0.210(3)	0.311(2)	0.05(1)
H(82)	-0.329(5)	0.109(4)	0.247(2)	0.09(1)
H(91)	-0.210(4)	0.347(3)	0.229(2)	0.06(1)
H(92)	-0.311(4)	0.258(3)	0.173(2)	0.06(1)
Hm	-0.438(6)	0.370(5)	0.250(3)	0.10(2)
Ha(1)	-0.496(5)	0.441(4)	0.123(2)	0.11(1)
Ha(2)	-0.579(5)	0.500(4)	0.162(2)	0.07(1)
Ha(3)	-0.389(5)	0.505(4)	0.187(2)	0.08(1)
Hb(1)	-0.648(5)	0.310(5)	0.187(2)	0.09(2)
Hb(2)	-0.557(5)	0.185(4)	0.205(2)	0.06(1)
Hb(3)	-0.603(5)	0.233(4)	0.137(2)	0.08(1)
Hm(1)	-0.485(5)	0.226(5)	0.405(2)	0.10(1)
Hm(2)	-0.354(5)	0.417(5)	0.533(2)	0.09(1)
Hm(3)	0.317(5)	0.502(4)	0.450(2)	0.05(1)

TABLE 5

The observed structure amplitudes and the calculated structure factors for d,l-Brompheniramine maleate. Excluded reflections are marked with an asterisk and the amplitudes have been multiplied by 10.0.

Table with multiple columns and rows of numerical data, including headers like '201 202' and '203 204'.

260	259	258	257	256	255	254	253	252	251	250	249	248	247	246	245	244	243	242	241	240	239	238	237	236	235	234	233	232	231	230	229	228	227	226	225	224	223	222	221	220	219	218	217	216	215	214	213	212	211	210	209	208	207	206	205	204	203	202	201	200	199	198	197	196	195	194	193	192	191	190	189	188	187	186	185	184	183	182	181	180	179	178	177	176	175	174	173	172	171	170	169	168	167	166	165	164	163	162	161	160	159	158	157	156	155	154	153	152	151	150	149	148	147	146	145	144	143	142	141	140	139	138	137	136	135	134	133	132	131	130	129	128	127	126	125	124	123	122	121	120	119	118	117	116	115	114	113	112	111	110	109	108	107	106	105	104	103	102	101	100	99	98	97	96	95	94	93	92	91	90	89	88	87	86	85	84	83	82	81	80	79	78	77	76	75	74	73	72	71	70	69	68	67	66	65	64	63	62	61	60	59	58	57	56	55	54	53	52	51	50	49	48	47	46	45	44	43	42	41	40	39	38	37	36	35	34	33	32	31	30	29	28	27	26	25	24	23	22	21	20	19	18	17	16	15	14	13	12	11	10	9	8	7	6	5	4	3	2	1	0
-----	-----	-----	-----	-----	-----	-----	-----	-----	-----	-----	-----	-----	-----	-----	-----	-----	-----	-----	-----	-----	-----	-----	-----	-----	-----	-----	-----	-----	-----	-----	-----	-----	-----	-----	-----	-----	-----	-----	-----	-----	-----	-----	-----	-----	-----	-----	-----	-----	-----	-----	-----	-----	-----	-----	-----	-----	-----	-----	-----	-----	-----	-----	-----	-----	-----	-----	-----	-----	-----	-----	-----	-----	-----	-----	-----	-----	-----	-----	-----	-----	-----	-----	-----	-----	-----	-----	-----	-----	-----	-----	-----	-----	-----	-----	-----	-----	-----	-----	-----	-----	-----	-----	-----	-----	-----	-----	-----	-----	-----	-----	-----	-----	-----	-----	-----	-----	-----	-----	-----	-----	-----	-----	-----	-----	-----	-----	-----	-----	-----	-----	-----	-----	-----	-----	-----	-----	-----	-----	-----	-----	-----	-----	-----	-----	-----	-----	-----	-----	-----	-----	-----	-----	-----	-----	-----	-----	-----	-----	-----	-----	----	----	----	----	----	----	----	----	----	----	----	----	----	----	----	----	----	----	----	----	----	----	----	----	----	----	----	----	----	----	----	----	----	----	----	----	----	----	----	----	----	----	----	----	----	----	----	----	----	----	----	----	----	----	----	----	----	----	----	----	----	----	----	----	----	----	----	----	----	----	----	----	----	----	----	----	----	----	----	----	----	----	----	----	----	----	----	----	----	----	---	---	---	---	---	---	---	---	---	---

FIGURE 1

The atomic numbering scheme used in this analysis.

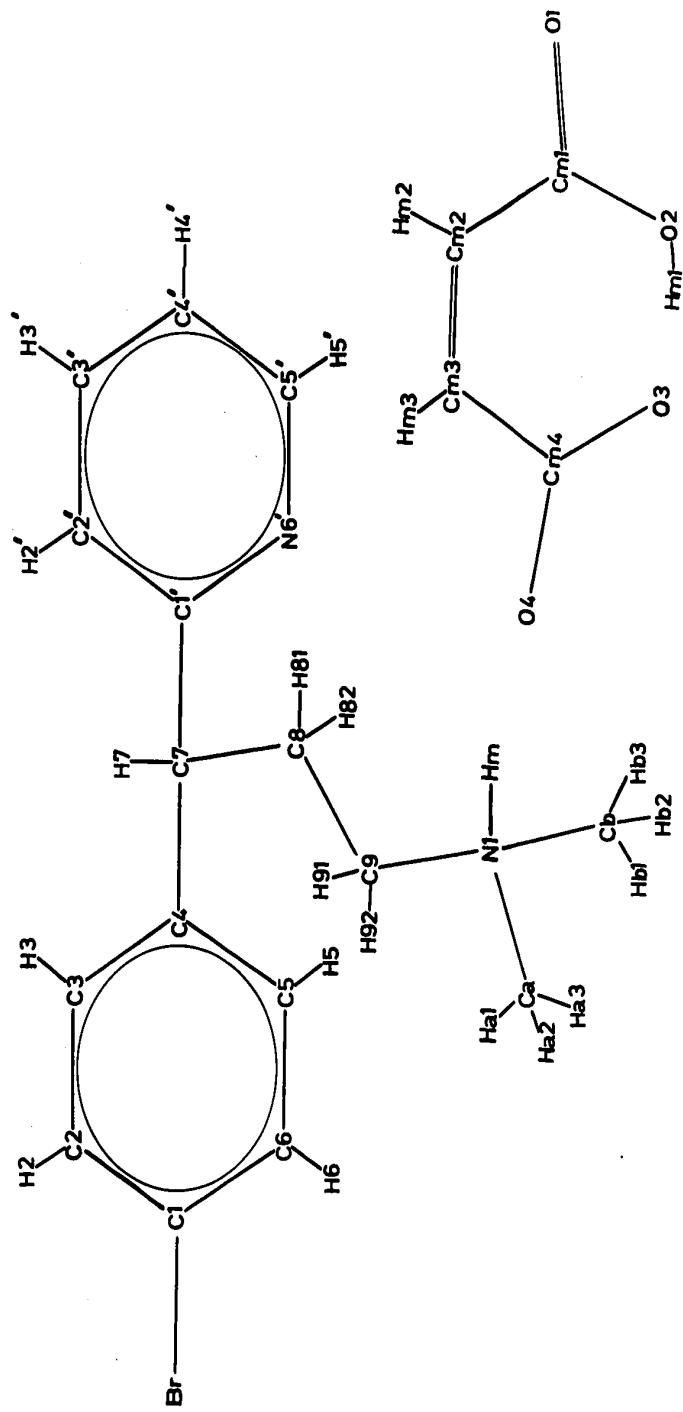


FIGURE 2

Bond distances and interbond angles for the non-hydrogen atoms of dl-Brompheniramine maleate. The e.s.d.'s in these distances and angles average 0.005Å and 0.4Å respectively.

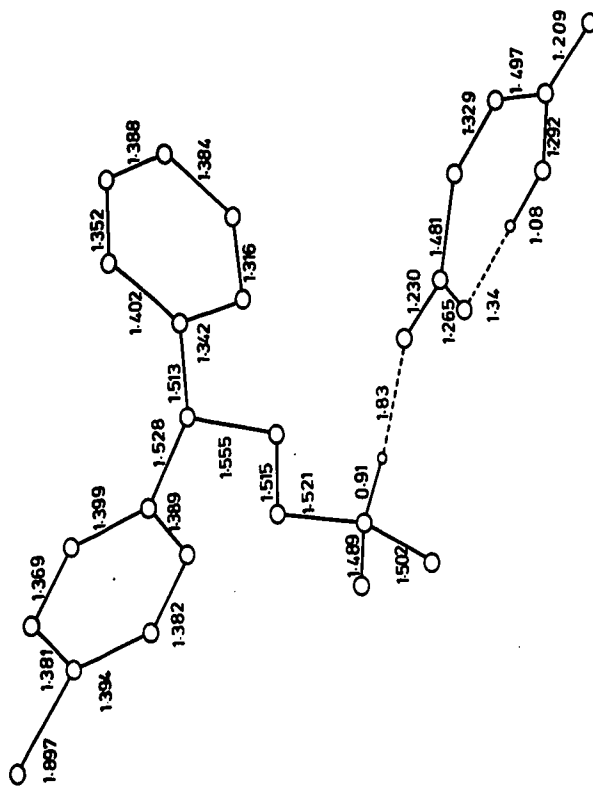
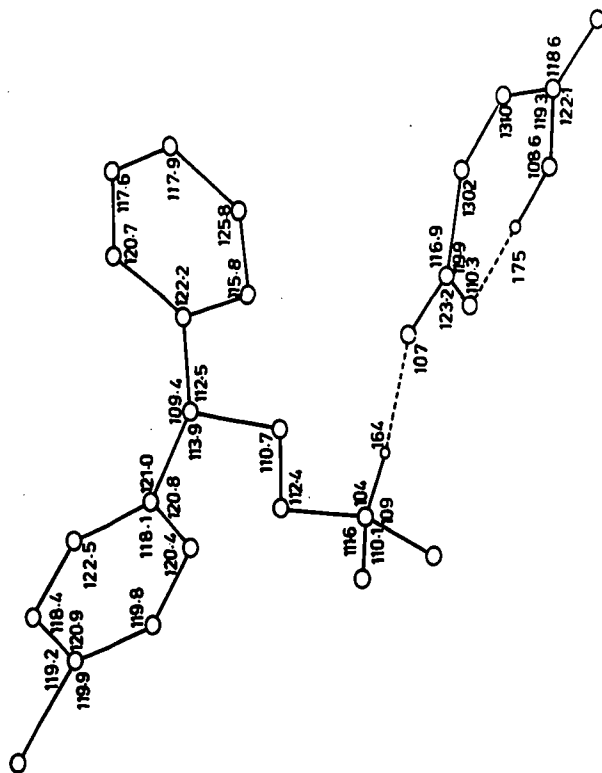


TABLE 6

Bond distances and interbond angles involving the hydrogen atoms of d,l-Brompheniramine maleate.

(a) Distances

C(2)-H(2)	0.96(4) Å	C(9)-H(91)	0.97(4) Å
C(3)-H(3)	1.00(6)	C(9)-H(92)	0.91(4)
C(5)-H(5)	0.95(5)	Ca-Ha(1)	0.93(6)
C(6)-H(6)	0.87(4)	Ca-Ha(2)	1.14(5)
C(7)-H(7)	1.11(5)	Ca-Ha(3)	1.01(5)
C(2')-H(2')	0.97(6)	Cb-Hb(1)	1.03(6)
C(3')-H(3')	0.89(5)	Cb-Hb(2)	0.91(4)
C(4')-H(4')	0.96(5)	Cb-Hb(3)	0.94(4)
C(5')-H(5')	0.76(5)	Cm(2)-Hm(2)	1.00(5)
C(8)-H(81)	0.98(4)	Cm(3)-Hm(3)	0.96(4)
C(8)-H(82)	1.01(5)		

(b) Angles

(i) The p-bromophenyl system

C(1)-C(2)-H(2)	120(3)°
C(3)-C(2)-H(2)	122(3)
C(2)-C(3)-H(3)	117(3)
C(4)-C(3)-H(3)	121(3)
C(4)-C(5)-H(5)	125(3)
C(6)-C(5)-H(5)	115(3)
C(1)-C(6)-H(6)	120(3)
C(5)-C(6)-H(6)	120(3)

(ii) The pyridyl system

C(1')-C(2')-H(2')	122(3)°
C(3')-C(2')-H(2')	117(3)
C(4')-C(3')-H(3')	121(3)
C(3')-C(4')-H(4')	125(3)
C(5')-C(4')-H(4')	117(3)
C(4')-C(5')-H(5')	124(5)
N(6')-C(5')-H(5')	109(5)
C(2')-C(3')-H(3')	121(3)

Continued.....

Table 6 (Continued)

(iii) The aliphatic portion			
C(4)-C(7)-H(7)	104(3) ^o	N(1)-Ca-Ha(2)	111(3) ^o
C(1')-C(7)-H(7)	107(2)	N(1)-Ca-Ha(3)	106(3)
C(8)-C(7)-H(7)	110(2)	Ha(1)-Ca-Ha(2)	109(4)
C(7)-C(8)-H(81)	105(2)	Ha(1)-Ca-Ha(3)	97(5)
C(7)-C(8)-H(82)	107(3)	Ha(2)-Ca-Ha(3)	123(4)
C(9)-C(8)-H(81)	111(2)	N(1)-Cb-Hb(1)	109(3)
C(9)-C(8)-H(82)	110(3)	N(1)-Cb-Hb(2)	112(3)
H(81)-C(8)-H(82)	113(4)	N(1)-Cb-Hb(3)	113(3)
C(8)-C(9)-H(91)	112(2)	Hb(1)-Cb-Hb(2)	110(4)
C(8)-C(9)-H(92)	114(3)	Hb(1)-Cb-Hb(3)	108(4)
N(1)-C(9)-H(91)	108(2)	Hb(2)-Cb-Hb(3)	105(4)
N(1)-C(9)-H(92)	106(3)	C(9)-N(1)-Hm	104(4)
H(91)-C(9)-H(92)	104(4)	Ca-N(1)-Hm	108(4)
N(1)-Ca-Ha(1)	110(4)	Cb-N(1)-Hm	109(4)

(iv) The maleate ion

Cm(1)-O(2)-Hm(1)	109(3) ^o
Cm(4)-O(3)-Hm(1)	110(2)
Cm(4)-O(4)-Hm	107(2)
Cm(1)-Cm(2)-Hm(2)	106(3)
Cm(3)-Cm(2)-Hm(2)	122(3)
Cm(2)-Cm(3)-Hm(3)	120(2)
Cm(4)-Cm(3)-Hm(3)	110(2)

If X denotes a carbon, oxygen or nitrogen atom, then the standard deviations in Br-X, X-X and X-H distances average 0.005, 0.006 and 0.06Å respectively. Bond angles of the types Br-X-X, X-X-X, H-X-X and X-H-X have average standard errors of 0.4, 0.4, 3.0 and 2.0° respectively. These error estimates were derived from the appropriate atomic positional e.s.d's using the independent atom method of Ahmed et al.⁽⁵¹⁾. The sigmas in the atomic parameters were derived from the elements of the atomic matrices after inversion, according to standard methods⁽⁵²⁾, by the block-diagonal least-squares refinement program⁽⁵³⁾. Because of the neglect of inter-atomic correlations, this procedure usually leads to an underestimate of the atom parameter standard deviations which may be corrected for if convergence has been achieved using the relaxation factor method of Hodgson and Rollet⁽⁵⁴⁾. This method was not employed in its published form because of the apparent inability of the least-squares process to recover from the use of relaxation factors greater than unity. Other workers have accommodated this difficulty by simply multiplying the least-squares estimates of the standard deviations by some constant - usually in the range 2-3. The arbitrariness of this procedure makes it unattractive, and accordingly the least-squares estimates are used unmodified here, but with the full realization that an overly precise description may be implied by this usage.

The details of this structure may conveniently be considered in three parts. At this point, the discussion will concentrate mainly on a description of the protonated Brompheniramine moiety. An interpretation of this structure in terms of antihistaminic potency will be

integrated into a section at the end of this portion of the thesis, and the maleate ion will be fully discussed in another part of this work.

The observed C(1)-Br bond distance for this structure is 1.897(6)Å whereas the estimate of the bromine-aromatic carbon bond length obtained by Sutton, on the basis of spectroscopic work most of which was performed before 1950, is 1.85(1)Å⁽⁵⁵⁾. There is a serious discrepancy between these values, and to obtain a better estimate of the Br-C_{aromatic} distance, those bond lengths of Table 7 were gathered from the literature. Entries in this representative tabulation were averaged according to the formula given below⁽⁵⁵⁾:

$$\langle l \rangle = \Sigma (l_i / \sigma_i^2) / \Sigma 1 / \sigma_i^2$$

and the associated error estimate derived from⁽⁵⁵⁾:

$$\sigma_{\langle l \rangle} = (\Sigma 1 / \sigma_i^2)^{-1/2}$$

The improved expectation value obtained from this analysis is 1.895Å and the statistical standard deviation is 0.0015Å.

Agreement between this latter value and the observed magnitude of this quantity in Brompheniramine is good and lends some credence to both this experimental value and the e.s.d. in the observed bond length.

Other distances within the cation fall close to expected values; the six C...C bonds of the phenyl ring average 1.386Å, a value which is near the 1.394Å expected for such systems⁽⁵⁵⁾. The C(2)-C(3) separation is 0.017Å shorter than this average but the discrepancy is less than 3 x 0.006Å and so no statistical significance can be attached to it. Despite the unaccounted for errors in the standard deviations, the

TABLE 7

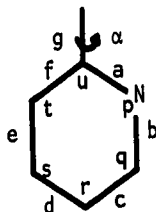
Bromine-C aromatic bond lengths: a representative survey.

Authors	Reference	Bond Lengths
A.T. McPhail and G.A. Sim	J. Chem. Soc. B, 1104 (1968)	1.96(3)
F.W. Comer and J. Trotter	J. Chem. Soc. B, 11 (1966)	1.91(5)
H.G. Rossmann and W.N. Lipscomb	Tetrahedron, 4, 275 (1958)	1.905(35), 1.972(35)
T.L. Charlton and J. Trotter	Acta Cryst., 16, 313 (1963)	1.88(5)
A.K. Pant	Acta Cryst., 19, 440 (1965)	1.90(5), 1.89(5)
R.P. Shibaeva and L.O. Atovmyan	Zh. Struct. Khim., 9, 90 (1968)	1.87(3)
A. Camerman, N. Camerman and J. Trotter	Acta Cryst., 19, 449 (1965)	1.87(3), 1.96(3)
A.C. MacDonald and J. Trotter	Acta Cryst., 19, 456 (1965)	1.90(1)
A.T. McPhail and G.A. Sim	J. Chem. Soc. B, 1235 (1966)	1.87(1)
P.B. Rerat	Acta Cryst., 225, 1392 (1969)	1.88(1), 1.93(1), 1.89(1), 1.95(1)
H. van Meersche and G. Leroy	Bull. Soc. Chim. Belges, 69, 204 (1960)	1.88(4)
K.A. Kerr, J.M. Robertson and G.A. Sim	J. Chem. Soc. B, 1305 (1967)	1.85(3)
O. Lefebvre-Soubeyran	Bull. Soc. Chim. Fr., 1242 (1966)	1.96(2)
H.M. Zacharis and L.H. Trefonis	J. Heterocycl. Chem., 5, 343 (1968)	1.886(5)
H.G. Newton, J.A. Kapecki, J.E. Baldwin and I.C. Paul	J. Chem. Soc. B, 189 (1967)	1.87(1)
B. Nilsson	Acta Chem. Scand., 22, 518 (1968)	1.93(2)
K. Bjamer, G. Ferguson and R.P. Melville	Acta Cryst., 224, 855 (1968)	1.910(13)
Y. Iitaka, I. Watanabe, I.T. Harrison and S. Harrison	Acta Cryst., 225, 1299 (1969)	1.88(1)
S. Abrahamsson and B. Nilsson	Acta Chem. Scand., 20, 1044 (1966)	1.93(2)
G. Kartha and D. Haas	J.A.C.S., 86, 3630 (1964)	1.94(3)
S. Abrahamsson	Acta Cryst., 16, 409 (1963)	1.88(2), 1.88(2), 1.90(2)
A. Griffiths and R. Hine	Acta Cryst., 226, 29 (1970)	1.908(13)
A. Griffiths and R. Hine	Acta Cryst., 226, 34 (1970)	1.876(31)
S.N. Srivastava and M. Przybylska	Acta Cryst., 226, 707 (1970)	1.91(2)
J.Z. Gougoutas and B.A. Kaski	Acta Cryst., 226, 853 (1970)	1.886(5)
A.T. Christensen	Acta Cryst., 226, 1519 (1970)	1.919(9)
J.C. Porthelne and C. Romers	Acta Cryst., 226, 1971 (1970)	1.889(9)
M. Uramoto, N. Otake, Y. Ogawa, H. Yonehara, F. Harumo and Y. Saito	Acta Cryst., 227, 236 (1971)	1.87(3)
P.A. Chiaroni	Acta Cryst., 227, 448 (1971)	1.886(15)
E. Thom and A.T. Christensen	Acta Cryst., 227, 573 (1971)	1.901(7)
E. Thom and A.T. Christensen	Acta Cryst., 227, 794 (1971)	1.881(8)
M.N. Sabesan and K. Venkatesan	Acta Cryst., 227, 986 (1971)	1.867(12)
V.F. Brandl, M. Röhrl, K. Zechmeister and W. Hoppe	Acta Cryst., 227, 1718 (1971)	1.91(2)
W. Dreissig and K. Pilleth	Acta Cryst., 227, 1140 (1971)	1.891(7)
D.J. Duchamp and C. Chidester	Acta Cryst., 228, 1092 (1972)	1.902(2)
R. Norrestam and M. Von Glehn	Acta Cryst., 228, 434 (1972)	1.891(6)
R. Takahashi and Y. Iitaka	Acta Cryst., 228, 764 (1972)	1.93(2)
I.K. Larsen	Acta Cryst., 228, 1136 (1972)	2.01(2), 1.92(1), 1.89(1), 1.92(1), 1.90(5), 1.82(4)
B. Jensen	Acta Cryst., 228, 771 (1972)	1.87(3)
B. Jensen	Acta Cryst., 228, 774 (1972)	1.878(7)
J.C. Porthelne, C. Romers and E.W.H. Rutter	Acta Cryst., 228, 849 (1972)	1.901(5)
S. Kashino, Y. Sumida and M. Haise	Acta Cryst., 228, 1374 (1972)	1.910(10)
J.P. Schaefer and L.L. Reed	Acta Cryst., 228, 1743 (1972)	1.93(2)
S.C. Nyburg, A.G. Brook, J.D. Pascoe and J.T. Szymański	Acta Cryst., 228, 1785 (1972)	1.892(6)
A.T. Christensen and K.O. Strömme	Acta Cryst., 225, 657 (1969)	1.886(16), 1.891(16), 1.896(16)

6σ (0.042Å) shortening of the C(2')-C(3') bond in the 2-pyridyl function is probably significant. Non-equality of the nominally equivalent C \cdots N bonds within this ring is also apparent, the C(1')-N(6') distance being longer than that for C(5')-N(6') by 0.026Å.

Inspection of the internal bond angles of the 2-pyridyl ring also reveals some departures from the geometry one might expect on the basis of an assumed "nearly symmetric" system. A regular hexagonal form for this ring may be discounted because it is known that C \cdots N bonds are shorter than similar linkages between carbon atoms⁽⁵⁵⁾, but if it is assumed that only small electronic disturbances are associated with the presence of a -CHPhCH₂- substituent, then there seems little reason for angles C(1')-N(6')-C(5') and N(6')-C(5')-C(4') differing by 4.2° and 5.8° respectively from 120°, whereas the other ring angles only deviate by a maximum of 2.2° from this value.

The 2-pyridyl moiety forms part of all three of the antihistamine structures determined here and certain consistencies may be noted if these three features are studied. However, in order to set a firmer base for these comparisons, another literature search was performed. With reference to the key figure (XVI) the data of Table 8 may be interpreted in terms of the following generalities.



(XVI) Key figure for Table 8

- (i) There is no inherent tendency for one C ~~---~~ N bond to be longer than the other.
- (ii) The internal ring angle at the nitrogen atom is about 3° less than 120° .
- (iii) Angles q and u , which are the internal ring angles at those atoms flanking the nitrogen atom, are usually greater than the trigonal value by about 3° .

The last entry in Table 8 summarises the results obtained spectroscopically for pyridine and demonstrates that the bond angle distortions noted above are an intrinsic property of this heterocycle. The spectroscopic workers assumed that the molecule had a 2-fold axis of symmetry in interpreting their results.

The two aryl systems are individually planar with maximum exoplanar displacements of 0.012\AA and 0.010\AA for the phenyl and pyridyl rings respectively. With respect to an orthogonal axial system measured in angstroms and with x, y, z parallel to the crystallographic a, b and c^* axes, these two planes may be described by the direction cosine equations $-0.4273x + 0.6013y - 0.6751z + 1.1812 = 0$, and $-0.3878x + 0.7369y + 0.5538z - 5.3962 = 0$ respectively.

The goodness of fit of the atomic positions to a plane is often inferred from the χ^2 parameter⁽⁶³⁾. This quantity is defined by $\chi^2 = \sum (p_i^2 / \sigma(p_i)^2)$. The summation being taken over all atoms used to define the plane, p_i is the deviation of atom i from the plane and $\sigma(p_i)$ is the e.s.d. in that distance. Small χ^2 values indicate good planarity of the group. The benzyl and pyridyl rings have χ^2 values of 25.6 and 5.6 respectively and they maintain an interplanar dihedral angle of

103.6° between them. The dihedral angle between the aryl planes describes their mutual disposition but gives no indication of their orientation with respect to the rest of the molecule. Torsion angles about the C(4)-C(7) and C(1')-C(7) bonds are important in describing the geometry and so are quoted here. The torsion angles C(6)-C(4)-C(7)-C(8) and N(6')-C(1')-C(7)-C(8) are -55.1° and 33.3° respectively. Figure 3, which is a stereoscopic pair of the complex, displays the conformation.

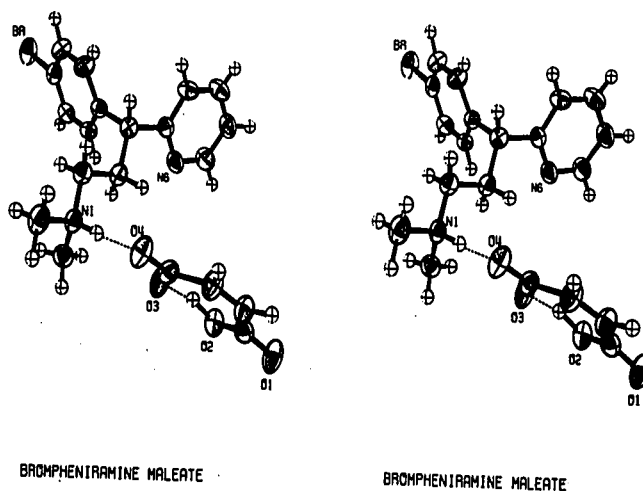


FIGURE 3

A stereoscopic pair of the d,l-Brompheniramine maleate complex showing the R absolute configuration. This and the other stereoscopic drawings in this thesis are computer produced diagrams (64).

The three bond angles at C(7) not presented in Figure 2 are those involving H(7). When C(4), C(1') and C(8) are the second bonded atoms

the bond angles are $104^{\circ}26'$, $106^{\circ}31'$ and $109^{\circ}31'$ respectively (standard error in each case being $2^{\circ}18'$). Deviations from ideality here are small but may be attributed to non-collinear bisectors of the angles $C(4)-C(7)-C(1')$ and $C(8)-C(7)-H(7)$.

Because of the greater basicity of the dimethylpropylamine group-
ing over the pyridyl function, it is not surprising that the maleate
ion is hydrogen-bonded to this former structural unit. The $N(1)-O(4)$
distance is 2.718\AA , the separation of $O(4)$ and Hm is 1.84\AA , and the
bond angles at Hm and $O(4)$ are $163^{\circ}54'$ and $107^{\circ}12'$ respectively.
These parameters describe a $N-H\dots O$ bond which, although slightly
shorter than those tabulated by Donohue⁽⁶⁵⁾, only extends this range
($2.73 - 3.07\text{\AA}$) by 0.01\AA and so nothing special can be inferred from
these dimensions.

The alkylamine chain is fully extended and directed away from the
diaryl system. Repulsive interactions are minimised by this arrange-
ment which implies a trans conformation about the $C(8)-C(9)$ bond; the
torsion angle $C(7)-C(8)-C(9)-N(1)$ is $-171^{\circ}39'$. Because of the appar-
ent importance of the conformation about this bond a view of the
molecular complex projected down the $C(9)-C(8)$ bond is included in
Figure 4.

Another conformational feature of interest is depicted in the
molecular packing diagram, Figure 5. The molecule in the bottom left
corner of this diagram most clearly shows that the alkylamine chain is
not symmetrically disposed with respect to the two aromatic rings. The
nature of this asymmetry is such as to partially occlude the p-bromo-
phenyl moiety and expose the pyridyl ring to functional groups which

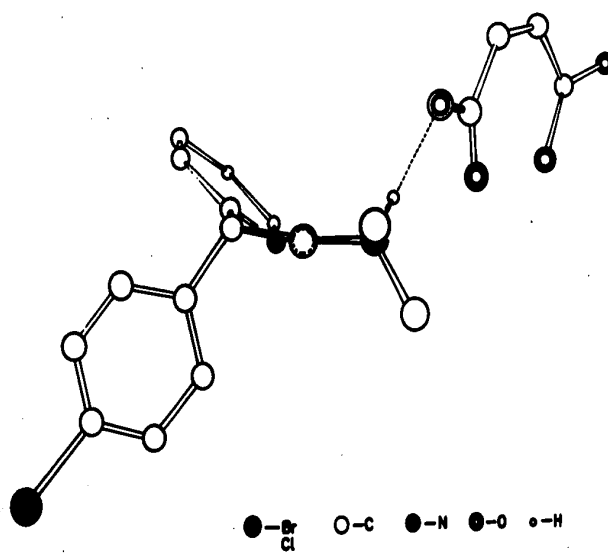
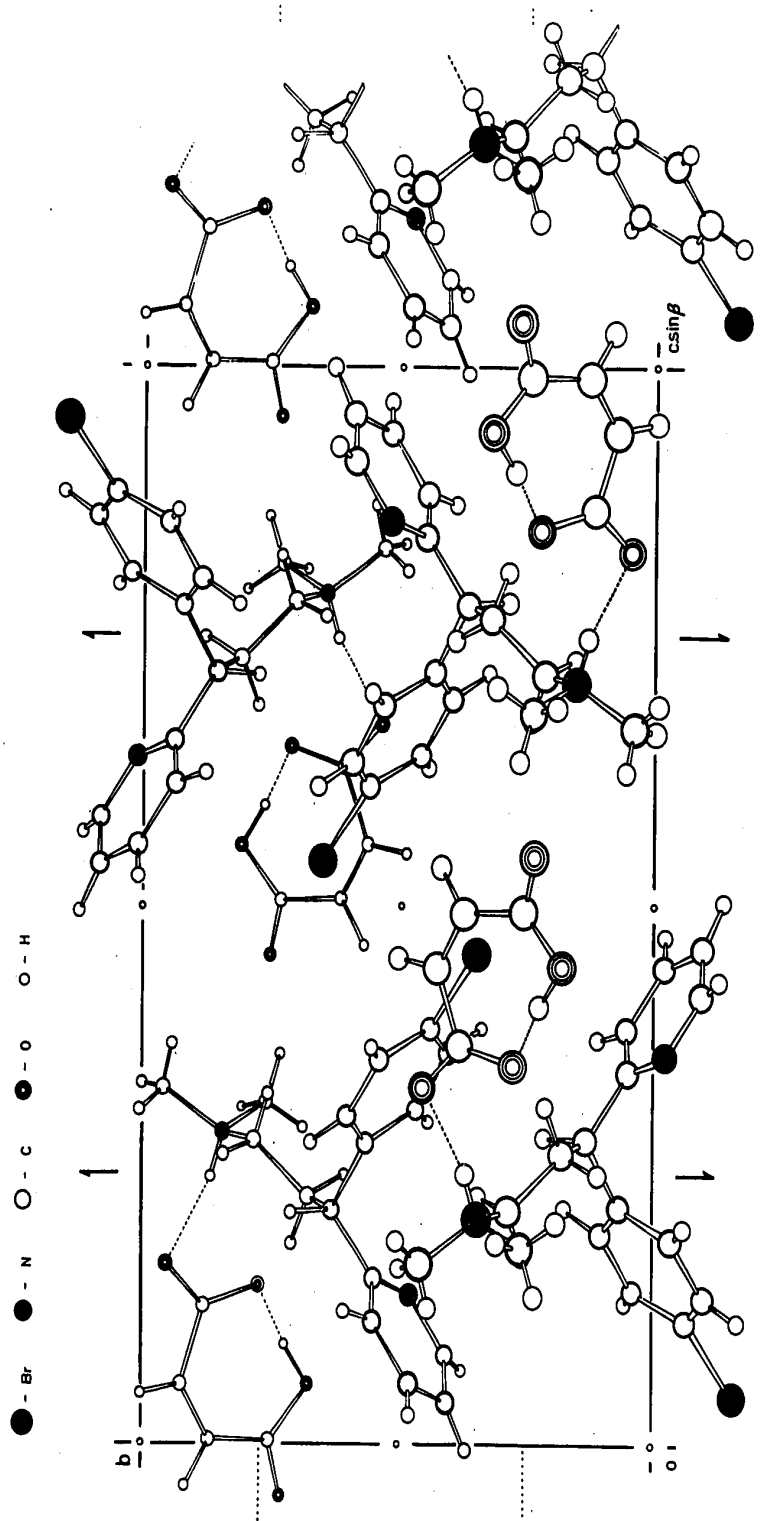


FIGURE 4

A drawing of the d,l-Brompheniramine maleate complex as viewed down the C(9)-C(8) bond direction.

FIGURE 5

A packing diagram of several molecules viewed parallel to a. The conformation is most clearly shown by the molecule in the bottom left corner.



approach this "open face" of the cation in directions permitting hydrogen bonding to the dimethylamino group. It may be thought that repulsive interactions might be responsible for the molecular dissymmetry, but neither an extensive search through lists of computed interatomic distances nor a close examination of a space filling CPK molecular model has revealed any such interactions. The unsymmetrical nature of this conformation may most easily be described by quoting the distances from the alkylamine nitrogen to the centroids of the aromatic rings. These parameters are 6.212Å and 5.568Å respectively for the pyridyl and benzene rings.

Despite the presence of two basic functions and a diprotic acid molecule, the only intermolecular interaction of a polar nature is the hydrogen bond previously mentioned. The aromatic base and the second maleic carboxyl group do not participate in any specific bonding interactions, although they and the other parts of this structure participate in many Van der Waals type attractive forces⁽⁶⁶⁾.

In this space group the eight centres of symmetry per unit cell fall into two non-equivalent classes. One Van der Waals contact worthy of mention is that between bromine atoms related by centres of symmetry equivalent to that of the origin. The separation of these two atoms is 4.025Å, a value which is in agreement with the 3.90Å expected on the basis of Pauling's Van der Waals radius for bromine⁽⁶⁷⁾. Another intermolecular contact across a centre of symmetry involves an edge of the pyridyl rings and may be seen at the right-hand side of Figure 5. The closest carbon-carbon contact here is 3.680Å and although the pyridyl rings are parallel no stacking interactions occur,

and so this is another normal dispersion type interaction which contributes to the stability of the crystalline solid.

* * * * *

The gift of the sample of d&l-Brompheniramine maleate by Drs. R.R. Ison and A.F. Casy is gratefully acknowledged.

1.3 (+)-CHLORPHENIRAMINE MALEATE

Experimental

A powdered sample (5 gm) of this compound was supplied from batch number 1171-29-1 by Dr. J.G. Topliss of the Schering Corporation. This isomer is reported to have an optical rotation of $[\alpha]_D^{26} = +43.5^\circ$ for a 1% solution in dimethylformamide (DMF)⁽⁶⁸⁾. An optical rotation of $41.0 \pm 0.8^\circ$ was obtained independently after evaluation of experimental readings on a 0.25% solution in DMF using a Cary model 60 recording spectropolarimeter.

Some difficulty was experienced in growing crystals suitable for data collection because of the very high solubility of (+)-Chlorpheniramine maleate in simple alcohols and because of the readiness with which this compound supersaturates in anisole, pyridine, dimethylsulphoxide (DMSO), chloroform, sec. propanol, tert. amylalcohol and water. Well shaped needles were obtained by slowly cooling a hot solution of the molecular complex in ethylacetate. One of these crystals was cut under the microscope with a scalpel and a columnar fragment measuring 0.25 x 0.30 x 0.60 mm mounted along its length in the usual way.

Preliminary oscillation and Weissenberg photographs revealed 2/m diffraction symmetry and the fact that the direction of elongation of the crystals was not the monoclinic unique axis. The space group of these crystals was uniquely determined as $P2_1$ by noting that the odd orders of the $0k0$ reciprocal lattice row had zero intensity, and that the compound possessed optical activity.

The crystal was transferred to the diffractometer and aligned using

customary techniques. The refined unit cell constants and some other physical parameters are contained in Table 9.

Because of the geometry of the diffractometer and the manner of the crystal mounting, it was necessary to collect the data from two regions of reciprocal space. These two regions were both within the spherical shell defined by $4.0^\circ \leq 2\theta \leq 128^\circ$. The first part of the set encompassed all those reflections for which $-6 \leq h < 3$ and $-23 \leq k \leq 0$ and $0 \leq l \leq 10$; the remainder of the set collected was from the $\bar{h}, \bar{k}, \bar{l}$ octant for which $h \leq -3$. These data were combined and the indices transformed to yield hkl and $\bar{h}\bar{k}\bar{l}$ reflections (see later).

The data reduction procedure employed corrections for the minor intensity falloff in the three monitor reflections which occurred during the data collection, as well as the Lorentz and polarization corrections appropriate for the moving crystal/moving counter technique with normal beam equatorial geometry⁽⁴³⁾. Also at this time observational weights were calculated according to the procedure outlined above (page 19). Of the 1784 independent and space group permissible reflections collected, 1679 were found to have net intensities greater than $3\sigma_{\text{net}}$. The remaining 105 data points were assigned a threshold intensity and coded as unobserved; they were excluded from all subsequent calculations.

A Patterson map was computed using F_o^2 modified by the $1/Lp$ curve as coefficients in the synthesis. Despite this sharpening procedure, the vector map obtained showed poor resolution. An unsharpened Patterson map was computed for comparison and two well shaped peaks were shown to have been enhanced by the sharpening. A symmetry minimum

TABLE 9

(±)-Chlorpheniramine maleate physical data.

molecular formula	$C_{20}H_{23}N_2O_4Cl$
molecular weight	390.87
crystalline habit	needles along <u>a</u>
space group	$P2_1$
<u>a</u>	5.7669(4) Å
<u>b</u>	20.3382(16) Å
<u>c</u>	9.1347(8) Å
<u>β</u>	103.73(2)°
V	1040.75 Å ³
ρ_{calc} (2 formula units/cell)	1.248 gm/cc
ρ_{obs} (density gradient column)	1.248 gm/cc
$[\alpha]_D^{26}$ 1% DMF (lit.) (68)	+43.5°
$[\alpha]_D^{26}$ 1% DMF (obsd.)	+41 ± 0.8°
$\bar{\mu}$ (Cu K_α)	18.5 cm ⁻¹
crystal size	0.25 x 0.30 x 0.60 mm
2θ range explored	4°-128°
no. unique reflections	1784
no. observed reflections	1679 (94.1% of total)
no. variable parameters	308
ratio observations/parameters	5.45
final unweighted R	5.02%
final weighted R	6.64%
mean sigma in C-C bond	0.005 Å
mean sigma in C-C-C angle	0.4°

superposition map⁽⁶⁹⁾ calculated on the basis of these two positions revealed the chlorobenzene fragment and the maleate ion. Successive structure factor computations and electron density syntheses revealed the remainder of the structure. The relationship of the final model as input to the least-squares refinement to the $u \cdot \frac{1}{2} \cdot w$ harker section is depicted in Figure 6. The model was refined by the difference Fourier method and through two cycles of unit-weighted block-diagonal least-squares⁽⁵³⁾ to yield a conventional R factor⁽⁴⁰⁾ of 25%.

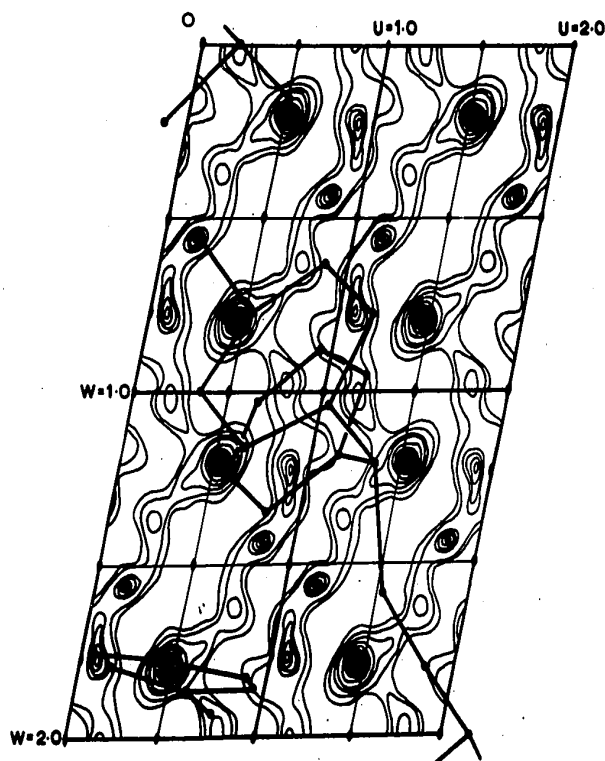


FIGURE 6

The $u \cdot \frac{1}{2} \cdot w$ section of the three dimensional Patterson synthesis and the relationship of the initial model to this section.

Throughout the refinement the y coordinate for the chlorine atom was fixed at 0.50. The scattering factors used were derived from the analytical coefficients of Cromer and Mann⁽⁴⁵⁾ except for the hydrogen curve which was that of Stewart, Davidson and Simpson⁽⁷⁰⁾. The $\Delta f'$ correction terms for the non-hydrogen atoms were applied here and subsequently. These quantities for Cu K_α radiation are: Cl = 0.375, O = 0.055, N = 0.036, C = 0.021 electrons⁽⁵⁰⁾. The $\Delta f''$ terms for chlorine and oxygen, 0.685 and 0.034 electrons respectively⁽⁵⁰⁾, were applied later. Convergence of the isotropic model was achieved at R = 17.8% after two further cycles of block-diagonal least-squares refinement. The temperature factors were then allowed to assume their anisotropic form and the refinement continued through four further cycles. The residual at this stage had been reduced to 10.4% and a difference map calculated on the basis of these new parameters revealed chemically sensible locations for all of the hydrogen atoms except the second base dissociable proton of the maleate ion. It was also possible at this time to deduce which of the atoms of the pyridyl ring was the nitrogen - all atoms of this moiety had hitherto been treated as carbons.

The hydrogen atoms were included, with their temperature parameters fixed at the final isotropic value assumed by the atoms to which they were bonded, and six more least-squares cycles performed. The reliability index was thereby decreased to 6.8% but a difference map computed at this stage did not allow reliable positioning of the remaining hydrogen atom.

In an attempt to remove residual errors in the model and to determine the absolute configuration of the (+)-Chlorpheniramine molecule,

several adjustments were made:

(i) The reflection data were transformed back to the $h\bar{k}l$ and $\bar{h}k\bar{l}$ quadrants originally collected. The $\bar{h}k\bar{l}$ reflections which had $h \leq -3$ were denoted by $h\bar{k}l$. The validity of this procedure lies in the Laue group symmetry of these crystals of $2^{(71)}$ and in the fact that the two forms of the reflection do not differ significantly in transmission factor.

(ii) The molecule was inverted by reflection through the plane $y = \frac{1}{2}$. Only three of the parameters used to describe each atom need be modified by this procedure. They are: $y' = 1.0 - y$, $B'_{12} = -B_{12}$, and $B'_{23} = -B_{23}$ ⁽⁷²⁾. The original molecule had the R configuration at the methine optic centre and the inverted molecule is denoted S according to the convention of Cahn, Ingold and Prelog⁽²⁹⁾.

(iii) The $\Delta f''$ terms for the chlorine and oxygen atoms were included in the calculations and parallel least-squares refinement performed.

(iv) Five reflections of high intensity and small scattering angle and for which F_o was significantly less than F_c were excluded from the refinement.

After each model had been refined through seven cycles using observational weights the following information was obtained:

<u>Model</u>	$R = \frac{\sum F_o - F_c }{\sum F_o }$	$R' = \left[\frac{\sum w (\Delta F)^2}{\sum w F_o^2} \right]^{\frac{1}{2}}$
R	5.57%	7.34%
S	5.76%	8.21%

During this refinement 308 parameters were varied using 1674 independent observations. The R factor ratios⁽⁷³⁾ R_{R1} and R_R are 1.119 and 1.034 for the weighted and unweighted reliability indices respectively. Interpolation on the tables of Hamilton⁽⁷³⁾ shows that these ratios are significant at the 99.5% confidence level and that the true absolute configuration is R. This finding is at variance with that previously reported on the basis of chemical arguments⁽³²⁾. No fault could be found with these chemical arguments but it was felt that original assignment on which they rested was not firmly based, and so it was decided to carry out more experimental work in the hope of clarifying the situation.

The original crystal used for the data collection was remounted on the diffractometer as it had been previously. Those reflections which satisfied the three criteria:

- (i) the reflection should not belong to any special reciprocal lattice zone, i.e., $h \neq 0$, $k \neq 0$ and $l \neq 0$. Only the $h0l$ zone is centrosymmetric here and cannot give useful information with regard to absolute configuration. Reflections from the $0kl$ and $hk0$ zones were excluded purely for convenience;
- (ii) the observed intensity should be great enough to permit statistically reliable measurement but not sufficiently large to necessitate concern over such effects as absorption, extinction and counter paralysis, i.e., $10.0 \leq F_0 \leq 40.0$ electrons; and
- (iii) the contribution of the chlorine atom to the overall structure factor should be large enough for the $\Delta f_{Cl}''$ term to be observable, i.e., $F_c(Cl) \geq 0.25 F_c(a11)$,

were recollected as were their Friedel pairs. The 106 $hk\ell/h\bar{k}\bar{\ell}$ pairs obtained on this basis were processed in the normal way. The goniostat settings for the two members of a pair differed only in ϕ and since the greatest and least correction factors for the various orientations available by ϕ rotation are 1.59 and 1.46 respectively, absorption corrections were not applied. Two cylinders of diameters 0.30 and 0.25 mm respectively were assumed in determining these figures by interpolation in a table of correction factors for absorption in a cylindrical specimen⁽⁷⁴⁾. This procedure would overestimate the difference between the correction factors.

Structure factors were calculated for these data using the "R" and "S" parameter sets as they stood before the above parallel refinement was performed. When the $\Delta f''$ terms for the chlorine and the oxygen atoms were included in the calculations, the "S" set of parameters was clearly identified as being correct. The agreement summary for these calculations is:

<u>Model</u>	<u>R</u>	<u>R'</u>
R	6.74%	9.13%
S	5.87%	8.05%

A tabulation of the observed and calculated structure amplitudes for the correct parameter set is given in Table 10 and shows that in all but three cases the observed and calculated $|F(k)| - |F(\bar{k})|$ differences agree with regard to sign.

Having thus established the correct chirality, it became possible to concentrate on only one parameter set. The intraion hydrogen-bonded

TABLE 10

Observed and calculated structure factor amplitudes
for the $hk\ell/hk\ell$ Friedel pairs used to determine the
absolute configuration of (+)-Chlorpheniramine maleate.

II	IKI	L	FO(K)	FO(-K)	FR(K)	OBS'D		CALC'D		CONTRA-DICTION
						F(K):F(-K)	F(K):F(-K)	F(K):F(-K)	F(K):F(-K)	
1	1	1	30.66	30.13	34.39	33.85	>	>		
-1	1	1	18.47	17.63	14.93	14.27	>	>		
2	1	1	11.91	12.26	11.75	12.27	<	<		
-2	1	1	26.87	25.73	25.34	24.65	>	>		
2	2	1	15.85	17.07	14.77	16.10	<	<		
-2	2	1	27.62	27.01	24.26	23.82	>	>		
3	2	1	16.60	17.34	17.07	17.88	<	<		
1	3	1	43.60	44.61	51.53	53.07	<	<		
-1	3	1	30.08	36.33	39.43	38.06	>	>		
-2	3	1	31.25	30.80	28.53	28.32	>	>		
2	3	1	16.36	15.80	15.95	15.57	>	>		
2	4	1	16.20	15.00	15.64	14.65	>	>		
-2	4	1	26.83	27.22	25.10	25.47	<	<		
-2	5	1	14.21	14.94	13.76	14.54	<	<		
1	6	1	15.55	15.84	14.03	14.34	<	<		
-1	6	1	22.58	22.05	21.14	20.84	>	>		
-2	6	1	16.36	16.86	16.33	16.63	<	<		
3	6	1	14.23	13.66	15.41	15.01	>	>		
-1	7	1	26.56	25.84	26.94	26.12	>	>		
-2	7	1	12.07	11.88	11.80	11.61	>	>		
-1	8	1	13.94	13.94	13.88	14.06	<	<		X
1	8	1	17.26	17.58	16.36	16.71	<	<		
2	8	1	26.20	25.07	24.59	23.55	>	>		
-2	8	1	15.58	16.02	14.88	15.45	<	<		
1	8	1	16.12	15.70	15.57	15.41	>	>		
-3	8	1	14.20	14.24	13.88	13.10	>	>		
1	9	1	20.00	20.21	20.44	20.68	<	<		
-1	9	1	19.26	19.82	19.35	19.60	<	<		
1	10	1	15.52	15.32	14.67	14.54	>	>		
-1	10	1	13.56	13.68	12.97	12.97	<	<		
2	10	1	15.44	15.64	15.43	15.84	<	<		
-2	10	1	17.14	16.45	16.07	15.57	>	>		
-3	10	1	4.32	9.91	10.24	10.77	<	<		
1	11	1	13.60	12.82	12.25	11.47	>	>		
-1	11	1	17.90	17.32	16.50	15.74	>	>		
1	11	1	11.00	11.50	11.09	12.14	<	<		
1	1	2	15.29	16.75	15.70	17.39	<	<		
2	1	2	16.27	15.94	15.51	15.40	>	>		
-2	1	2	31.14	31.89	32.52	33.50	<	<		
-3	1	2	14.39	13.46	13.66	12.84	>	>		
1	2	2	13.85	14.76	13.82	14.85	<	<		
-1	2	2	17.38	16.84	15.74	14.87	>	>		
-2	2	2	20.26	20.20	21.66	21.73	<	<		X
2	3	2	26.13	25.44	25.38	24.69	>	>		
-3	3	2	9.95	9.81	11.36	10.99	>	>		
1	4	2	10.57	11.72	9.45	10.80	<	<		
-1	4	2	9.09	10.83	10.76	12.44	<	<		
-2	4	2	17.81	16.70	16.94	15.85	>	>		
2	5	2	24.92	25.60	26.48	27.22	<	<		
-1	6	2	20.31	19.15	17.17	15.90	>	>		
-2	6	2	10.84	11.77	12.35	13.01	<	<		
1	7	2	19.01	18.20	18.64	17.83	>	>		
2	7	2	19.40	20.11	19.89	20.64	<	<		
-3	7	2	11.67	11.08	11.40	10.87	>	>		
2	9	2	16.78	15.58	16.51	15.56	>	>		
-2	9	2	10.53	11.20	11.23	11.95	<	<		
1	11	2	12.87	13.21	13.38	13.72	<	<		
3	11	2	9.64	9.69	10.49	10.62	<	<		
1	1	3	28.37	28.10	28.32	29.38	<	<		
-1	1	3	15.49	13.69	14.76	12.85	>	>		
-2	1	3	13.84	13.21	12.33	11.88	>	>		
1	2	3	17.53	17.88	17.99	18.19	<	<		
2	2	3	9.02	9.67	10.38	10.39	<	<		
3	2	3	15.12	14.54	15.74	15.16	>	>		
-3	2	3	21.90	21.65	21.00	20.79	>	>		
-1	3	3	28.88	28.53	29.97	29.73	>	>		
1	3	3	15.01	14.43	14.06	13.33	>	>		
-2	3	3	30.58	31.08	29.80	30.74	<	<		
3	3	3	9.56	9.95	10.39	10.73	<	<		
1	4	3	24.13	25.23	24.26	25.54	<	<		
2	4	3	16.53	16.06	16.29	16.13	>	>		
-3	4	3	14.17	14.00	13.51	13.45	>	>		
-1	5	3	9.49	10.52	10.50	11.61	<	<		
1	6	3	20.56	20.79	20.82	20.12	>	>		
-2	6	3	14.03	17.60	16.31	15.87	>	>		
-2	8	3	14.73	14.71	14.07	14.04	>	>		
-1	9	3	11.31	10.67	11.58	10.86	>	>		
-1	11	3	9.63	10.28	9.95	10.64	<	<		
1	1	4	14.21	13.15	14.08	13.02	>	>		
-1	2	4	10.51	10.75	11.06	12.25	<	<		
-2	1	4	12.32	11.94	11.16	10.84	>	>		
1	12	3	11.89	12.10	11.85	12.07	<	<		
2	10	3	17.71	17.52	18.39	18.24	<	<		
-1	4	4	16.53	15.86	18.14	17.59	<	<		
1	5	4	11.11	11.23	10.32	10.46	>	>		
-1	6	4	12.00	13.28	12.38	13.33	<	<		
-2	6	4	12.05	11.53	12.22	11.81	>	>		
1	7	4	16.52	17.34	17.15	17.91	<	<		
-1	8	4	16.85	16.68	17.65	17.40	>	>		
-2	8	4	11.58	11.43	11.48	11.38	>	>		
1	9	4	13.35	13.92	13.66	13.25	>	>		
2	11	4	12.10	12.42	13.13	13.45	<	<		
-1	1	5	31.92	31.56	31.64	31.29	>	>		
2	2	5	12.87	12.35	12.55	11.96	>	>		
-2	3	5	16.42	15.74	15.57	14.71	>	>		
1	4	5	9.57	9.79	10.35	10.56	<	<		
-2	2	6	12.71	13.10	12.86	13.32	<	<		
-2	4	6	9.52	9.26	10.36	10.08	>	>		
-1	6	6	9.86	10.08	10.71	11.09	<	<		
-1	4	7	6.56	6.69	6.86	6.98	<	<		
-1	5	7	7.70	7.76	8.14	8.27	<	<		
1	5	7	6.16	6.18	7.08	7.02	>	>		
-2	5	7	4.84	4.87	4.82	4.90	<	<		X
-2	2	8	6.14	5.85	6.79	6.53	>	>		
-3	2	8	5.78	5.94	6.23	6.39	<	<		
-1	3	9	3.99	3.91	4.25	4.16	>	>		

hydrogen atom was found to occur, in its expected position and at a peak height of $0.25 \text{ e}/\text{\AA}^3$, in a difference electron density map computed on the basis of the correct set of parameters at the termination of the parallel refinement. The next four least-squares cycles employed the contributions from all atoms, but the B_{iso} terms for the hydrogen atoms were invariant as was the y coordinate of the chlorine atom. Relaxation factors⁽⁵⁴⁾ of 0.7 were applied to the indicated parameter shifts for each of these cycles. Although the third and fourth cycles resulted in only small reductions in $\sum w\Delta^2$, the lack of convergence was indicated by the magnitude of the shifts, which varied between 1% and 75% of the associated estimated standard deviation, and by the almost perfect oscillation of the shifts. Convergence was forced by damping out these oscillations with two further cycles using relaxation factors of 0.5 and 0.4 for the first and second of these respectively. The final weighted and unweighted R factors over the 1674 included data were 6.64% and 5.02% respectively.

A listing of the observed and calculated structure amplitudes based on the final model is presented in Table 11. The positional and thermal parameters used to describe the final model are given in Tables 12, 13 and 14.

Results and Discussion

Those atomic parameters listed above were used with the independent atom method of Ahmed et al.⁽⁵¹⁾ in the derivation of molecular bond distances and angles. The distances and angles involving non-hydrogen atoms are shown in Figure 7 which also presents the numbering scheme and

TABLE 11

The observed and calculated structure factor amplitudes,
x 10, and the phase angles for (+)-Chlorpheniramine maleate.

TABLE 12

Atomic positional parameters ($\times 10^4$) for the
non-hydrogen atoms of (+)-Chlorpheniramine maleate.

Atom	x/a	y/b	z/c
C Σ	855(3)	5000(0)	2772(2)
C(1)	2561(9)	5639(3)	3765(5)
C(2)	4515(9)	5867(3)	3269(4)
C(3)	5829(7)	6374(2)	4031(4)
C(4)	5286(6)	6672(2)	5278(3)
C(5)	3301(6)	6427(2)	5735(4)
C(6)	1991(7)	5908(3)	4985(5)
C(7)	6818(5)	7220(2)	6120(4)
C(8)	7665(5)	7053(2)	7808(3)
C(9)	9432(6)	7549(2)	8661(4)
N(1)	10838(4)	7284(1)	10133(3)
C(10)	9339(6)	7063(2)	11156(4)
C(11)	12632(6)	7772(2)	10887(5)
C(1')	5559(6)	7878(2)	5858(4)
C(2')	6025(10)	8315(2)	4798(5)
C(3')	4802(15)	8901(3)	4565(6)
C(4')	3171(11)	9044(3)	5376(7)
C(5')	2843(11)	8591(3)	6436(10)
N(6')	4003(8)	8022(2)	6669(6)
O(1)	13788(4)	6330(1)	9640(3)
O(2)	10807(4)	5632(1)	8940(4)
O(3)	10289(4)	4441(1)	8735(5)
O(4)	12565(6)	3591(1)	8769(6)
Cm(1)	13011(5)	5770(1)	9293(3)
Cm(2)	14808(5)	5247(1)	9294(4)
Cm(3)	14525(5)	4599(2)	9148(5)
Cm(4)	12348(6)	4180(2)	8866(5)

TABLE 13
Anisotropic thermal parameters ($\times 10^4$)
used to describe the atoms of Table 12.

Atom	U_{11}^*	U_{22}	U_{33}	U_{12}	U_{23}	U_{13}
C ₁	641 (5)	564 (5)	496 (4)	-81 (4)	-131 (4)	-24 (4)
C (1)	430 (11)	394 (11)	316 (8)	47 (10)	-4 (8)	-28 (8)
C (2)	411 (11)	548 (16)	278 (8)	59 (11)	-56 (9)	90 (8)
C (3)	307 (8)	488 (13)	293 (8)	53 (9)	40 (9)	104 (6)
C (4)	242 (6)	360 (9)	278 (7)	41 (6)	57 (6)	75 (6)
C (5)	278 (7)	424 (11)	302 (7)	-7 (8)	-9 (8)	97 (6)
C (6)	296 (9)	496 (14)	344 (9)	-15 (9)	10 (9)	60 (7)
C (7)	235 (6)	349 (9)	313 (7)	26 (6)	71 (6)	101 (6)
C (8)	228 (6)	269 (7)	316 (7)	9 (5)	67 (6)	68 (5)
C (9)	237 (6)	236 (7)	379 (8)	1 (5)	67 (6)	97 (6)
N (1)	187 (4)	197 (5)	357 (6)	11 (4)	-11 (4)	68 (4)
C (10)	250 (6)	276 (7)	303 (7)	10 (6)	24 (6)	66 (5)
C (11)	235 (7)	251 (7)	493 (11)	-21 (6)	-47 (8)	30 (7)
C (1')	249 (6)	322 (8)	329 (8)	-23 (6)	102 (7)	55 (6)
C (2')	541 (15)	345 (11)	313 (8)	-76 (10)	59 (8)	119 (9)
C (3')	863 (28)	329 (11)	401 (13)	-42 (16)	152 (11)	88 (15)
C (4')	496 (16)	349 (12)	589 (17)	58 (11)	157 (12)	104 (13)
C (5')	438 (14)	356 (12)	923 (29)	126 (11)	224 (16)	288 (17)
N (6')	408 (10)	396 (11)	732 (16)	138 (9)	261 (11)	324 (11)
O (1)	277 (5)	206 (4)	385 (6)	5 (4)	-14 (4)	130 (4)
O (2)	208 (4)	258 (5)	753 (12)	33 (4)	-15 (7)	99 (6)
O (3)	218 (5)	267 (6)	817 (13)	-36 (5)	-84 (7)	136 (6)
O (4)	356 (8)	229 (5)	972 (18)	-14 (6)	-17 (8)	236 (10)
Cm (1)	224 (6)	215 (6)	332 (7)	5 (5)	3 (5)	107 (5)
Cm (2)	181 (5)	229 (6)	431 (9)	-5 (5)	-33 (6)	103 (6)
Cm (3)	203 (6)	247 (7)	470 (10)	26 (5)	-29 (7)	116 (6)
Cm (4)	262 (7)	211 (6)	478 (11)	-9 (5)	-19 (7)	137 (7)

* These coefficients are defined on page 24.

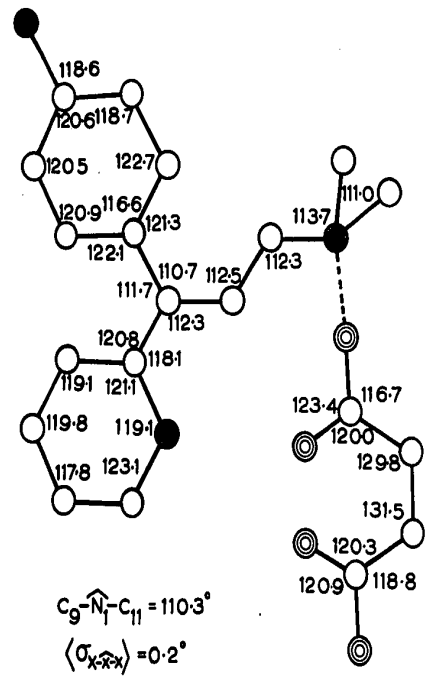
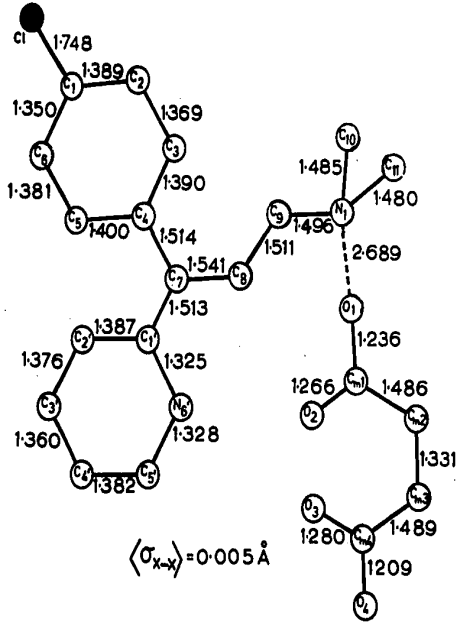
TABLE 14

Atomic parameters ($\times 10^3$) for the hydrogen atoms of (+)-Chlorpheniramine maleate.

Atom	x/a	y/b	z/c	U_{iso}
H(1)	1127(5)	706(2)	1000(3)	43
H(2)	469(8)	559(2)	263(5)	82
H(3)	700(7)	652(2)	370(4)	73
H(5)	309(6)	657(2)	659(4)	60
H(6)	90(7)	581(2)	532(4)	74
H(7)	821(6)	728(2)	558(4)	58
H(81)	643(5)	700(2)	823(3)	48
H(82)	794(5)	668(1)	795(3)	48
H(91)	1053(6)	762(2)	790(3)	56
H(92)	864(6)	795(2)	890(3)	56
H(111)	1338(6)	792(2)	1001(4)	64
H(112)	1334(7)	766(2)	1180(4)	64
H(113)	1174(6)	819(2)	1115(4)	64
H(101)	840(6)	667(2)	1062(4)	59
H(102)	866(6)	741(2)	1167(4)	59
H(103)	1042(6)	698(2)	1197(4)	59
H(2')	692(7)	812(2)	413(4)	75
H(3')	532(6)	926(2)	387(4)	64
H(4')	248(6)	948(2)	528(4)	64
H(5')	146(6)	873(2)	712(4)	64
Hm(1)	1034(6)	486(2)	857(3)	57
Hm(2)	1640(6)	538(2)	966(3)	54
Hm(3)	1582(7)	429(2)	916(4)	74

FIGURE 7

Bond distances and angles for the non-hydrogen atoms
of (+)-Chlorpheniramine maleate.



the atomic coding used in this work. Comparable molecular parameters for the hydrogen atoms are to be found in Table 15. Using X to denote a carbon, nitrogen or oxygen atom, then the e.s.d.'s in the distances C-X, X-X and H-X average 0.005, 0.005 and 0.03 \AA respectively. Error estimates for the angles C-X-X, X-X-X, X-X-H, H-X-H and X-H-X average 0.3, 0.4, 3.0, 3.0 and 3.7 $^\circ$ respectively.

In keeping with the procedure adopted for d,l-Brompheniramine maleate, only the structure of the protonated (+)-Chlorpheniramine entity will be discussed in this section.

Other authors have shown that the chlorine-aromatic carbon bond distance has a preferred magnitude of 1.737(16) \AA in cases where the halogen atom is univalent^(75,76,77). The value of 1.748(5) \AA obtained for the present compound is insignificantly different from this expected value and supports the conclusions in the above citations that Sutton's 1.70(1) \AA is an underestimate.

The phenyl ring of this compound is planar, $\chi^2 = 8.8$, with no member of this grouping displaced more than 0.01 \AA from the plane with equation $-0.4624x + 0.6535y - 0.5992z - 5.1817 = 0$. The ring, however, does exhibit several distortions from ideality; of the six intra-ring C...C bonds, three are within 0.005 \AA of 1.394 \AA and a fourth is within 3σ of this accepted value⁽⁵⁵⁾. However, the C(1)-C(6) and C(2)-C(3) bonds are both abnormally short, being 1.350(5) and 1.369(5) \AA respectively. An inspection of the thermal vibration ellipsoids of the atoms C(2), C(3) and C(6) reveals that the principal axes of vibration are not perpendicular to the plane of the benzene ring (see Figure 8) as would be expected for this rigid body. In situations where the major compon-

TABLE 15

Distances and angles involving the hydrogen atoms
of (+)-Chlorpheniramine maleate.

(a) Distances*

C(2)-H(2)	0.83Å	C(9)-H(92)	0.99Å
C(3)-H(3)	0.86	N(1)-H(1)	0.55
C(5)-H(5)	0.87	C(10)-H(101)	1.02
C(6)-H(6)	0.79	C(10)-H(102)	0.98
C(2')-H(2')	0.98	C(10)-H(103)	0.87
C(3')-H(3')	1.06	C(11)-H(111)	1.04
C(4')-H(4')	0.97	C(12)-H(112)	0.86
C(5')-H(5')	1.16	C(12)-H(113)	1.05
C(7)-H(7)	1.05	Cm(2)-Hm(2)	0.94
C(8)-H(8')	0.90	Cm(3)-Hm(3)	0.97
C(8)-H(82)	0.78	O(3)-Hm	0.87
C(9)-H(91)	1.06		

(b) Angles*

(i) The p-chlorophenyl system

C(1)-C(2)-H(2)	104°
C(3)-C(2)-H(2)	136
C(2)-C(3)-H(3)	118
C(4)-C(3)-H(3)	119
C(4)-C(5)-H(5)	117
C(6)-C(5)-H(5)	122
C(5)-C(6)-H(6)	114
C(1)-C(6)-H(6)	126

(ii) The pyridyl system

C(1')-C(2')-H(2')	114°
C(3')-C(2')-H(2')	126
C(2')-C(3')-H(3')	119
C(4')-C(3')-H(3')	121
C(3')-C(4')-H(4')	118
C(5')-C(4')-H(4')	124
C(4')-C(5')-H(5')	116
N(6')-C(5')-H(5')	121

Continued.....

Table 15 (Continued)

(iii) The aliphatic portion			
C(4)-C(7)-H(7)	106°	C(10)-N(1)-H(1)	104°
C(1')-C(7)-H(7)	103	C(11)-N(1)-H(1)	111
C(8)-C(7)-H(7)	114	N(1)-C(10)-H(101)	105
C(7)-C(8)-H(81)	112	N(1)-C(10)-H(102)	116
C(7)-C(8)-H(82)	113	N(1)-C(10)-H(103)	101
C(9)-C(8)-H(81)	114	H(101)-C(10)-H(102)	124
C(9)-C(8)-H(82)	118	H(101)-C(10)-H(103)	117
H(81)-C(8)-H(82)	85	H(102)-C(10)-H(103)	91
C(8)-C(9)-H(91)	100	N(1)-C(11)-H(111)	102
C(8)-C(9)-H(92)	112	N(1)-C(11)-H(112)	113
N(1)-C(9)-H(91)	111	N(1)-C(11)-H(113)	109
N(1)-C(9)-H(92)	106	H(111)-C(11)-H(112)	129
H(91)-C(9)-H(92)	115	H(111)-C(11)-H(113)	105
C(9)-N(1)-H(1)	106	H(112)-C(11)-H(113)	150

(iv) The maleate ion

O(2)-Hm-O(3)	159°
Cm(1)-Cm(2)-Hm(2)	115
Cm(3)-Cm(2)-Hm(2)	114
Cm(2)-Cm(3)-Hm(3)	124
Cm(4)-Cm(3)-Hm(3)	104

* Standard deviations average
0.03Å for these distances and
3.0° for the angles.

ent of the atomic vibration is not aligned with the direction of least constraint (usually perpendicular to the bond directions), it is probable that the atom is not being described in a meaningful way. Such poor descriptions can arise from the refinement of a structure using data containing uncorrected errors such as those of extinction and/or absorption⁽⁷⁸⁾. As mentioned above on page 50, serious errors arising from secondary extinction effects were largely eliminated by excluding five reflections of high intensity and small scattering angle from the final stages of the refinement.

Making the reasonable approximation that the crystalline specimen used was a cylinder with mean radius 0.14 mm, the value of μr is seen to be 0.26. For this crystalline shape and value of μr the absorption correction factor which must be applied is essentially invariant with scattering angle, being 1.55 and 1.52 at $\theta = 0^\circ$ and 60° respectively⁽⁷⁴⁾. This calculation is only valid, however, if the cylindrical axis remains perpendicular to the scattering vector, a situation which is achieved only in zero layer rotation or Weissenberg photography and on the diffractometer at $\chi = 0^\circ$. Since χ varied over a large range during the data collection, and because the length of the cylindrical crystal was approximately twice its diameter, the implication is that the effects of absorption may be a significant contributor to inaccuracies in the final model.

Another, little recognised, area where an inaccurate description of a structure may arise is in the refinement process. Srinivasan has shown that very large correlations are to be expected when non-centrosymmetric structures containing centrosymmetric atomic groupings are

refined using least-squares techniques⁽⁷⁹⁾ and that the neglect of these terms in a block-diagonal situation is not warranted. An example where refinement of the same structure using both full-matrix and block-diagonal procedures led to differences of up to 0.097\AA in atomic position has been provided by Parthasarathy, Sime and Speakman⁽⁸⁰⁾, thus illustrating that the block-diagonal approximation can lead to serious discrepancies between the "true" structure and the final model.

In the present case, there are two important centrosymmetric groupings, viz. the phenyl and pyridyl rings, both of which surround the real-space 2_1 screw axis at $\frac{1}{2}\cdot y \cdot \frac{1}{2}$ (refer to Figure 6). In light of the above comments, it may be expected that the existence of these features would present some problems in the refinement and perhaps lead to a final model which, in so far as the phenyl and pyridyl rings are concerned, may not be correct. Rae and Maslen have shown that neither full-matrix least-squares nor Fourier refinement procedures can be expected to alleviate these problems⁽⁸¹⁾ and so we must accept the present structure with its limitations on the accuracy of the two rings.

The fact that the deviations from ideality are not gross may be taken as evidence that neither one of these groupings dominates the scattering to an extent that would make the above effect important enough to force complete failure of the block-diagonal least-squares refinement. It may be, however, that at least part of the reason for the initial failure of the absolute configuration assignment may be ascribed to this cause, and so this example could possibly serve as another "cautionary tale" of block-diagonal refinement in acentric space groups.

The good planarity of the pyridyl ring is indicated by the χ^2 value of 11.3 and by the fact that the maximum exoplanar displacement of a ring atom is 0.01Å from the plane with equation $-0.5736x - 0.4311y - 0.6955z + 11.6439 = 0$.

One view of the molecule which indicates that the benzyl and pyridyl rings adopt a similar conformation to those in d&l-Brompheniramine is given in the stereoscopic Figure 8. The dihedral angle between these two planes is 113.6° and the torsion angles C(6)-C(4)-C(7)-C(8) and N(6')-C(1')-C(7)-C(8) are 53.7° and -43.4° respectively. It will be noticed that although these angles are similar in magnitude to those of the previous structure they are opposite in sign. This is because the two molecules under consideration have opposite absolute configurations.

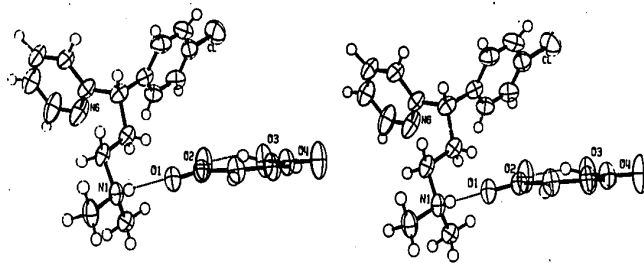


FIGURE 8

A stereo pair of the (+)-Chlorpheniramine maleate complex. The correct S absolute configuration is shown. The two upper carbon atoms of the benzene ring are C(2) and C(3).

The bond distances and interbond angles for the alkylamine chain of (+)-Chlorpheniramine maleate are not significantly different from those obtained for d,l-Brompheniramine maleate. In both cases the C-C-C angles at C(8) and C(9) are significantly greater than the tetrahedral value of 109.5° , and the C(8)-C(9) bonds are shorter than the 1.54\AA expected here. One obvious explanation for these results would be in terms of partial double bond character for the C(8)-C(9) bond. However, because all of C(7), C(8), C(9) and N(1) have four substituents, it is difficult to justify the invocation of this explanation. The opening of the bond angles at C(8) and C(9) would tend to increase the C(7)-N(1) separation, whereas the bond shortening would decrease this distance. Because of these facts, and also because the fully extended alkylamine chains are not subjected to any apparent end-on forces, these observations must have their genesis in some electronic effect which is not understood at this time.

The alkylamine chain is again oriented unsymmetrically with respect to the two aromatic rings (refer to Figure 8). In this case, however, it is the 2-pyridyl ring which is partially obstructed by the dissymmetry and the p-chlorophenyl ring is exposed. In the previous structure, nitrogen atom N(1) was found to be 6.212\AA from the centroid of the exposed pyridyl ring and 5.568\AA from the centroid of the phenyl system. In the present case, the alkylamine basic centre is 6.154\AA from the centroid of the exposed ring (p-chlorophenyl) and 5.402\AA from the occluded 2-pyridyl moiety. The similarity of these numbers is striking, and if the identity of the aryl systems is ignored, Figures

4 and 9 reveal that d,l-Brompheniramine maleate and (+)-Chlorpheniramine maleate adopt very similar solid state conformations; this point will be discussed further in a later section.

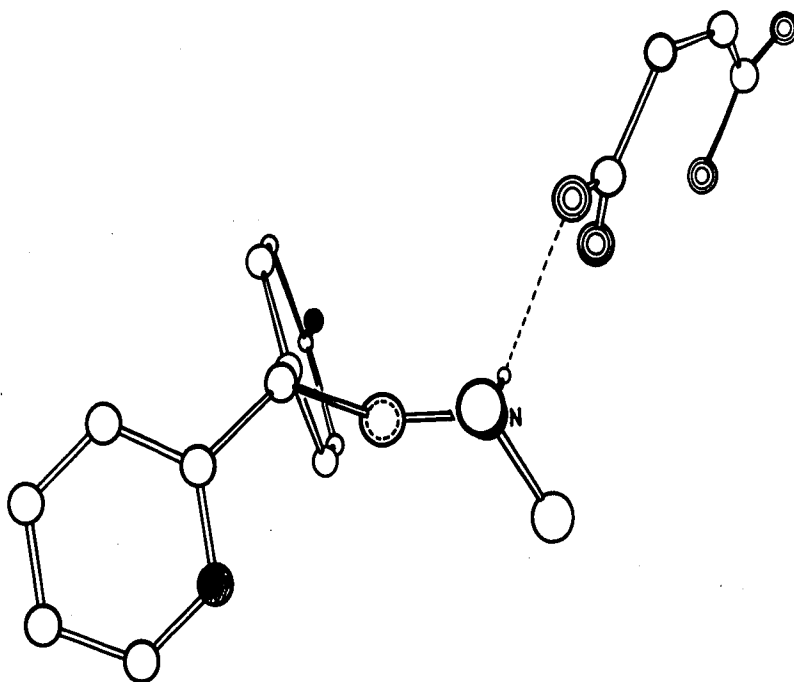


FIGURE 9

A drawing of the (+)-Chlorpheniramine maleate structure viewed down the C(9)-C(8) bond direction. The atomic coding is consistent with that of Figure 4 (page 41).

It may be thought that the presence of the aromatic rings around a 2_1 screw axis would imply that π electron overlap between symmetry related molecules might be a significant binding force which stabil-

ises the solid state structure. That the plane of the phenyl ring of one molecule is approximately parallel to the plane of the pyridyl ring of a symmetry related molecule is evident from a study of the stereoscopic packing diagram presented as Figure 10. The closest

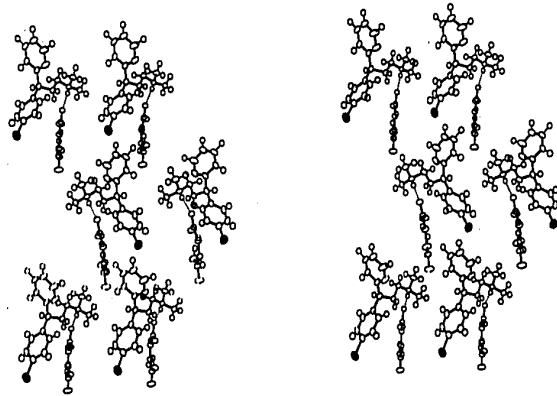


FIGURE 10

A stereoscopic packing diagram of several (+)-Chlorpheniramine maleate molecules viewed parallel to a^* .

approach of non-hydrogen atoms is 4.010\AA between C(1) of the p-chlorophenyl ring and C(4') of the pyridyl ring in another molecule. The chlorine atom is separated by 4.190\AA from the centroid of the aromatic base's π electron system. These distances are both significantly greater than the appropriate Van der Waals radius sums, and

so no specific interactions can be said to occur.

The maleate mono-anion is involved in two interactions which contribute to the stability of the solid. The first of these is

the hydrogen bond between N(1) and O(1). The distance N(1)-O(1) is 2.689(3)Å, angle N(1)-H(1)····O(1) is 164(4)°, and the bond angle at the acceptor atom is 117.0(8)°. The second bonding force is between oxygen O(4) and the "umbrella" of CH₂ and CH₃ groups bonded to N(1) which sits over this oxygen. The carbon-oxygen distances involved are 3.55, 3.30 and 3.51Å respectively for C(9), C(10) and C(11). The chain of polar and Van der Waals type bonding forces which runs up the b axis is illustrated in Figure 11.

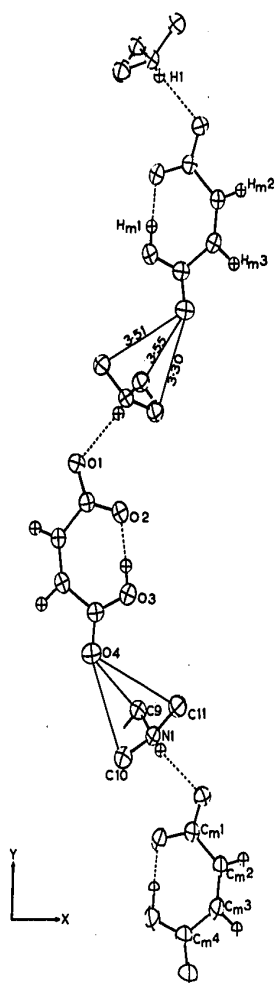


FIGURE 11

The chain of polar and non-polar bonding interactions involving the maleate ion.

* * * * *

The (+)-Chlorpheniramine maleate sample used in this work was kindly supplied by Dr. J.G. Topliss of the Schering Corporation, Bloomfield, New Jersey, U.S.A.

1.4 TRIPROLIDINE HYDROCHLORIDE MONOHYDRATE

Experimental

A crystalline sample of this compound was supplied by Dr. A.F. Casy of the Faculty of Pharmacy at this University. The specimen originated from Burroughs Wellcome and Company (Canada) Ltd., and was from the batch with analysis number 31104. Recrystallization was achieved by cooling a warm solution of the compound in anisole. The space group and initial measurements of the lattice parameters were determined photographically and the crystal then aligned on the diffractometer in the manner appropriate for a monoclinic lattice mounted down a non-unique axis. The refined cell parameters and some other physical data are given in Table 16.

During the preliminary photography it was observed that the tendency of these crystals to become rose-coloured on standing in air was greatly enhanced by X-irradiation. To minimise the effects of any attendant decomposition due to the X-rays, the total exposure time was kept as short as possible by:

- (i) Choosing the fastest $\theta/2\theta$ scan speed available, i.e., $2^\circ/\text{min}$ in 2θ .
- (ii) Decreasing the basic scan width to barely accommodate the reflections. This width was 1.3° in 2θ and was modified as a function of θ to cope with the dispersion of the $\text{Cu } K_\alpha$ doublet⁽⁴²⁾.
- (iii) The fixed position background counts on either side of the reflection were taken for 4 seconds each.
- (iv) Firstly measuring those reflections with $2\theta \leq 100^\circ$ and then

TABLE 16

Some physical constants and other quantities
relating to Triprolidine hydrochloride mono-
hydrate.

formula	$C_{19}H_{25}ClN_2O$
molecular weight	332.88 Daltons
M.P. (Thomas Hoover, uncorrected)	112-115°C
M.P. (lit.) ⁽⁸²⁾	116-118°C
space group	$P2_1/c$
a	14.777(2) Å
b	9.5785(8) Å
c	13.099(1) Å
cos β	-0.0082(2)
β	90.48(2)°
V	1854.02 Å ³
Z	4
ρ_{obs} (Dioxane/Bromobenzene)	1.202(4) gm/cm ³
ρ_{calc}	1.192 gm/cm ³
$\bar{\mu}$ (Cu K α)	16.68 cm ⁻¹
crystal size	0.20 x 0.25 x 0.30 mm
2 θ range explored	4°-129°
no. unique reflections	3123
no. observed reflections	2516 (80% of total)
no. variable parameters	282
ratio observations/parameters	8.92
final unweighted R	5.06%
final weighted R	7.69%
mean sigma in C-C bond	0.003 Å
mean sigma in C-C-C angle	0.2°

examining the region of reciprocal space with $100 \leq 2\theta \leq 129^\circ$.

As well as these stratagems, the amount of radiation falling on the crystal was diminished by using an incident beam graphite monochromator.

Despite the colouration of the crystal, which became progressively more severe as the intensity collection proceeded, the monitor reflections had shown only insignificant intensity changes at the end of the low θ data set and were still 98% of their original value at the end of the entire data collection. Of the 1911 reflections measured in the first part, 1716 (89%) satisfied the observed/unobserved criteria that the net counts should not be less than the smaller of 95 counts or 60% of the total background for that reflection. These selection parameters correspond to a limiting fractional error in the net intensity of approximately 0.33. In a similar manner 2516 (80%) of the 3123 reciprocal lattice points comprising the full set were considered observed.

The Lorentz and polarization corrections as appropriate to the normal-beam-equatorial geometry of the FACS-1 system with partially polarized incident X-radiation were applied⁽⁴³⁾. During this data reduction process, minor intensity variations in the data were accommodated by applying a reflection number dependent scale factor. This scale factor was derived from the periodic measurements of three monitor reflections according to the procedure of Ahmed et al.⁽⁸³⁾. Observational weights were calculated according to the procedure given above (page 19) and stored with each reflection.

Structure solution was achieved without difficulty by means of the

Patterson synthesis, and a program⁽⁸⁴⁾ written to apply the symmetry minimum technique of Simpson et al.⁽⁶⁹⁾. Refinement of the initial model by difference Fourier and least-squares methods resulted in weighted (observational weights) and unweighted R factors of 7.38% and 4.67% respectively for the observed reflections of the low θ data set. These discrepancy indices have the values 7.69% and 5.06% for the 2516 observed data of the complete set. During the least-squares part of this refinement the temperature parameters for the hydrogen atoms were held constant at the final isotropic value of the heavy atom to which they were bonded. Scattering factor tables for the non-hydrogen atoms were derived from the analytical coefficients of Cromer and Mann⁽⁴⁵⁾, and were corrected for the effects of anomalous dispersion by the terms $\Delta f'_O = 0.055$, $\Delta f'_N = 0.036$, $\Delta f'_C = 0.021$, $\Delta f'_{Cl} = 0.375$ and $\Delta f''_{Cl} = 0.685$ ⁽⁵⁰⁾. The hydrogen atom curve used was that of Stewart, Davidson and Simpson⁽⁷⁰⁾.

Experience with other compounds, in both centric and non-centric space groups, had shown that the indiscriminate use of the relaxation factor series of Hodgson and Rollet⁽⁵⁴⁾ can lead to divergence of the refinement when used with the single-atom-block block-diagonal procedure. In particular, and independent of the stage of the refinement, the use of relaxation factors greater than unity is correlated with large increases in $\Sigma w\Delta^2$. Continued use of the method does not, in this author's experience, result in a lowering of $\Sigma w\Delta^2$ sufficient to overcome the increase previously induced. To obviate this difficulty, relaxation factors greater than unity were replaced by 0.7, and to remove terminal oscillations in the model the final four cycles were

calculated using shift multipliers of 0.5, 0.6, 0.8 and 0.5 respectively.

The set of atomic parameters and their e.s.d's obtained from the final least-squares cycle using the complete data set are contained in Tables 17, 18 and 19. The observed structure amplitudes and the structure factors calculated from the final model are listed in Table 20.

Results and Discussion

The positional parameters for the atoms of this structure were used to calculate the interatomic bond distances and interbond angles. These molecular parameters for the non-hydrogen atoms are displayed, together with the numbering scheme and the atomic coding, in Figure 12. Distances and angles involving the hydrogen atoms are to be found in Table 21. Using X as before to denote a C, N or O atom, the e.s.d's in the distances C-X, X-X and H-X average 0.003, 0.003 and 0.03Å respectively. The angles X-X-X, H-X-X, C-H-X and H-X-H have average error estimates of 0.2, 1.6, 2.3 and 2.5° respectively. The same method as was used previously (page 33) was adopted for the calculation of the e.s.d's.

Bond distances within the benzene ring average 1.384Å and the four C...C bonds of the pyridyl ring average 1.378Å, the associate error estimates being 0.011Å in each case. For deriving these e.s.d's the formula given below for the error estimate in a simple average was used because it was felt that this method yielded realistic estimates of these e.s.d's:

$$\sigma_{\bar{x}} = \sqrt{\frac{(\bar{x} - x_i)^2}{n - 1}}$$

The values of 0.0012 and 0.0015Å for the error estimate in these averages,

TABLE 17

Positional parameters ($\times 10^4$) for the non-hydrogen atoms of Triprolidine hydrochloride monohydrate.

Atom	x/a	y/b	z/c
C(1)	8588(1)	921(1)	-702(1)
O(1)	9295(2)	-1451(3)	910(2)
N(10)	8699(1)	2169(2)	1476(2)
C(7)	6549(2)	559(3)	2359(2)
C(8)	7222(2)	1069(3)	1799(2)
C(9)	8186(2)	1201(3)	2140(2)
C(11)	8350(2)	3630(3)	1447(3)
C(12)	9128(3)	4461(4)	1181(4)
C(13)	9953(2)	3675(4)	1315(3)
C(14)	9682(2)	2287(3)	1749(2)
C(1')	5623(2)	480(3)	1923(2)
N(2')	5397(1)	1443(2)	1217(2)
C(3')	4581(2)	1343(3)	794(2)
C(4')	3957(2)	344(3)	1014(2)
C(5')	4190(2)	-641(3)	1742(3)
C(6')	5024(2)	-572(3)	2201(2)
C(1)	6703(2)	7(3)	3412(2)
C(2)	7330(2)	-1030(3)	3610(2)
C(3)	7438(2)	-1580(3)	4580(2)
C(4)	6930(2)	-1119(3)	5382(2)
C(5)	6305(2)	-48(3)	5198(2)
C(6)	6197(2)	480(3)	4233(2)
C(15)	7016(2)	-1778(4)	6415(3)

TABLE 18

Thermal parameters ($\times 10^4$) describing the atomic vibration of the atoms in Table 17.

Atom	U_{11}^*	U_{22}	U_{33}	U_{12}	U_{23}	U_{13}
C(1)	351 (3)	619 (4)	241 (2)	6 (2)	-44 (2)	-21 (2)
O (1)	446 (9)	477 (9)	527 (10)	-63 (7)	45 (8)	55 (7)
N (10)	188 (5)	247 (6)	187 (5)	-6 (4)	16 (4)	9 (4)
C (7)	196 (6)	178 (6)	194 (7)	22 (5)	-1 (5)	11 (5)
C (8)	206 (7)	256 (7)	192 (7)	0 (6)	35 (6)	0 (5)
C (9)	207 (7)	313 (8)	212 (8)	-27 (6)	53 (6)	10 (6)
C (11)	258 (8)	275 (8)	377 (10)	15 (7)	41 (7)	-27 (7)
C (12)	332 (11)	338 (12)	932 (24)	-67 (9)	244 (13)	-36 (13)
C (13)	236 (8)	377 (11)	501 (13)	-86 (8)	54 (10)	0 (8)
C (14)	189 (7)	310 (9)	268 (8)	-8 (6)	0 (7)	-7 (6)
C (1')	190 (6)	181 (6)	192 (7)	23 (5)	-13 (5)	17 (5)
N (2')	215 (6)	248 (6)	227 (6)	29 (5)	14 (5)	-10 (5)
C (3')	236 (7)	285 (8)	271 (8)	56 (6)	25 (7)	-25 (6)
C (4')	219 (7)	336 (10)	293 (9)	39 (6)	-71 (7)	-22 (6)
C (5')	227 (8)	266 (8)	344 (10)	-35 (6)	-64 (7)	38 (7)
C (6')	215 (7)	240 (7)	247 (8)	-9 (6)	6 (6)	15 (6)
C (1)	178 (6)	197 (6)	194 (7)	-10 (5)	7 (5)	5 (5)
C (2)	204 (7)	213 (7)	223 (7)	2 (5)	-4 (6)	16 (6)
C (3)	226 (7)	217 (7)	237 (7)	-3 (6)	37 (6)	-38 (6)
C (4)	266 (8)	246 (8)	192 (7)	-67 (6)	33 (6)	-16 (6)
C (5)	244 (7)	279 (8)	207 (7)	-38 (6)	-12 (6)	35 (6)
C (6)	212 (7)	234 (7)	232 (7)	24 (6)	8 (6)	16 (6)
C (15)	363 (10)	393 (10)	278 (9)	-92 (8)	73 (8)	-45 (8)

* These coefficients are defined on page 24.

TABLE 19

Positional and isotropic vibration parameters ($\times 10^3$) for
the hydrogen atoms of Triprolidine hydrochloride monohydrate.

Atom	x/a	y/b	z/c	U_{iso}
H(10)	868(2)	185(3)	91(2)	48
H(8)	706(2)	144(2)	109(2)	46
H(3')	448(2)	198(3)	33(2)	64
H(4')	334(2)	34(3)	66(2)	64
H(5')	377(2)	-137(3)	189(2)	59
H(6')	521(2)	-123(3)	266(2)	57
H(2)	767(2)	-133(3)	315(2)	61
H(3)	787(2)	-234(3)	463(2)	61
H(5)	587(2)	30(3)	568(2)	66
H(6)	580(2)	108(2)	416(2)	42
H(91)	848(2)	31(3)	205(2)	66
H(92)	819(2)	163(3)	278(2)	49
H(111)	818(2)	382(3)	218(2)	84
H(112)	787(2)	367(3)	99(2)	67
H(121)	908(2)	536(3)	128(2)	91
H(122)	905(2)	478(4)	61(3)	102
H(131)	1043(2)	363(4)	81(3)	114
H(132)	1043(2)	402(3)	167(2)	81
H(141)	974(2)	229(3)	246(2)	72
H(142)	997(2)	146(3)	149(2)	66
H(151)	714(2)	-110(3)	688(2)	80
H(152)	754(2)	-186(3)	656(2)	62
H(153)	650(2)	-218(3)	662(2)	90
WH(1)	903(2)	-95(3)	38(2)	75
WH(2)	-1(2)	-129(4)	80(3)	106

TABLE 20

The observed structure amplitudes and calculated structure factors based on the final model for Triprolidine hydrochloride monohydrate. Excluded reflections are marked with an asterisk. These amplitudes have been scaled by a factor of 10.0.

A large grid of data, likely a table with columns and rows containing alphanumeric characters and numbers, possibly representing a catalog or index of items.

Continued.....

FIGURE 12

Bond distances and angles for the non-hydrogen atoms of Triprolidine hydrochloride monohydrate.

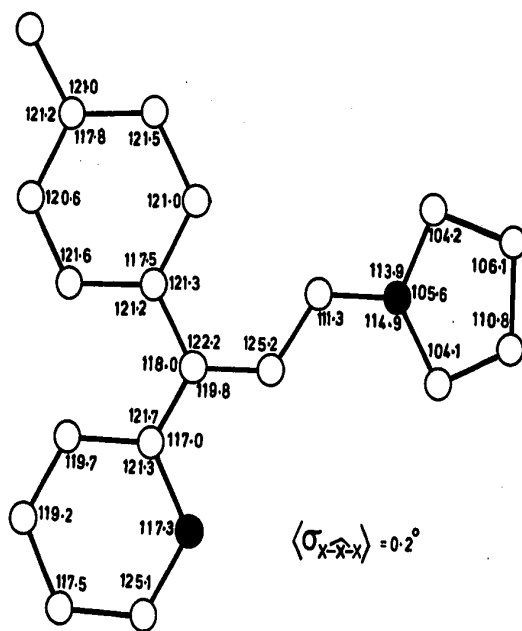
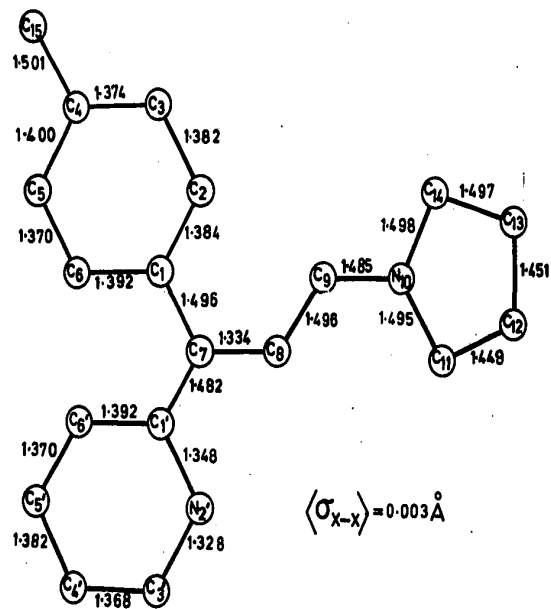


TABLE 21

A listing of the bond distances and angles involving the hydrogen atoms of Triprolidine hydrochloride monohydrate.

(a) Distances*

O(1)-WH(1)	0.89Å	C(8)-H(8)	1.00Å
O(2)-WH(2)	1.04	C(9)-H(91)	0.99
C(2)-H(2)	0.84	C(9)-H(92)	0.95
C(3)-H(3)	0.95	N(10)-H(10)	0.82
C(5)-H(5)	0.95	C(11)-H(111)	0.96
C(6)-H(6)	0.86	C(11)-H(112)	0.93
C(3')-H(3')	0.84	C(12)-H(121)	0.91
C(4')-H(4')	0.98	C(12)-H(122)	0.70
C(5')-H(5')	0.96	C(13)-H(131)	0.97
C(6')-H(6')	0.88	C(13)-H(132)	0.93
C(15)-H(151)	0.91	C(14)-H(141)	0.86
C(15)-H(152)	0.82	C(14)-H(142)	0.94
C(15)-H(153)	0.92		

(b) Angles*

(i) The p-tolyl system

C(1)-C(2)-H(2)	119.6°
C(3)-C(2)-H(2)	119.4
C(2)-C(3)-H(3)	112.6
C(4)-C(3)-H(3)	125.7
C(4)-C(5)-H(5)	125.4
C(6)-C(5)-H(5)	113.5
C(5)-C(6)-H(6)	121.7
C(1)-C(6)-H(6)	116.6
C(4)-C(15)-H(151)	108.4
C(4)-C(15)-H(152)	111.5
C(4)-C(15)-H(153)	114.8
H(151)-C(15)-H(152)	76.8
H(153)-C(15)-H(152)	129.9
H(151)-C(15)-H(153)	105.2

(ii) The pyridyl system

N(2')-C(3')-H(3')	125.1°
C(4')-C(3')-H(3')	113.9
C(3')-C(4')-H(4')	122.5
C(5')-C(4')-H(4')	120.1
C(4')-C(5')-H(5')	118.5
C(6')-C(5')-H(5')	122.3
C(5')-C(6')-H(6')	120.6
C(1')-C(6')-H(6')	119.5

Continued.....

Table 21 (Continued)

(iii) The aliphatic portion			
C(7)-C(8)-H(8)	117.2°	C(13)-C(12)-H(121)	124.3°
C(9)-C(8)-H(8)	117.5	C(11)-C(12)-H(122)	111.7
C(8)-C(9)-H(91)	108.8	C(13)-C(12)-H(122)	117.7
N(10)-C(9)-H(91)	104.1	H(121)-C(12)-H(122)	67.4
C(8)-C(9)-H(92)	107.3	C(12)-C(13)-H(131)	117.8
N(10)-C(9)-H(92)	105.2	C(14)-C(13)-H(131)	114.6
C(9)-N(10)-H(10)	105.5	C(12)-C(13)-H(131)	117.8
C(11)-N(10)-H(10)	108.5	C(14)-C(13)-H(132)	114.1
C(14)-N(10)-H(10)	109.6	H(131)-C(13)-H(132)	78.8
N(10)-C(11)-H(111)	104.6	N(10)-C(14)-H(141)	107.8
C(12)-C(11)-H(111)	109.6	C(13)-C(14)-H(141)	112.2
N(10)-C(11)-H(112)	108.5	N(10)-C(14)-H(142)	106.1
C(12)-C(11)-H(112)	112.5	C(13)-C(14)-H(142)	116.6
H(111)-C(11)-H(112)	116.4	H(141)-C(14)-H(142)	109.3
C(11)-C(12)-H(121)	117.8		

(iv) The water molecule

WH(1)-O(1)-WH(2) 105°

* Estimated standard deviations average 0.03Å for the distances and, except for H-X-H, 1.6° for the angles. For H-X-H the error estimates average 2.5°.

obtained from the formula of Sutton⁽⁵⁵⁾ are almost certainly spuriously low. Using these former standard deviations, it may be seen that no statistical significance can be attached to the apparent shortening of these C-C bonds. Bond angles and distances for the 2-pyridyl ring are contained in Table 8 (entry #3) and may be seen to conform to the generalisations derived from this tabulation.

The phenyl and pyridyl rings are individually planar with χ^2 values of 41.8 and 3.9 respectively. The maximum deviation of a defining atom from the phenyl plane, equation $-0.6958x - 0.6892y - 0.2024z + 7.7804 = 0$, is 0.008\AA . In the case of the pyridyl ring, the maximum displacement is 0.003\AA and the plane is defined by the equation $0.3797x - 0.5862y - 0.7157z - 1.0727 = 0$. These two planes have an interplanar dihedral angle of 106.5° . Despite the similarity of this quantity with the interaryl dihedral angles in the previous two structures (103.6° and 113.6° for *dl*-Brompheniramine maleate and (+)-Chlorpheniramine maleate respectively), Figure 13, which is a projection of the structure down the C(9)-C(8) bond direction, shows that only the pyridyl ring in the present compound is similarly arranged with respect to the alkylamine chain. Torsion angles about the ring to double bond linkages are given by $N(2')-C(1')-C(7)-C(8) = 29.7^\circ$ and $C(2)-C(1)-C(7)-C(8) = 55.3$. In this case it will be noticed that these angles both have the same sign and the "butterfly wing" arrangement of aromatic rings observed for the Pheniramines is not evident here. This point will be discussed later.

The presence of a double bond between C(7) and C(8) forces coplanarity of the atoms C(1), C(1'), C(7), C(8), C(9) and H(8). A least-

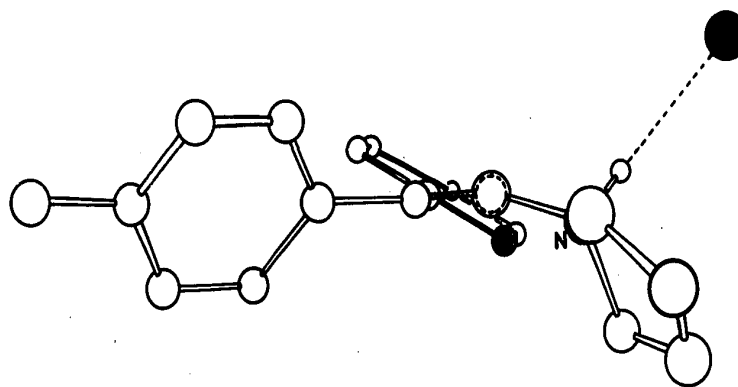


FIGURE 13

A view of the Triprolidine hydrochloride structure viewed in the C(9)-C(8) bond direction.

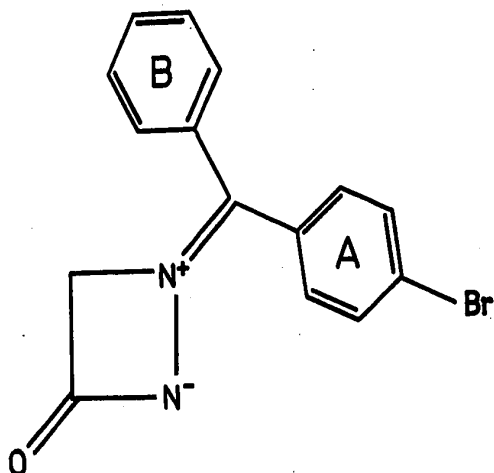
squares plane defined by the positions of these six atoms was determined to have equation $0.1913x - 0.9107y - 0.3661z - 0.2405 = 0$, $\chi^2 = 54.5$, and maximum displacement of a defining atom of 0.036\AA for H(8).

Of the two aromatic systems, the pyridyl ring is more nearly coplanar with the ethylenic system than is the p-tolyl function, the dihedral angles between the appropriate planes being 29.7° and 55.3° respectively. This finding is in agreement with the substance of those results obtained by Adamson et al. ⁽¹⁷⁾ and may have been predicted on steric grounds. The serious overcrowding involved in the close approaches of hydrogen atoms is evident when attempt is made to build a coplanar cis Ph/CH₂ ethylene system from CPK space filling models. The lack of an ortho hydrogen substituent on the 2-pyridyl moiety and the fact that the cis substituent to the aromatic base is hydrogen permits

this greater approach to coplanarity of the pyridyl and ethylenic systems. The fact that the coplanarity is not perfect is probably a result of steric interference between H(8) and the unshared electron pair on the heterocyclic nitrogen; evidence for this comment being derived from the 2.47(3)Å distance between the pyridyl nitrogen and H(8), and the fact that the closest approach expected on a Van der Waals radii basis is 2.7Å⁽⁶⁷⁾. It is possible that intermolecular base stacking interactions (see page 92) may be partially responsible for this 29.7° deviation from coplanarity, but it is felt that the above-mentioned effect is probably more important in this regard.

The two bond lengths C(7)-C(1) (1.496(3)Å) and C(7)-C(1') (1.482(3)Å) differ by 0.014Å, the distance from the ethylenic system to the more nearly coplanar pyridyl ring being the shorter of the two. That the 29.7° torsion angle about the C(8)-C(7)-C(1')-N(2') bond precludes extensive π electron overlap between these two systems is indicated by this small difference and the fact that the 1.334(3)Å bonding distance between C(7) and C(8), is just that expected for an isolated C=C bond⁽⁵⁵⁾.

That significant shortening of the bond joining an aromatic system to a coplanar exocyclic double bond is expected may be inferred from the crystal structure analysis of the compound illustrated below⁽⁸⁵⁾. The dihedral angle between ring A and that of the methylene-oxoazetidinium system is 6° and the linkage between these two units is 1.45Å long. Comparable figures for ring B are 89.5° and 1.51Å respectively.



(XVII) α -1-(p-bromophenyl)phenylmethylen-3-oxo-1,2-diazetidinium inner salt

As with the previous two antihistaminic drugs studied here, the conformation about the C(8)-C(9) bond is trans. In the present case the N(10)-C(9)-C(8)-C(7) torsion angle is 162.5° (refer to Figure 13).

The tetrahydropyrrolidino structural feature as a whole is not planar, although the four carbon atoms do define a good plane with a χ^2 value of 32.5 and equation $-0.0575x - 0.3633y - 0.9299z + 3.7422 = 0$. The largest displacement of a defining atom is 0.02\AA from this plane, but nitrogen N(10) is 0.455\AA out of the plane. Although there are serious difficulties to be faced in defining a simple and widely applicable terminology for use in describing the conformation of cyclic systems, in this case it seems reasonable to adopt the "E" (envelope)⁽⁸⁶⁾ designation for this ring. An alternative description, although one that tends to obscure the essence of the conformation, may be given in

terms of the torsion angles about the five bonds of this system. These torsion angles are: $N(10)-C(11)-C(12)-C(13) = 16.1^\circ$, $C(11)-C(12)-C(13)-C(14) = 2.5^\circ$, $C(12)-C(13)-C(14)-N(10) = -20.1^\circ$, $C(13)-C(14)-N(10)-C(11) = 30.0^\circ$, and $C(14)-N(10)-C(11)-C(12) = -28.6^\circ$.

The centres of symmetry are again in this structure the loci of important intermolecular bonding interactions. Figure 14 portrays the immediate environment of those centres equivalent to that at the origin.

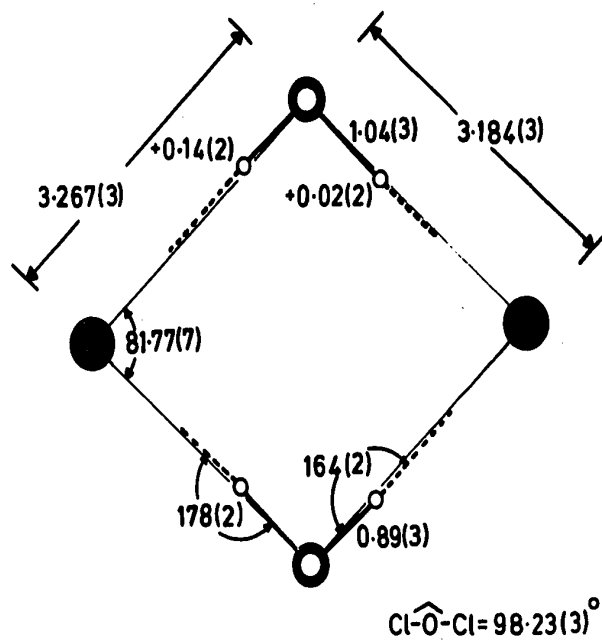


FIGURE 14

A drawing showing the immediate environment of one class of inversion centres in the crystals of Triprolidine hydrochloride monohydrate.

The water molecule is involved in two hydrogen bonds with chloride ions and each chloride ion is hydrogen bonded to two waters as well as the protonated nitrogen atom of the tetrahydropyrrole ring. This cluster of polar bonding forces is instrumental in linking together the various molecules of this structure, and may be seen in the stereoscopic Figure 15. The $N^+—H \cdots Cl^-$ bond is $3.094(3)\text{\AA}$ in length and has an angular deviation from linearity of $1^\circ 4'$ at the hydrogen atom. The distances and angles describing the $O—H \cdots Cl^-$ bonds are given in Figure 15.

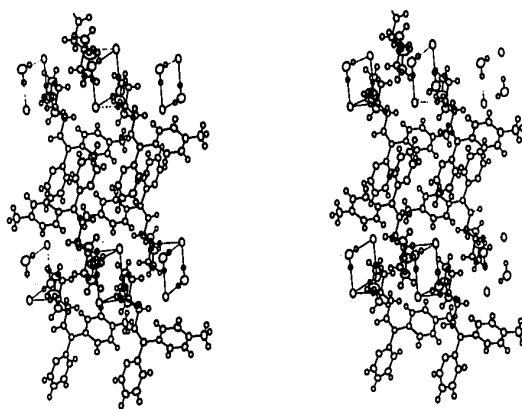


FIGURE 15

A stereoscopic pair packing diagram for
Triprolidine hydrochloride monohydrate.

The completely filled valence electron shell of a chloride ion has three mutually orthogonal p orbitals and it may be expected that these three hydrogen bonds would have interbond angles near 90° at the chloride ion.

The angles $N(10)-Cl-O(1)$, $N(10)-Cl-O(1)'$, and $O(1)-Cl-O(1)'$ (where $O(1)'$ is the symmetry equivalent atom to $O(1)$) are $70^{\circ}78'$, $88^{\circ}42'$ and $81^{\circ}78'$ respectively. A chloride ion has an effective radius of $1.81\text{\AA}^{(87)}$ and the Van der Waals radius of a hydrogen atom is $1.2\text{\AA}^{(67)}$. On the basis of these figures the expected non-bonded separation of these atoms is $\sim 3.0\text{\AA}$. The actual distances are $2.27(3)\text{\AA}$, $2.40(3)\text{\AA}$ and $2.14(3)\text{\AA}$ for $Cl-H(10)$, $Cl-WH(2)$ and $Cl-WH(1)'$ respectively, the $70^{\circ}47'$ angle at the chloride ion being that between the two longer $Cl\cdots H$ distances. Inspection of Figure 15 does not reveal any dominant steric repulsion which would force the above 20° departure from orthogonality.

The arrangement of pyridyl rings around the centres of symmetry equivalent to that at the centre of the cell represents another intermolecular bonding interaction which contributes to the stability of the crystals. The stacking of these aromatic systems is clearly seen near the viewer and slightly above the centre of Figure 15. These planes are parallel and are separated by $3.466(3)\text{\AA}$, the displacement of their centroids is $4.004(3)\text{\AA}$ and closest approach of non-hydrogen atoms is the $3.533(3)\text{\AA}$ between $C(3')$ and its inverted equivalent.

These two interactions are the most easily characterised and probably the most important in stabilising the crystalline state, but as well as these there are numerous Van der Waals attractions which are instrumental in accomplishing this.

* * * * *

The gift of the sample of Triprolidine hydrochloride monohydrate from Dr. A.F. Casy is gratefully acknowledged.

1.5 CONCLUSIONS

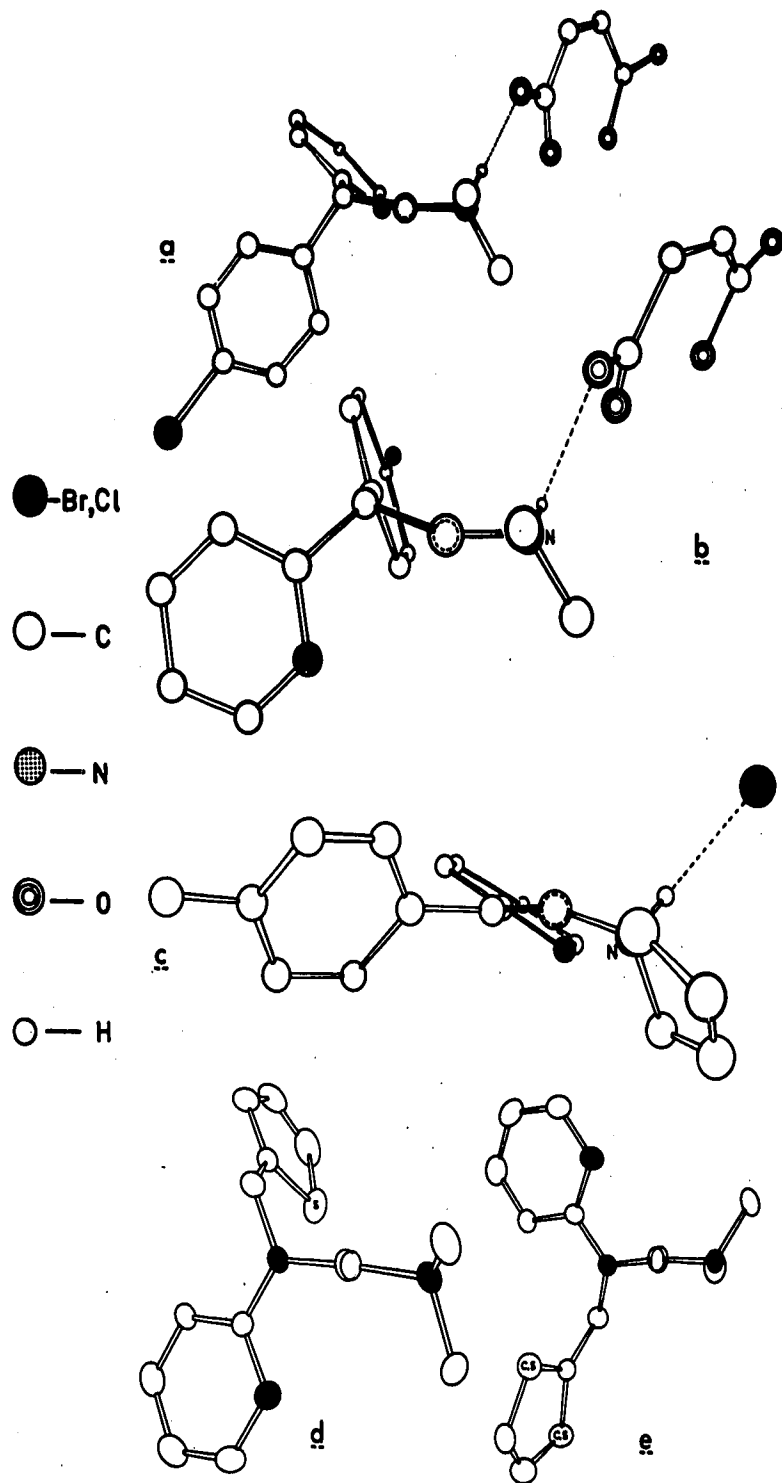
The work presented in sections 1.2, 1.3 and 1.4, together with that of Clark and Palenik on Histadyl⁽⁸⁸⁾, comprise the only four studies of antihistaminic drugs which have been pursued by the X-ray crystallographic method. Although this is meagre evidence on which to build a theory, there are certain similarities among these structures which permit some tentative generalisations on antihistaminic activity to be made. The structures of some stereochemically constrained antihistamines may be used as corroborative evidence and, where possible, these will be introduced.

For the convenience of the reader, the diagrams which show the molecular conformation viewed in the C(9)-C(8) bond direction of the three structures determined here, given above as Figures 4, 9 and 13, are reproduced again below as Figure 16. Accompanying these diagrams are similar views of the two crystallographically independent molecules of Histadyl.

The most immediately obvious similarity between these five species is their common trans arrangement of non-hydrogen substituents about the bond equivalent to $C_{\alpha}-C_{\beta}$ in histamine (1). The proposal that this conformation was a necessary prerequisite for antihistaminic activity was noted above (page 7). Evidence given for the proposal at that time was from the EHT work of Kier⁽¹⁵⁾ which purported to show that the trans $C_{\alpha}-C_{\beta}$ conformer of the histamine mono-cation was energetically preferred over the gauche form. The apparent ability of Triprolidine to mimic the assumed form of histamine was cited as supporting evidence. Reasoning on the basis of the trans conformation found for the histamine di-

FIGURE 16

A composite diagram showing five antihistamine molecules viewed in the C(9)-C(8) (C-C₉) bond direction. The structures labelled a, b and c are Brompheniramine maleate, Chlorpheniramine maleate and Triprolidine hydrochloride monohydrate, respectively. The two independent molecules of Histadyl are denoted d and e.

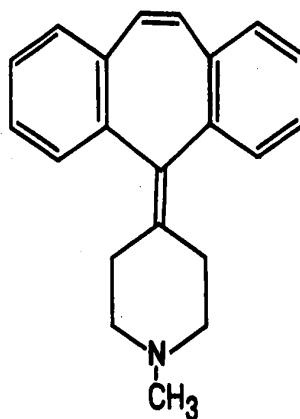


cation⁽¹⁹⁾ and from the published structure for d,l-Brompheniramine maleate⁽⁸⁹⁾, as well as from their own work on Histadyl, Clark and Palenik have indicated their belief that the trans conformation is necessary. Ham⁽⁹⁰⁾, however, has pointed out that this reasoning depends on the assumptions that, (a) the receptors for histamine and an antihistamine are identical, and (b) the receptor-bound conformation of the drug is the same as that in solution or in the solid state. This first point seems particularly important if it is interpreted to mean that not only do histamine and antihistamines compete for the same site, but also that they bind with this site in a similar manner. Because of their agonist/antagonist properties, it is unlikely that this is strictly true, but the possibility that similar binding does occur and that some part of the antihistamine blocks the onset of allergic symptoms cannot be discounted.

Ham went on to show, by pmr studies on four antihistamines with conformationally mobile $-CH_2-CH_2-$ alkyl chains, that in three cases approximately equal proportions of the trans and gauche forms existed in solution, and that in the fourth case the predominating conformation was gauche. The implication of this work in relation to the crystallographic studies is that antihistaminic drugs need not have a strong preference for the trans conformation but that they should be capable of assuming this form.

If it is accepted that binding to the receptor takes place through the amino group and the aryl function(s), then the distance between this former feature and the aromatic rings should have some measure of constancy in this class of molecules. An example of a potent antihistaminic where these moieties are constrained to be more widely separated than is

possible for a flexible molecule in a folded conformation is provided by Cyproheptadine⁽²²⁾ (XVIII). In this compound the nitrogen atom is



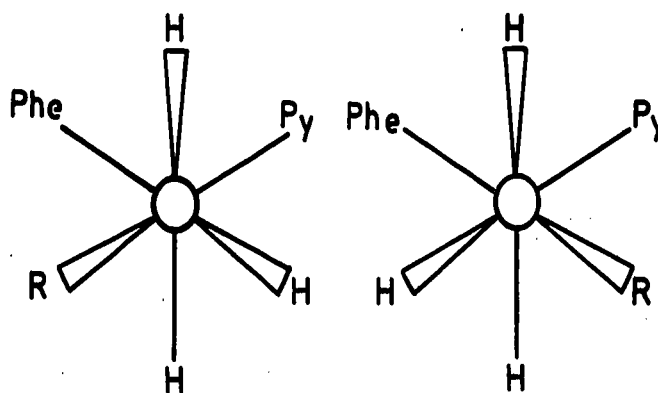
(XVIII) Cyproheptadine

(measured on a framework molecular model) ca. 6.3\AA from the centroids of the benzenoid rings. Because this distance can only be approached by molecules like the Pheniramines in fully extended form, it is assumed that a trans $C_{\alpha}-C_{\beta}$ conformation is necessary for binding to the H1 site.

The existence of various active drugs which conform to the generalised antihistamine formulation given above (page 9), but which do not possess an aromatic base as part of their structure, led Casy and Parulkar⁽²³⁾ to suggest that "the distance between the side chain nitrogen and the centre of the aromatic ring attached to C-1 more truly represents the critical parameter for activity in these compounds". This comment was directed at those who had been assuming that the alkyl N-pyridyl N

separation was the important parameter.

The essential difference between the d&l-Brompheniramine and the (+)-Chlorpheniramine structures is the torsion angle about the C(7)-C(8) bond. In the former, the $-\text{CH}_2\text{N}^+\text{HMe}_2$ (R) group bonded to C(8) is gauche with respect to the phenyl substituent of C(7), and trans with respect to the pyridyl ring. In (+)-Chlorpheniramine, the molecule assumes the trans/gauche Phe/Py conformation with respect to the R group. Newman projections with the correct S absolute configuration and illustrating these two arrangements are given below.



(a) gauche/trans : Phe/Py (b) trans/gauche : Phe/Py

(IX) Newman projections down C(8)-C(7)
for the Pheniramines

Because of the steric hindrance involved in a gauche/gauche : Phe/Py conformation for the alkylamine feature, it is proposed that either of the two arrangements observed above is permitted, but that gauche/gauche

is not.

These two staggered conformations are probably energetically favoured over the eclipsed conformer which has C-H bonds overlying the C-Ar linkages, but examination of a space filling molecular model indicates that steric interference is small. There would only be a small energy difference between this possible symmetric arrangement of the alkylamine chain and the gem diaryl system and the asymmetric disposition of these features as observed here, with the latter conformations representing the overall minima.

Having thus established that the precise nature of the aryl system interacting with the receptor is not critically important, although there does seem to be a slight preference for a pyridyl ring⁽²⁴⁾, and that the observed dissymmetry of the Pheniramines probably represents their most stable form, attention can now be turned to the generalities which can be drawn from these structures.

In each of the three crystal structures determined here, the molecule has an open side. In the d,l-Brompheniramine and Triprolidine cases, this side is formed by the pyridyl ring(s) and the alkylamine chains. The exposed face of the (+)-Chlorpheniramine molecule is formed by the saturated chain and the p-chlorophenyl feature, but as was noted above, the form with the pyridyl ring exposed is energetically very similar.

The distance from the saturated nitrogen atom to the centroid of the exposed ring is very similar in all three cases. These distances are: 6.212Å for d,l-Brompheniramine, 6.154Å for (+)-Chlorpheniramine, and 6.013Å for Triprolidine. The measurement of ~6.3Å for Cyproheptadine (XVIII) correlates nicely with these determinations and lends some support to the

argument of Casy and Parulkar⁽²³⁾.

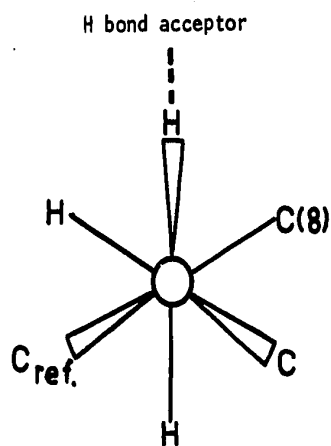
Although the existence of an open side is not so obvious in either of the two conformations presented for the Histadyl molecule, it is present in both. Clark and Palenik have demonstrated that the exocyclic nitrogen atoms both have a planar arrangement of the three atoms to which they are bonded. It was also shown that the dihedral angle between the mean plane of the four atoms just mentioned and that of the pyridyl ring was small in both cases; resonance stabilization of this structure was indicated by the shortening of the C-N (exocyclic) bond.

The presence of this rigid structural feature and the above implication that an extended alkyl chain is necessary for receptor binding means that sites which require both a hydrogen bond donor and an aromatic π electron system on the same side of the molecule cannot effectively utilize the pyridyl ring in binding a Histadyl molecule. Interestingly, however, the required arrangement is presented by the thenyl ring and the saturated nitrogen function in the (observed) case that the two methyl groups are directed away from the former moiety. The separation of the quaternary nitrogen atom from the centroid of the thenyl rings is 6.47Å and 5.93Å for the two independent molecules of that crystallographic analysis.

From the apparent constancy of this parameter, and from the similar arrangement of functional groups that these molecules could present to a receptor site, it is inferred that the H1 site is such as to bind a substance having a positively charged hydrogen bonding donor separated by 6.0 - 6.2Å from the centre of a π electron cloud with the approximate dimensions of a benzene ring.

Calculating from the published structural parameters for the fully extended form of histamine⁽¹⁹⁾, it is possible to determine that the primary nitrogen and the centroid of the imidazole ring are separated by 4.94Å. The magnitude of the difference between these two distances (ca. 1.2Å) probably means that the binding of histamine and antihistamines to the H1 receptor site is not identical.

Another remarkable point of similarity in the five established structures is that in each case the non-hydrogen substituents of the tertiary nitrogen atom are directed away from the exposed aromatic ring. Choosing the nitrogen substituent nearest the viewer as a reference atom here, the torsion angles $C_{ref.}-N-C(9)-C(8)$ for the five molecules of Figure 16 are 172.4, 177.1, 177.2, 158.6 and 184.4° respectively for parts a, b, c, d and e. A Newman projection down the N-C(9) bond illustrating this common conformation is given below. The fact that four different molecules in



(XX) The observed conformation about the N-C_{alkyl chain} bond in antihistaminic drugs

five different solid state environments adopt conformations which are so similar in all respects must be regarded as strong evidence that the observed structures typify the most probable conformation of an active drug.

Turning now to the function of a third binding interaction, a few points can be made. That there are three points of attachment of an antihistaminic molecule to the receptor site is to be inferred by the site specificity with respect to the absolute configuration of the antagonist (see page 13). Since the H1 site is capable of distinguishing an R arrangement of phenyl, pyridyl and alkylamine substituents of C(7) from the enantiomorphous S configuration, it must interact with all three of these substituents. Clark and Palenik have stated that "the bulky groups found in most antihistamines are therefore selected to prevent the response triggered by the imidazole ring". That the selection is not based simply on size may be inferred from the total lack of active drugs which have large, but inert, groups in place of, for example, the p-tolyl function of Triprolidine. A diaryl system seems necessary here and it is probable that the third interaction involves π electrons in some way.

Reasonable constancy is observed in the distances between the side chain nitrogen atoms and the centroids of the p-bromophenyl, 2-pyridyl, p-tolyl, and 2-pyridyl rings of d,l-Brompheniramine, (+)-Chlorpheniramine, Triprolidine and Histadyl. These distances are 5.57, 5.40, 5.56, 5.54 and 5.49Å respectively for the above substances.

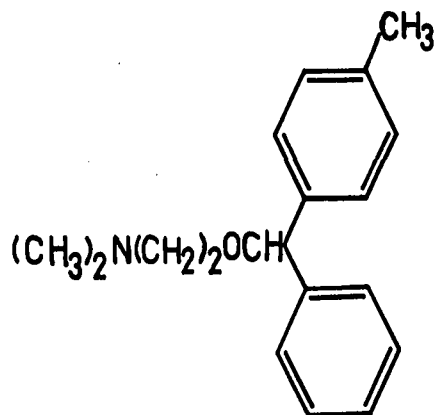
The possibility that these last quoted distances represent that parameter of the antagonist which mimics the agonist cannot be discounted entirely on the evidence available, but the ca. 6.3Å found for this quan-

tity in Cyproheptadine (XVIII), which is incapable of assuming a shorter distance, and like distances in other inflexible molecules would argue against this postulate.

Implicit in most of the above has been the assumption that the receptor site is a stereochemically rigid entity. It has long been recognized that the original characterization of a receptor site (page 1) needed modification to include the concept of flexibility, and it seems that the available facts regarding antihistaminic receptors can most easily be accommodated by a model with this attribute.

Based on the hypothesis by Rocha e Silva⁽⁹²⁾ that the protonated $-\text{NH}_3^+$ group of the histamine side chain is anchored to N_{ϵ_1} of a histidyl group in the receptor, and that a second binding interaction is via N_{δ_1} of the histamine and the carbonyl group of an adjacent peptide linkage, Nauta, Rekker and Harms have proposed a very detailed model for the histamine receptor⁽⁹³⁾. This model is not reproduced here but it can be easily described. The receptor site is visualised as an alpha helical polypeptide chain having (in part) the amino acid sequence, ...phe-his-gly-gly-ser... . The agonist molecule is thought to bind to this receptor via two hydrogen bonds which involve N_{α} and N_{δ_1} of the drug with the imidazole and hydroxyl features of the α -helical chain.

In the proposal of Nauta et al., the antihistamine 4-methyldiphenhydramine (XXI) was assumed bound at three points. These three points involve: (i) a hydrogen bond between N_{δ_1} of the histidine and the alkylamine nitrogen atom of the drug, (ii) another hydrogen bond between the serine hydroxyl and the ether oxygen, and (iii) a π - π overlap attraction between the benzenoid section of the phenylalanine residue



(XXI) 4-methyldiphenhydramine

and one of the like features on the antihistamine.

There are several aspects of this proposal which make it unattractive as a general model for the H1 receptor:

- (i) The presence of one of the aryl groups is ignored; as noted above, the presence of two aromatic rings seems mandatory in antihistamines, and it must be presumed that these are both utilized in some fashion.
- (ii) One of the binding interactions is postulated to take place through a feature which is not present in many active drugs, i.e., the ether oxygen. The presence of a nitrogen atom, which could act as a hydrogen bond acceptor, in place of the ether oxygen of Diphenhydramine in some antagonists detracts only slightly from this objection since some of the most potent antihistamines do not have this functional group, viz. the Pheniramines.

(iii) The model is essentially a static acceptor of an antihistaminic molecule, no functional characteristics are implied, and it is difficult to see how the proposal can explain the dramatically different physiological responses induced by agonists and antagonists.

This writer feels that until a receptor site has actually been isolated and characterized, it is unreasonable to propose a very specific model of the kind outlined above. More general descriptions may, however, be proposed, and that given below represents an attempt to synthesize an H1 receptor site from the available facts.

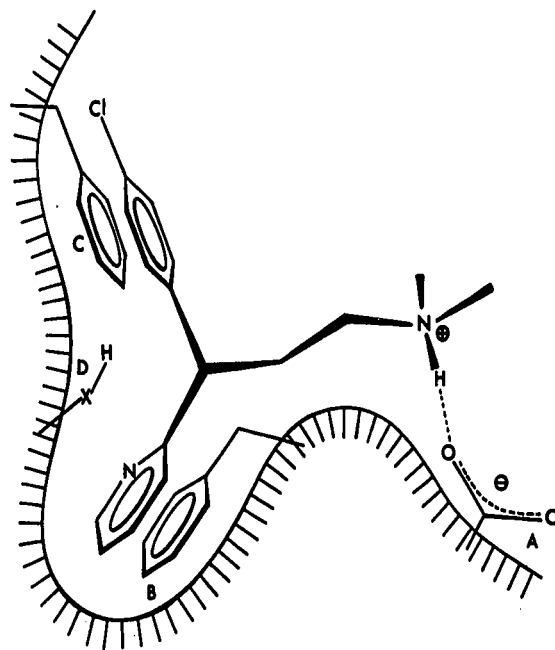


FIGURE 17

A sketch of the proposed model for the H1 receptor showing a (+)-Chlorpheniramine molecule bound to the site.

Figure 17 presents one of many possible protein surfaces with the required specificity and size parameters for the binding of antihistaminic molecules. Feature A of this model is chosen to be an ionized carboxyl group since this function would form a strong hydrogen bond with a protonated amino moiety. Ring B is drawn as a benzenoid system attached to the protein (possibilities include phe, tyr, trp). It is difficult to obtain a good estimate of the distance between these features, but the 5.25Å separation of the hydrogen bond accepting chloride ion and the π electron system to which the 2-pyridyl group in Triprolidine is attracted is probably a reasonable measure of the distance between these similar functions of the H1 site. Point of attachment C in Figure 17 is again envisaged as a benzene ring which, in this case, can interact with the second π electron system of the antagonist. Hydrogen bond donor D of this model is presumed latent when an antihistamine is bound, its function being to form a linkage to the agonist molecule.

The proposed model has the diaryl portion of the drug in a hydrophobic region formed by the receptor, and the protonated amino function is exposed to the solvent. The reasons for postulating this arrangement rather than any other are three:

(i) No effective drug has a large substituent bonded to the aromatic ring(s) on the sides remote from the alkylamine chain. This is taken to imply that the receptor cannot accommodate too great a bulk and is therefore a pocket on the surface of some protein (cf. the tosyl hole in α -chymotrypsin⁽⁹⁴⁾).

(ii) Although they are unusual, several antihistamines have more

bulky groups replacing the methyl substituents of the saturated nitrogen atom (e.g., piperidine, diethyl). It is felt that these could best be accommodated by allowing this extra bulk to protrude outside the immediate site.

(iii) The greatest amount of stabilization energy arising from hydrophobic bonding interactions⁽⁹⁵⁾ can be achieved when the non-polar parts of the molecule are removed from the, supposed aqueous, environment.

When a molecule of histamine is bound to the site it is thought that a major conformational change of the site occurs. The proposed binding of a histamine molecule is illustrated below.

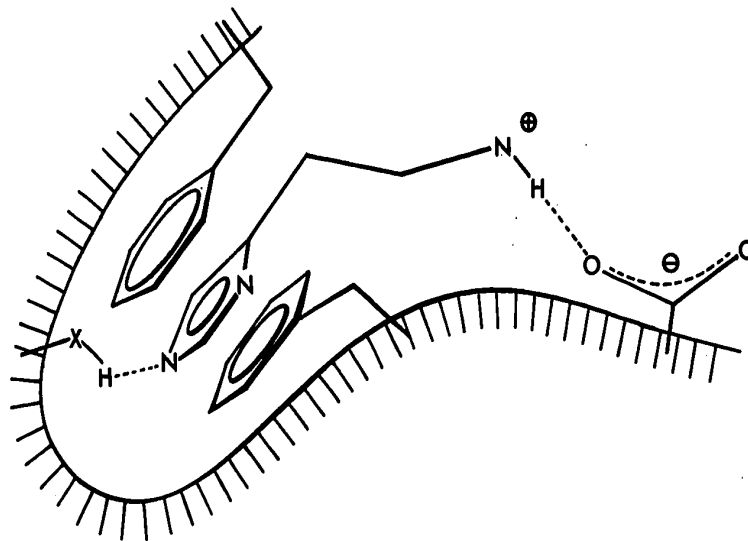


FIGURE 18

The binding of a histamine molecule to the proposed site.

It is envisaged that the change is such as to reduce the volume of the cavity by a folding inward of the receptor protein. By this means, the previously free hydrogen bonding donor (D) could be brought into a position where it could link with the imidazole group of histamine.

A strong hydrogen bond between an imidazole group and an acidic donor in a hydrophobic environment has been implicated in the mechanism of action of serine proteases⁽⁹⁶⁾, and it is felt that the agonist's binding may well have some of the characteristics proposed for the active site of chymotrypsin or elastase⁽⁹⁷⁾. It is even possible that the histamine, when bound to the receptor, becomes part of a catalytic site!

The aryl ring labelled C in Figure 17 comes down and sandwiches the imidazole ring between itself and ring B which in turn has changed position to accommodate the smaller distance from the basic centre to the aromatic group in this species. The existence of binding group D and its hydrogen bonding to the histamine imidazole ring is postulated to account for the fact that methylation of either aromatic nitrogen atom produces an agonist of greatly reduced potency⁽⁹⁸⁾.

Refinement of this model would probably involve the addition of subsidiary point(s) of attachment, e.g., one involving a hydrogen bonding donor which could interact with either N_{δ_1} of the imidazole ring or features similar to the ether oxygen of Diphenhydramine (XXI). Concrete proposals along these or other lines should, however, await the accumulation of more data.

One attractive feature of the present model is that it does involve different conformations for the receptor when either an agonist or an antagonist is bound. In this way, it is possible to understand the

108.

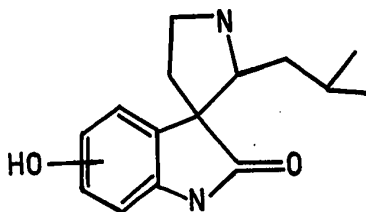
differing physiological effects of the two classes of compound. It must be stressed that this proposal is not intended to be definitive but rather it is hoped that these ideas will stimulate further work and thought on this problem.

PART 2

*An Oxindole Alkaloid*2.1 INTRODUCTION

A previously unknown alkaloid of molecular formula $C_{15}H_{20}N_2O_2$ was isolated from the dried root bark of *Eleagnus Commutata* (Wolf Willow or Silverberry) by Drs. Locock and Slywka of the Faculty of Pharmacy at this University during their work on the phytochemistry of this species.

Extensive work on the chemical and physical characterization of the compound implied that it was a phenolic derivative of an oxindole skeleton with a spiro linked secondary alkylamine moiety bearing a methylpropyl side chain. The molecular structure proposed by Slywka⁽⁹⁹⁾ is given below.



(XXII) The proposed structure for the alkaloid

The major point of uncertainty with this structure was the location of the phenolic hydroxyl, although the bonding pattern of the spiran ring and its associated alkyl chain was not firmly settled at the time the crystallographic study was initiated.

In cases such as this, X-ray crystallography can very often settle

such questions of structure unambiguously, and as a side benefit provide conformational details which may not be available by other means.

Because of this, and because of our willingness to embark upon a problem which would extend our familiarity with the "direct" methods of structure solution, we agreed to Dr. Locock's request that we attempt to resolve the remaining difficulties.

2.2 THE STRUCTURE ANALYSIS

Experimental

Columnar crystals, with either a triangular or rhombic cross section, were grown from hot ethanol by Dr. G.W.A. Slywka and supplied in a form suitable for diffraction studies. Preliminary rotation and Weissenberg photographs of a rhombic specimen measuring 0.20 x 0.13 x 0.30 mm and rotated about the needle axis revealed $2/m$ diffraction symmetry and the systematic zonal absences $h0\ell$, $\ell = 2n+1$; $0k0$, $k = 2n+1$. The space group was thus uniquely determined as $P2_1/c$ and the c axis shown to be the direction of elongation of the crystals. The lattice constants and some other physical quantities appear below as Table 22. The unit cell parameters, originally obtained from films, were refined as part of the alignment process⁽³⁸⁾ on a Picker FACS-1 diffractometer.

Reflection intensities were collected using Ni filtered Cu K radiation with the diffractometer in the coupled $\theta/2\theta$ scan mode. The 2397 reflections obtained were subjected to the usual examination for significance (see page 19). Lorentz and polarization correction terms were applied and observational weights calculated. Twenty percent (482 reflections) of the 2397 data points examined within the sphere limited by $2\theta \leq 130^\circ$ had net counts less than $3\sigma_{\text{net}}$ and so were assigned a threshold intensity and coded "unobserved". These were omitted from all further calculations except the scaling and generation of the normalised structure factors (E 's). Wilson's method⁽¹⁰⁰⁾ was used to place the data on an approximate absolute scale; the experimental intensity distribution plot and the linear least-squares regression line derived from this are displayed in Figure 19.

TABLE 22

Some physical constants and other data
for oxindole alkaloid crystals.

formula	$C_{15}H_{20}N_2O_2$
molecular weight	260.34 Daltons
space group	$P2_1/c$
a	13.1949(10) Å
b	9.4525(6) Å
c	12.1186(6) Å
β	109°47(1)'
V	1422.3 Å ³
ρ_{obs} (chlorobenzene/chloroform)	1.220(2) gm/cm ³
ρ_{calc} (4 formula units/cell)	1.216 gm/cm ³
Z	4
$\bar{\mu}$ (Cu K_α)	6.61 cm ⁻¹
M.P. (99)	250-252°C
2 θ range explored	4°-128°
no. unique reflections	2397
no. observed reflections	1915 (79.9% of total)
no. variable parameters	252
ratio observations/parameters	7.6
final unweighted R	4.30%
final weighted R	6.25%
mean sigma C-C bond	0.003 Å
mean sigma C-C-C angle	0.2°

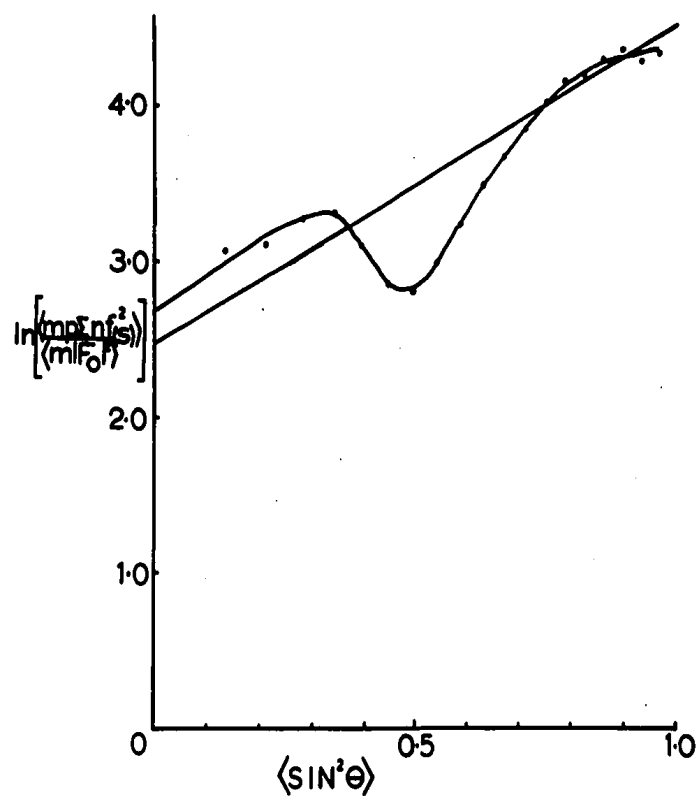


FIGURE 19

The intensity distribution (Wilson plot) for the oxindole alkaloid.

Normalised structure factors were calculated according to the expression given below⁽¹⁰¹⁾.

$$|E_{\bar{h}}| = \left\{ \frac{K(s)}{N \sum_{i=1}^P f_i^2(s)} \right\}^{\frac{1}{2}} \cdot |F_{\bar{h}}|$$

where:

$|E_{\bar{h}}|$ is the amplitude of the normalized structure factor appropriate to the reciprocal lattice point defined by the vector \bar{h} ;

$|F_{\bar{h}}^-|$ is the observed structure factor magnitude on the arbitrary scale;

$$s = \sin \theta/\lambda;$$

$K_{(s)}$ is the value of the normalization curve, at the appropriate value of s , which puts the $F_{\bar{h}}^{-2}$ on an absolute scale for point atoms at rest;

p is a small integer, which varies according to reflection class, and is designed to place all of the data on the same statistical footing (101);

$\sum_{i=1}^N f_i^2(s)$ is the value of the scattering power curve at the $\sin \theta/\lambda$ value of $|F_{\bar{h}}^-|$;

N is the total number of atoms in one unit cell.

It was found that the distribution statistics of the derived E 's closely followed those expected for a centrosymmetric structure (102):

	<u>Experimental</u>	<u>Theoretical</u>
$\langle E \rangle$	0.831	0.798
$\langle E ^2 \rangle$	0.999	1.000
$\langle E ^2 - 1.0 \rangle$	0.913	0.968
Fraction with $ E > 3.0$	0.36%	0.3%
Fraction with $ E > 2.0$	3.39%	5.0%
Fraction with $ E > 1.0$	31.87%	32.0%

Three hundred and forty-three reflections were found with $|E|$'s greater than 1.5. These were sorted in order of decreasing magnitude and written to a permanent storage device (magnetic tape). Reflections

which satisfied the relation $\bar{h} = \bar{h}' + \bar{h}''$ were then searched for and stored in groups according to the index triple \bar{h} , and in descending order of $|E_{\bar{h}}^-|$.

Theoretical considerations dictate that arbitrary phases may be assigned to three reflections which satisfy various parity criteria⁽¹⁰³⁾. In this case these reflections were selected automatically from the first 15 in the above list which did not have eee parity. Selection was made primarily by the number of sigma-two interactions found for the index triples and then according to the parity rule that the determinant of the indices, reduced modulo 2, should be non-zero. In this manner the 15th, 4th and 8th reciprocal lattice vectors were assigned phase angles of zero degrees, i.e., $E(\bar{1}, 2, 10) = +2.192$, $E(0, 8, 3) = +3.480$ and $E(\bar{3}, 3, 11) = +3.158$.

These preliminary calculations then allowed the iterative application of Sayre's equation⁽¹⁰⁴⁾ according to the symbolic addition procedure of Karle and Karle⁽¹⁰⁵⁾ with the technique of Hall and Ahmed⁽¹⁰¹⁾ to define and evaluate the symbols. By this means all but four of the 221 reflections with $|E_{\bar{h}}^-| > 1.7$ were reliably phased. A Fourier synthesis using these phased E's as coefficients revealed chemically sensible maxima corresponding to all of the non-hydrogen atoms comprising the molecule, except for the two methyl carbons.

Refinement of the model by conventional difference Fourier and least-squares techniques using the scattering factors of Cromer and Mann⁽⁴⁵⁾ in conjunction with the local version of the Busing, Martin and Levy program⁽⁴⁹⁾, ORFLS, led in a straightforward manner to the location of the hydrogen atoms. Inclusion of these positions with the scattering

factor curve of Mason and Robertson⁽⁴⁶⁾ and continued least-squares refinement, with the block-diagonal approximation, and observationally weighted structure factors resulted in final weighted and unweighted reliability indices of 6.25% and 4.30% respectively. Contributions to these indices were accepted from all but 3 of the 1915 observed data. The three reflections excluded are marked with an asterisk in the structure factor listing (Table 23) and are all of very high intensity and small Bragg angle. Tables 24 and 25 contain the positional and thermal parameters for the non-hydrogen atoms; the similar quantities used to describe the hydrogens are given in Table 26.

Results and Discussion

The atomic numbering scheme adopted in this analysis is given in Figure 20. Bond distances involving the non-hydrogen atoms are also displayed in this figure, while Figure 21 presents the interbond angles. The set of molecular parameters involving the hydrogen atoms is given in Table 27. Figure 22, which is a diagram of one molecule viewed parallel to the c axis, shows that the compound is a 6-hydroxy derivative of an oxindole nucleus with a spiro linked secondary alkylamine moiety attached to C(3). The existence of a methylpropyl side chain bonded to C(4') is confirmed and the previous structural studies⁽⁹⁹⁾ shown to be essentially correct. The fact that the phenolic hydroxyl function is a substituent of C(6) rather than C(5) is at variance with the previous tentative assignment⁽⁹⁹⁾ of this group to C(5).

The problem of deciding on a C(5) or C(6) placement of a hydroxyl function on an indole nucleus has been encountered before⁽¹⁰⁶⁾. In the

TABLE 23

The set of observed structure amplitudes and calculated structure factors ($\times 10$) based on the final model for the oxindole alkaloid. Excluded reflections are coded with an asterisk.

TABLE 24

The positional parameters for the non-hydrogen atoms of one molecule of 6-hydroxy-2'-(2-methylpropyl)-3,3'-spiro-tetrahydropyrrolidino-oxindole. The quantities have been multiplied by 10^4 .

Atom	x/a	y/b	z/c
N(1)	2090(1)	-65(2)	4144(1)
C(2)	1774(2)	1313(2)	3974(2)
C(3)	1593(2)	1705(2)	2700(2)
C(4)	1576(2)	-112(2)	1053(2)
C(5)	1775(2)	-1507(2)	826(2)
C(6)	2135(2)	-2482(2)	1738(2)
C(7)	2277(2)	-2092(2)	2889(2)
C(8)	2052(2)	-702(2)	3083(2)
C(9)	1717(1)	292(2)	2186(2)
O(2)	1671(1)	2100(2)	4724(1)
O(6)	2356(1)	-3821(1)	1469(1)
C(4')	2438(2)	2826(2)	2462(2)
N(5')	1999(1)	4193(2)	2847(2)
C(6')	811(2)	4063(2)	2341(2)
C(7')	5286(2)	2503(2)	2134(2)
C(8')	3583(2)	2577(2)	3444(2)
C(9')	4430(2)	3539(3)	3244(2)
C(10)	4591(3)	3284(5)	2087(3)
C(11)	5494(2)	3360(4)	4249(3)

TABLE 25

The parameters describing the anisotropic vibration of the atoms contained in Table 24. The quantities have been multiplied by 10^4 .

Atom	U_{11}^*	U_{22}	U_{33}	U_{12}	U_{23}	U_{13}
N(1)	322(5)	152(3)	159(3)	10(3)	4(3)	89(3)
C(2)	269(5)	162(4)	201(4)	-9(4)	-20(3)	93(4)
C(3)	214(5)	147(4)	187(4)	5(3)	-3(3)	65(4)
C(4)	238(5)	171(4)	165(4)	2(4)	20(3)	53(4)
C(5)	267(5)	184(4)	152(4)	-12(4)	-11(3)	69(4)
C(6)	226(5)	135(4)	193(4)	-10(3)	-15(3)	80(4)
C(7)	232(5)	142(4)	176(4)	-3(3)	13(3)	68(4)
C(8)	207(4)	148(4)	158(4)	-11(3)	-5(3)	59(3)
C(9)	199(4)	143(4)	174(4)	-4(3)	2(3)	54(3)
O(2)	467(5)	191(3)	230(4)	26(3)	-35(3)	163(4)
O(6)	395(5)	140(3)	220(3)	8(3)	-20(2)	147(3)
C(4')	219(5)	141(4)	196(4)	3(3)	3(3)	63(4)
N(5')	282(5)	146(4)	266(4)	11(3)	5(3)	103(4)
C(6')	241(6)	184(5)	435(8)	37(4)	50(5)	107(5)
C(7')	220(5)	185(5)	293(6)	24(4)	8(4)	66(4)
C(8')	228(5)	228(5)	260(6)	3(4)	12(4)	53(4)
C(9')	234(6)	316(7)	345(7)	-24(5)	-9(6)	86(5)
C(10)	394(9)	737(16)	405(10)	-112(10)	-18(10)	200(8)
C(11)	266(7)	592(12)	467(11)	-46(8)	-72(9)	42(7)

* These coefficients are defined on page 24.

TABLE 26

Positional and thermal parameters ($\times 10^3$) for the hydrogen atoms of
6-hydroxy-2'-(2-methylpropyl)-3,3'-spirotetrahydropyrrolidino-oxindole.

Atom	x/a	y/b	z/c	U_{iso}
H(1)	224(2)	-53(2)	488(2)	65(5)
H(4)	136(2)	59(2)	43(2)	76(6)
H(5)	168(1)	-185(2)	4(1)	53(5)
H(6)	230(2)	-453(3)	202(2)	97(8)
H(7)	257(1)	-281(2)	356(1)	60(5)
H(4')	238(1)	290(2)	179(1)	56(5)
H(5')	224(2)	429(3)	373(2)	108(8)
H(61')	53(2)	458(3)	168(2)	95(8)
H(62')	45(2)	449(3)	290(2)	105(9)
H(71')	30(2)	233(2)	131(2)	77(6)
H(72')	-1(2)	225(3)	244(2)	80(7)
H(81')	357(2)	268(2)	430(2)	73(6)
H(82')	386(2)	155(3)	335(2)	81(7)
H(9')	417(2)	455(3)	325(2)	90(8)
H(101)	518(3)	397(4)	201(3)	137(13)
H(102)	476(2)	211(3)	214(2)	121(10)
H(103)	387(3)	337(4)	140(3)	149(11)
H(111)	532(3)	356(3)	503(3)	146(10)
H(112)	568(3)	213(3)	419(3)	132(9)
H(113)	606(3)	404(3)	412(3)	151(12)

FIGURE 20

The numbering scheme and the bond distances involving the non-hydrogen atoms of the oxindole alkaloid. The bond distances have average standard errors of 0.003Å.

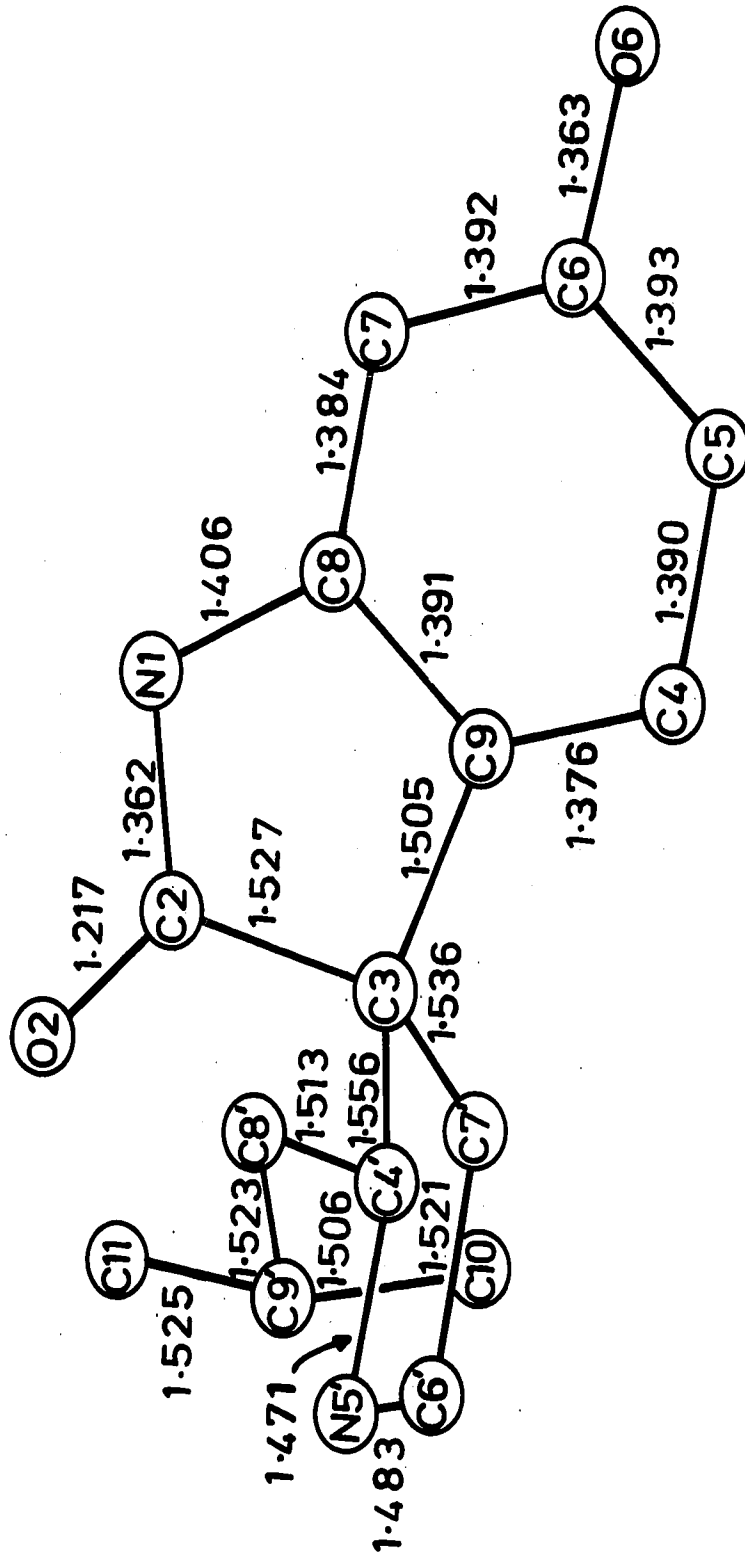


FIGURE 21

The interbond angles calculated on the basis of those parameters contained in Table 24. The average standard deviation of these quantities is 0.2° .

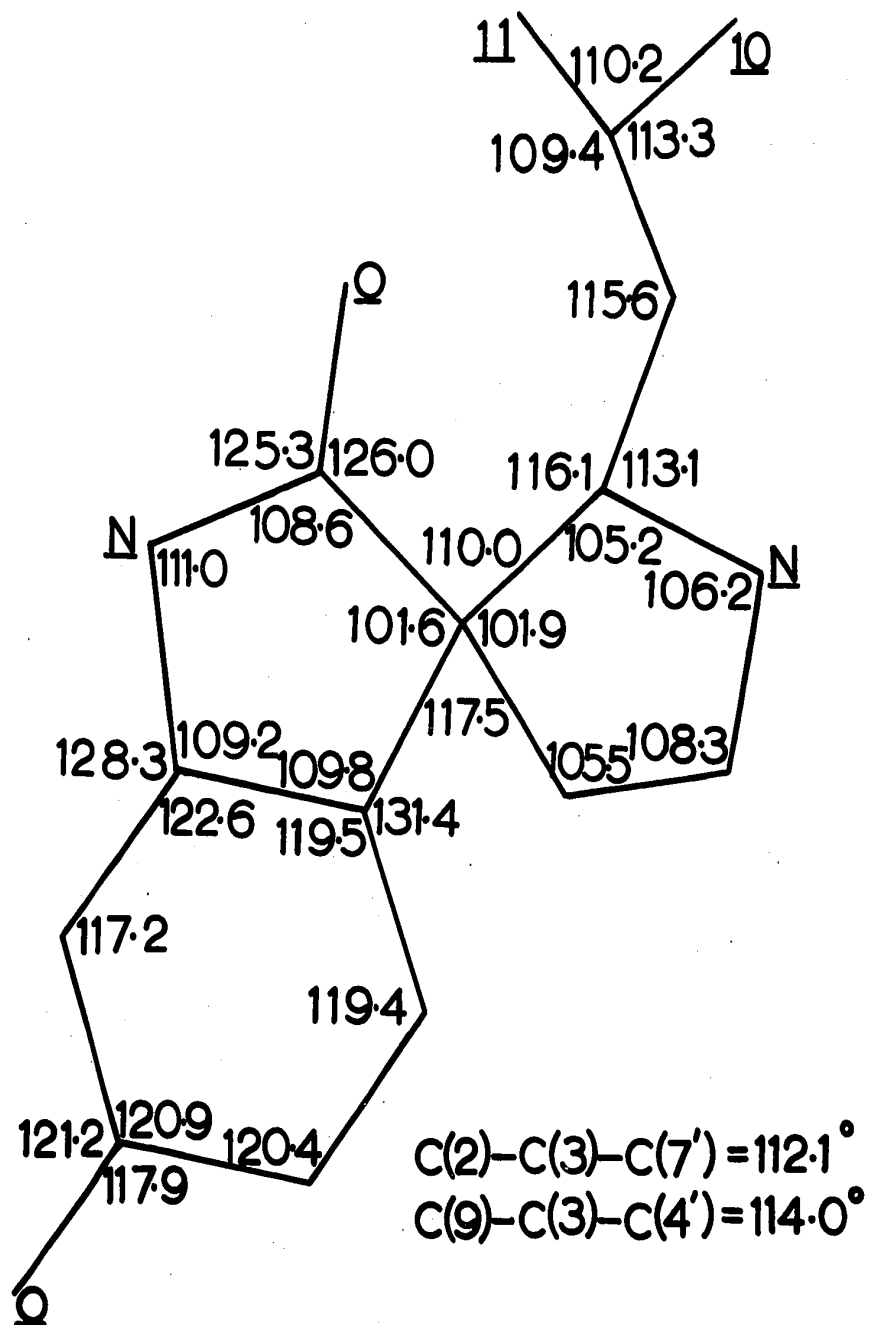


TABLE 27

Bond distances and angles for the hydrogen atoms of the oxindole alkaloid. Average standard errors are 0.02 Å and 1.0° for the distances and angles respectively.

(a) Distances

N(1)-H(1)	0.96(2) Å	C(7')-H(72')	0.94(2) Å
C(4)-H(4)	0.98(2)	C(8')-H(81')	1.04(2)
C(5)-H(5)	0.98(2)	C(8')-H(82')	1.05(2)
O(6)-H(6)	0.97(3)	C(9')-H(9')	1.02(3)
C(7)-H(7)	1.03(2)	C(10)-H(101)	1.04(4)
C(4')-H(4')	1.00(2)	C(10)-H(102)	1.13(3)
N(5')-H(5')	1.02(2)	C(10)-H(103)	1.03(4)
C(6')-H(61')	0.91(2)	C(11)-H(111)	1.07(4)
C(6')-H(62')	1.04(3)	C(11)-H(112)	1.20(4)
C(7')-H(71')	0.96(2)	C(11)-H(113)	1.03(3)

(b) Angles

H(1)-N(1)-C(2)	123(1)°	H(5')-N(5')-C(6')	111(1)°
H(1)-N(1)-C(8)	126(1)	H(61')-C(6')-N(5')	113(2)
H(4)-C(4)-C(5)	121(1)	H(61')-C(6')-C(7')	112(2)
H(4)-C(4)-C(9)	120(1)	H(61')-C(6')-H(62')	103(2)
H(5)-C(5)-C(4)	123(1)	H(62')-C(6')-N(5')	111(2)
H(5)-C(5)-C(6)	117(1)	H(62')-C(6')-C(7')	110(2)
H(6)-O(6)-C(6)	114(2)	H(71')-C(7')-C(3)	107(1)
H(7)-C(7)-C(6)	120(1)	H(71')-C(7')-C(6')	108(1)
H(7)-C(7)-C(8)	123(1)	H(71')-C(7')-H(72')	111(2)
H(4')-C(4')-C(3)	107(1)	H(72')-C(7')-C(3)	114(2)
H(4')-C(4')-N(5')	102(1)	H(72')-C(7')-C(6')	111(2)
H(4')-C(4')-C(8')	112(1)	H(81')-C(8')-C(4')	106(1)
H(5')-N(5')-C(4')	105(1)	H(81')-C(8')-C(9')	111(1)

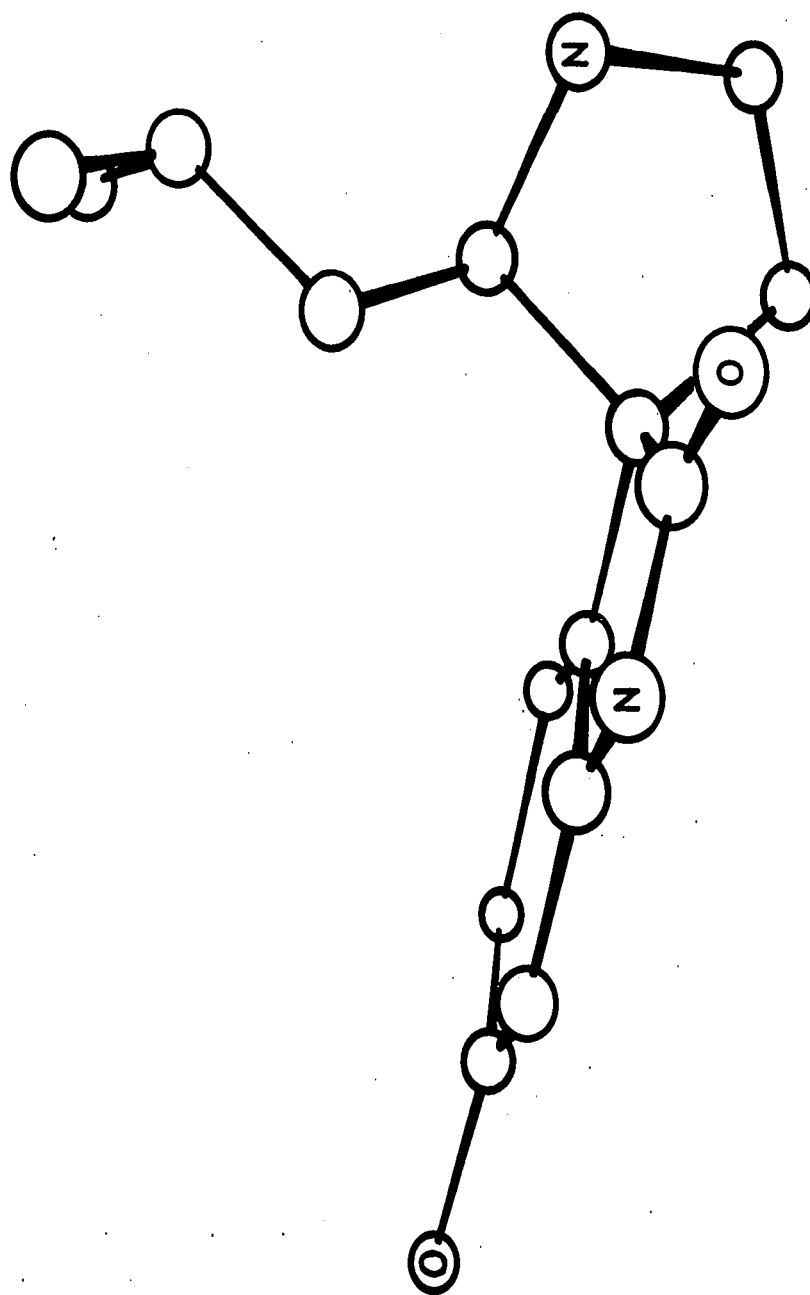
Continued.....

Table 27 (Continued)

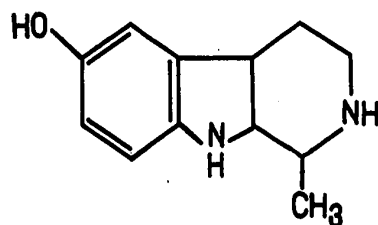
(b) <u>Angles</u> (Contd.)			
H(81')-C(8')-H(82')	109(2) ^o	H(102)-C(10)-C(9')	101(2) ^o
H(82')-C(8')-C(4')	112(1)	H(102)-C(10)-H(103)	103(3)
H(82')-C(8')-C(9')	103(1)	H(103)-C(10)-C(9')	111(2)
H(9')-C(9')-C(8')	107(1)	H(111)-C(11)-C(9')	106(2)
H(9')-C(9')-C(10)	108(1)	H(111)-C(11)-H(112)	110(2)
H(9')-C(9')-C(11)	109(1)	H(111)-C(11)-H(113)	114(3)
H(101)-C(10)-C(9')	109(2)	H(112)-C(11)-C(9')	102(2)
H(101)-C(10)-H(102)	119(3)	H(112)-C(11)-H(113)	115(2)
H(101)-C(10)-H(103)	113(3)	H(113)-C(11)-C(9')	109(2)

FIGURE 22

One molecule of the oxindole alkaloid
viewed parallel to the c axis.

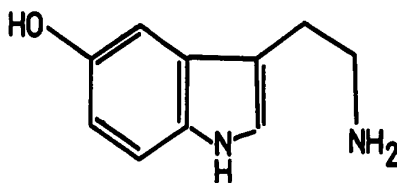


case of Shepherdine (XXIII), which was isolated from *Shepherdia canadensis*, a C(5) hydroxyl was postulated on the basis of similarities in the ir and pmr spectra of the unknown with those obtained from synthetic samples, and by analogy with other known compounds extracted from the same or similar sources. Proof of Browne's postulated structure



(XXIII) Shepherdine

was obtained by her showing that the unknown material was identical to that compound she was able to synthesize from 5-hydroxytryptamine (XXIV).

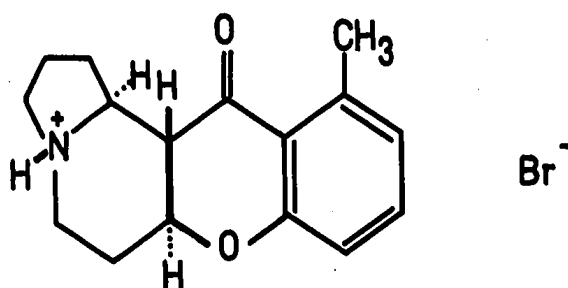


(XXIV) 5-hydroxytryptamine

Slywka's assignment of the phenolic hydroxyl group to C(5) was based largely upon pmr evidence - probably because of a paucity of closely related compounds for comparison by other methods. The difficulty with using this technique is that the compounds to be distinguished were both 1,2,4 tri-substituted benzenoid systems and these would be expected to give closely similar spectra. Solubility difficulties with the unknown alkaloid dictated that the pmr spectra be run in deuterated DMSO. Dimethylsulphoxide is a hydrogen bonding solvent and as well as this complicating factor, the presence of large extramolecular dipoles, some of which may be preferentially oriented with respect to the molecule, could impose unknown magnetic shielding effects on the system. Because of these factors the pmr spectrum of the present compound could be expected to present some difficulties in interpretation.

Both the proposed and found molecular structures for this alkaloid possess two asymmetric carbon atoms, [C(3) and C(4')]. Since the majority of potentially optically active compounds derived from biological sources are in fact synthesized as pure isomers, Slywka would not have been surprised with his determination of $+174.8^\circ$ for the optical rotation of this compound measured on a 0.1% ethanolic solution at 25°C (99). The fact that the crystals supplied by Slywka were found to crystallize in a centrosymmetric space group, $P2_1/c$, unequivocally demonstrates, however, that the material is a racemate. This finding when taken in conjunction with the very low likelihood that the recrystallization, done by Slywka from hot ethanol, would involve racemisation of a previously pure optical isomer and the existence of various precedents (99,106,107,108) for alkaloids being isolated in racemic form indicates that the composition of the mat-

erial studied polarimetrically was not the same as that of the crystals used in this work. A similar situation was found for Eleaocarpine (XXV) ⁽¹⁰⁸⁾ in that repeatedly recrystallized material was found to exhibit an optical rotation of $+0.1^\circ$, whereas the crystals were racemic. In this latter case the optical rotation of the pure (+) isomer is known to be $+206^\circ$ and so the postulate that the biosynthetic pathway for Eleaocarpine slightly favours the (+) rotamer appears reasonable. In the



(XXV) Eleaocarpine

present case, however, the apparently large rotation ($+174.8^\circ$) found for the natural product implies that the dextro rotatory isomer is strongly preferred over its antipode. Since all crystals examined belonged to space group $P2_1/c$, it seems reasonable to suggest that only a small fraction of the material was recovered from the recrystallization experiments, and to further suggest that the crystallization mother-liquor probably contained the (+) isomer in a reasonably pure state. Whatever the explanation for this seeming contradiction, it is probable

that the true optical rotation for the pure dextro isomer of this compound is not 174.8° .

When this structure is studied in detail, very few significant deviations from ideal molecular geometry are to be found. The benzenoid section of the oxindole system is planar with maximum exoplanar displacement of 0.01\AA from the plane with equation $-0.9603x - 0.2424y - 0.1378z + 1.7190 = 0$ ($\chi^2 = 69.9$). The phenoxy oxygen atom displacement is only $-0.043(2)\text{\AA}$ from this plane, but the phenolic hydrogen is displaced $+0.33(3)\text{\AA}$, thus permitting the O-H bond vector to point towards atom N(5') of another molecule (see Figure 23). The O-H...N bond is $2.659(2)\text{\AA}$ long and the relevant interbond angles are $\text{C}(6)\text{-O}(6)\text{-H}(6) = 114(2)^\circ$, $\text{O}(6)\text{-H}(6)\cdots\text{N}(5') = 171(2)^\circ$, $\text{H}(6)\cdots\text{N}(5')\text{-C}(4') = 110.4(0.9)^\circ$, $\text{H}(6)\cdots\text{N}(5')\text{-C}(6') = 103.9(0.9)^\circ$, and $\text{H}(6)\cdots\text{N}(5')\text{-H}(5') = 120(2)^\circ$. The distances involving the hydrogen atoms of this intermolecular linkage are $\text{O}(6)\text{-H}(6) = 0.97(3)\text{\AA}$, and $\text{H}(6)\cdots\text{N}(5') = 1.70(3)\text{\AA}$.

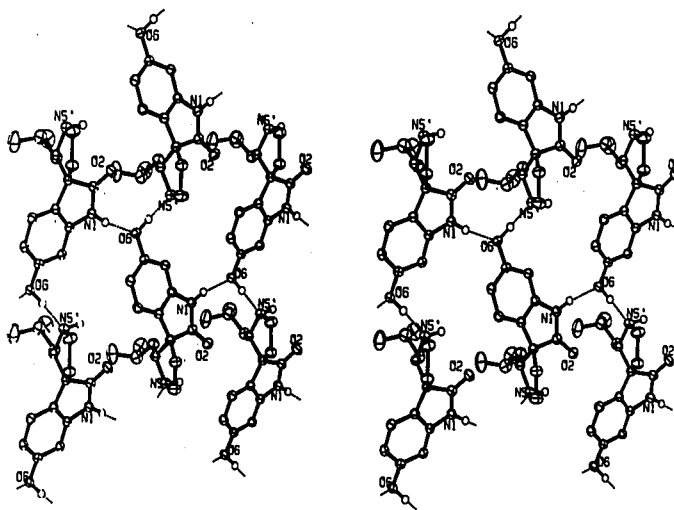


FIGURE 23

A packing diagram of several molecules of the alkaloid showing the sheet structure and the intermolecular hydrogen bonding.

The weighted average of the bond lengths within the benzenoid ring is 1.388Å with an associated e.s.d. of 0.006Å. The 0.006Å discrepancy between this average bond length and the 1.394Å found in highly accurate work⁽⁵⁵⁾ is not significant and indicates that the effects of rigid body libration⁽¹⁰⁹⁾ on this molecule in the solid state are small.

The five-membered ring of the oxindole nucleus is not planar; the spiro atom, C(3), deviates by -0.114(2)Å from the best four-atom least-squares plane which is defined by the atoms C(2), N(1), C(8) and C(9). This plane has equation $-0.9465x - 0.2723y - 0.1731z + 1.7989 = 0$ ($\chi^2 = 18.2$) and is nearly parallel to the plane of the benzenoid ring (dihedral angle = 2.8°). None of the four atoms which define the oxindole plane is displaced more than 0.005Å from it. The -C-NH-CO-C- grouping of this ring resembles a cis peptide bond and therefore may exhibit some of the features of this structural unit. All of the above six atoms are within 0.04Å of the five-atom least-squares plane, defined by the non-hydrogen members of this group, with equation $-0.9371x - 0.2572y - 0.2358z + 2.0524 = 0$ ($\chi^2 = 1113.5$). The amide bond, N(1)-C(2), distance of 1.362(3)Å is significantly shorter than the 1.475(5)Å⁽⁵⁵⁾ found in simple trivalent nitrogen compounds. The carbonyl carbon-oxygen distance, corrected according to the riding motion model⁽¹¹⁰⁾, is 1.248(3)Å and this is significantly longer than the comparable bond distances expected in simple aldehydes and ketones which are encompassed by 1.215(5)Å⁽⁵⁵⁾. Bond angle distortions imposed upon this system by virtue of its cyclic nature probably preclude the most favourable overlap of hybridized atomic orbitals, and so the shortening of the OC-N bond here is not as extreme as in normal peptide bonds where this linkage is found to be 1.325Å

long⁽¹¹¹⁾. Nitrogen atom, N(1), is engaged in forming the second intermolecular hydrogen bond of this structure to oxygen O(6) (refer to Figure 23). This bond deviates from linearity by 12(2)° at the hydrogen atom and has a donor...acceptor distance of 2.916(2)Å. When compared with the tabulated values of Donohue⁽⁶⁵⁾, or those of Hamilton and Ibers⁽¹¹²⁾, it may be seen that this bond typifies a normal N-H...O linkage.

The 1.505(3)Å bonding distance between atoms C(3) and C(9) appears abnormally short for a C-C single bond length. However, a comparison with documented values⁽⁵⁵⁾ shows that this value is exactly that expected for tetracoordinated carbon bonded to a benzenoid system. This observation reinforces the widely accepted principle that whenever bond length comparisons are to be made the hybridization states of the bonded atoms must be taken into account, and that comparisons made only on the basis of bond multiplicities are invalid.

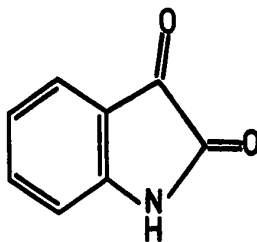
The best four-atom plane of the saturated spiran ring is defined by the positions of the atoms N(5'), C(6'), C(7') and C(3), and has equation $0.4359x - 0.0076y - 0.9000z + 2.3292 = 0$. The distances of the five ring atoms from this plane are: -0.020, 0.527, 0.017, -0.055 and 0.043Å respectively for C(3), C(4'), N(5'), C(6') and C(7'). These distances and the χ^2 value of 1007.8 imply that this plane has notional existence only and therefore should not be interpreted as an important structural feature. A more precise description of this ring's conformation may be given in terms of the relevant torsion angles. Using the definition of torsion angle given on page 6 of this thesis, these angles are: C(7')-C(3)-C(4')-N(5') = -36.2°, C(3)-C(4')-N(5')-C(6') = + 32.3, C(4')-N(5')-C(6')-C(7') = -15.5°, N(5')-C(6')-C(7')-C(3) = -7.7°, and C(6')-C(7')-

$C(3)-C(4') = +26.1^\circ$. An alternative description of this five-membered ring, and one that has been proposed for furanose ring forms⁽⁸⁶⁾, is in terms of atomic displacements from the plane through those three atoms which are common to both the best and the second best four-atom least-squares plane. In this case these atoms are N(5'), C(6') and C(7') and the plane has equation $0.3842x + 0.0724y - 0.9204z + 2.1370 = 0$ and the displacements of C(3) and C(4') are -0.197\AA and $+0.376\text{\AA}$ respectively. These two atoms are on opposite sides of the reference plane and so the ring has the twist (T) conformation.

The molecular packing is shown in the stereoscopic Figure 23 which is a projection onto (100). This diagram shows that the molecules form infinite layers with the hydrogen bond network shown being the principal intralayer bonding interaction. Interlayer bonding is the result of non-specific, non-directional Van der Waals dispersion forces between the methylpropyl side chains of different molecules.

A literature search for crystal structures of molecules sufficiently similar to the present one to permit fruitful comparisons to be made revealed only two compounds.

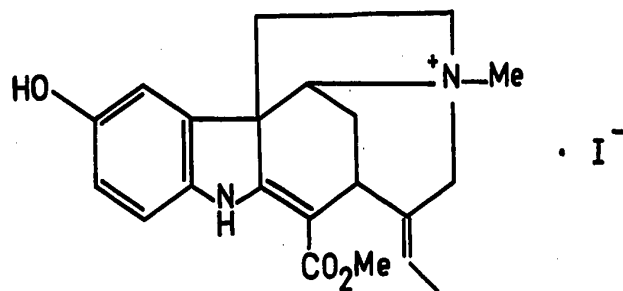
Isatin⁽¹¹³⁾ (XXVI) has the basic oxindole skeleton but the presence of the extra carbonyl group would impose electronic and structural con-



(XXVI) Isatin

straints on the skeleton which are not implied by the spiran ring of the present compound.

Sewarine⁽¹¹⁴⁾ (XXVII) has a phenolic indole system with an sp^2 hybridized carbon at the 2 position, but in this case the extended system



(XXVII) Sewarine

of fused rings makes detailed comparisons difficult. The Sewarine structure was solved by the heavy atom method (methiodide derivative of the parent alkaloid) using diffractometer data, and refined to an R factor of 11.0%. The estimated standard deviations for the Sewarine structure are 0.01Å in bond length and 1.0° for the interbond angles. Within the precision of this latter determination, only insignificant differences between it and the comparable features of the present structure are evident. Despite the claim that "the rather precise data obtained for the Sewarine molecule may serve as references for structure comparisons...." modern crystallography, especially that based on diffractometer data, is usually capable of higher precision than was obtained by these workers, and more accurate structural parameters are necessary before detailed

comparisons can be made.

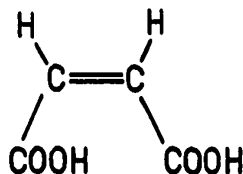
* * * * *

Thanks are expressed to Drs. Locock and Slywka for the sample of the alkaloid which can now be given the systematic name 6-hydroxy-2'-(2-methylpropyl)-3,3'-spirotetrahydropyrrolidino-oxindole.

PART 3

*Maleic Acid and Maleate Anions*3.1 INTRODUCTION

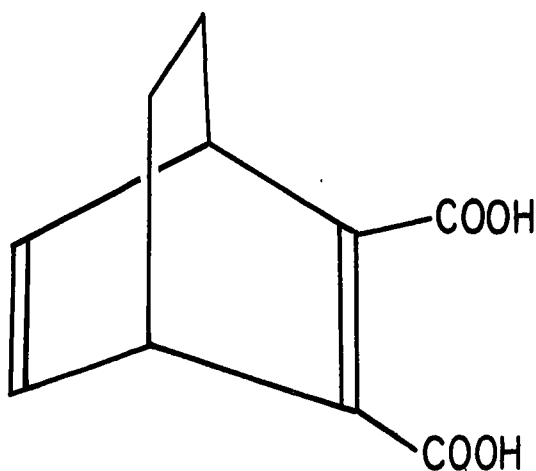
The relative ease with which the first base-dissociable proton of maleic acid (XXVIII) is removed ($pK_{a1} = 1.83$)⁽¹¹⁵⁾, and the much greater than usual difficulty experienced in titrating the second acidic function ($pK_{a2} = 6.07$)⁽¹¹⁵⁾ implies that neither of these two carboxyl groups is normal in its properties.



(XXVIII) Maleic acid

This information was used in conjunction with results from infrared spectroscopy to support the proposal of Cardwell, Dunitz and Orgel⁽¹¹⁶⁾ that the second base-dissociable proton of maleic acid resided between the two carboxyl groups. A previous paper by Shahat⁽¹¹⁷⁾, reporting the crystal structure of maleic acid, had shown that the two acidic functions were not equivalent with respect to carbon-oxygen bonding pattern, and so if the internal hydrogen bond suggestion is accepted then the implication is that this hydrogen is bonded more closely to one oxygen atom than it is to the other. The first crys-

tallographic investigation of a maleic acid system to directly verify the above postulate by locating the hydrogen atoms is that of bicyclo[2.2.2]octa-2,5-diene-2,3-dicarboxylic acid⁽¹¹⁸⁾ (XXIX).



(XXIX) Bicyclo[2.2.2]octa-2,5-diene-2,3-dicarboxylic acid

There are two molecules per crystallographic asymmetric unit in this structure, and both were observed to have an asymmetric intramolecular hydrogen bond. Donor oxygen to acceptor oxygen distances were calculated (by this author) to be 2.47 and 2.51Å for the two molecules which have O-H distances of 0.78 and 1.03Å respectively. The remaining hydroxyl group of the tricyclic molecule was utilized in linking the molecules together in an infinite helical chain. This disposition of hydrogen bonding power is essentially the same as that proposed by Shahat⁽¹¹⁷⁾, but with one major difference. In Shahat's final model, the hydrogen bearing oxygen atom not implicated in the intramolecular hydrogen bond was found 2.75Å and 2.98Å from two possible hydrogen bond accepting oxygen atoms. Shahat interpreted these findings as evi-

dence for the existence of a bifurcated hydrogen bond which linked his ribbons of maleic acid molecules into a two dimensional mesh. Donohue⁽⁶⁵⁾ recalculated the above contact distances from the published positional parameters and found that the 2.98Å previously mentioned was in reality 2.92Å. This minor revision did not in itself invalidate Shahat's postulate, but Donohue's more reasonable proposed placement of the hydrogen atom in question along an interoxygen line implied that the bifurcated hydrogen bond was non-existent. To date, no more accurate study of maleic acid (hereinafter referred to as $H_2Ma\&$) has appeared, and because of the importance of having accurate structural parameters for this parent substance, it was made the subject of a refinement study.

Our interest in the structural chemistry of the maleic acid/maleate mono-anion/maleate di-anion system was first stimulated by our findings that the maleate counterions to the *dl*-Brompheniramine and (+)-Chlorpheniramine species both possessed short but definitely asymmetric hydrogen bonds. That a symmetric position for the hydrogen atom under discussion was expected was inferred from previous crystallographic and theoretical studies on the maleate mono-anion. The first relevant crystal structure published was that of Darlow and Cochran⁽¹¹⁹⁾ on potassium hydrogen maleate (hereinafter called $KHMa\&$). The results of these workers were less clear cut than was hoped because in their studies the maleate mono-anion, ($HMa\&^-$), was found to reside across a crystallographic mirror plane perpendicular to the $C=C$ bond. Although circumstances such as this would normally require that the intra-ion linked hydrogen atom occupy a position on the mirror plane, the existence

of two half-hydrogens on either side of the mirror is a possibility. Because of this ambiguity, Darlow and Cochran were unable to state whether their hydrogen bond was symmetric or not. They were, however, able to give evidence for a central hydrogen position by providing diagrams of a well shaped electron density maximum located at the position where an ordered hydrogen atom would be expected to reside. The oxygen-oxygen separation for the two participants in this bond was given as $2.437(4)\text{\AA}$ in an interpretive paper by Darlow⁽¹²⁰⁾. An apparent space group ambiguity between $Pbcm$ and $Pbc2_1$ does not seem to have been adequately resolved in this study; no analysis of the intensity data or other statistical tests were reported. In view of the molecular constraints imposed by these authors' choice of $Pbcm$, reasonable uncertainty regarding this structure exists, even though a final R value of 4.9% was achieved. There seems to be a valid reason for redetermination of this structure and refinement in the acentric space group.

More conclusive evidence for a central position of the hydrogen atom in question was provided by a neutron diffraction study of potassium hydrogen chloromaleate⁽¹²¹⁾ (referred to here as $KHC\&M\&$). These workers introduced a chlorine atom into the organic ion to avoid any methodological bias of the type experienced by the previous workers. This stratagem was successful in that Ellison and Levy were able to demonstrate a central hydrogen atom position between two oxygen atoms separated by 2.403\AA .

Theoretical studies stimulated by the publication of an empirical curve which indicated that "for the particular case of $O-H\dots O$, the $O-H$ distance increases as the $O\dots O$ distance decreases"⁽¹²²⁾ have consoli-

dated the belief that the $\text{HMa}\bar{\ell}$ ion is one of the few species that has a truly symmetric hydrogen bond. A molecular orbital study of Murthy, Bhat and Rao⁽¹²³⁾ on this species, with the oxygen-oxygen separation constrained to be 2.4\AA , has resulted in their proposal of a symmetric single minimum potential energy function for this system. Kollman and Allen⁽¹²⁴⁾ have approached the hydrogen bonding energetics problem from a more general standpoint - their ab initio calculations on the H_5O_2^+ species being relevant here. The results of these workers indicate that at $0\cdots 0$ separations of 2.487\AA and 2.302\AA the same minimum energy was obtained, the difference between the two situations being that in the former case a double well function resulted, whereas in the latter a single minimum was obtained. At the intermediate separation of 2.381\AA , a lower energy well with a broad profile resulted from their calculations. In fact, these computations simply say, in sophisticated terms, what Coulson had suggested ten years earlier⁽¹²²⁾. It would be exceedingly dangerous, of course, to carry these latter results over to the maleic acid system directly, but the principle of a central positioning of the hydrogen atom in short hydrogen bonds seems well founded.

The problem remains to determine what factor or factors lead to oxygen-oxygen separations of 2.403\AA and 2.437\AA (and symmetric hydrogen bonds) in two $\text{HMa}\bar{\ell}$ structures, but result in $0\cdots 0$ distances of 2.417\AA (dℓ-Brompheniramine maleate) and 2.444\AA [(+)-Chlorpheniramine maleate] in two others which have asymmetrically positioned hydrogen atoms. The symmetric nature of the bond is presumed to be the result of a decrease in the $0\cdots 0$ distance rather than a cause of it.

In order to more fully characterise this system, and hopefully to

141.

answer some of the outstanding questions, the crystal structure of disodium maleate was also undertaken.

3.2 MALEIC ACID

Experimental

The same difficulties encountered by previous workers^(117,125,126) in obtaining a single crystal of maleic acid were experienced here. Several different solvents were used in an attempt to overcome the twinning problem, but to no avail. Only by cooling a warm solution of the acid in acetone were crystals of usable size obtained, and all of these were twinned by reflection across (100). In some instances, however, one member of the twin protruded past the other and by taking advantage of the extremely facile cleavage parallel to (001), a suitable single crystal could be obtained. The specimen (0.9 x 0.7 x 0.3 mm) acquired in this manner was mounted so as to rotate about the monoclinic unique axis and then encapsulated in Canada balsam to avoid atmospheric effects.

Diffraction data at room temperature were collected out to a minimum d spacing of 0.584Å (2θ max = 75°) on a Picker FACS-1 diffractometer using graphite monochromatised Mo K radiation (λ = 0.70926Å). Refined cell parameters and some other quantities relating to this analysis are contained in Table 28. With the exception of the b repeat distance, the unit cell obtained here is insignificantly different from that reported by Shahat⁽¹¹⁷⁾.

The usual θ/2θ scan mode was used over a basic width of 1.8° in 2θ at a scan speed of 2°/min. A total of 2534 unique and space group permitted reflections were collected and of these 727 (28.7%) were excluded from subsequent structure factor and electron density computations on the basis that their net intensities were not greater than 3σ_{net}. Sev-

TABLE 28

The unit cell constants and some other quantities relating to the crystal structure analysis of maleic acid.

molecular formula	$C_4H_4O_4$
molecular weight	116.07 Daltons
space group	$P2_1/c$
a	7.473(1) Å
b	10.098(2) Å
c	7.627(2) Å
cos β	-0.5545(1)
β	123.59(2)°
V	478.921 Å ³
Z	4
ρ_{obs} (117)	1.590 gm/cm ³
ρ_{calc}	1.610 gm/cm ³
$\bar{\mu}$ (Mo K_α)	1.6 cm ⁻¹
2 θ range explored	4°-75°
no. unique reflections	2534
no. observed reflections	1807 (71.3% of total)
no. variable parameters	89
ratio observations/parameters	20.3
final unweighted R	5.04%
final weighted R	7.31%
mean sigma in C-C bond distance	0.002 Å
mean sigma in C-C-C angle	0.1°
standard deviation of difference electron density map	0.032 e/Å ³

enty-two reflections were considered to be suffering from the effects of counter paralysis and so were remeasured with a diffracted beam attenuator in position. By multiplying the recollected intensities and the experimentally determined attenuator factor together, it was possible to overcome this problem.

Because the crystal had been thickly coated with Canada balsam prior to the data collection, it was realized that if absorption corrections were to be applied then this would have to be done empirically rather than analytically. Accordingly, an absorption profile of the crystal was prepared by examining the net intensities of three ϕ independent reflections as a function of ϕ . Only minor variation with scattering angle was found for these plots, and the average curve used to correct the intensities is given below as Figure 24. This semi-empirical

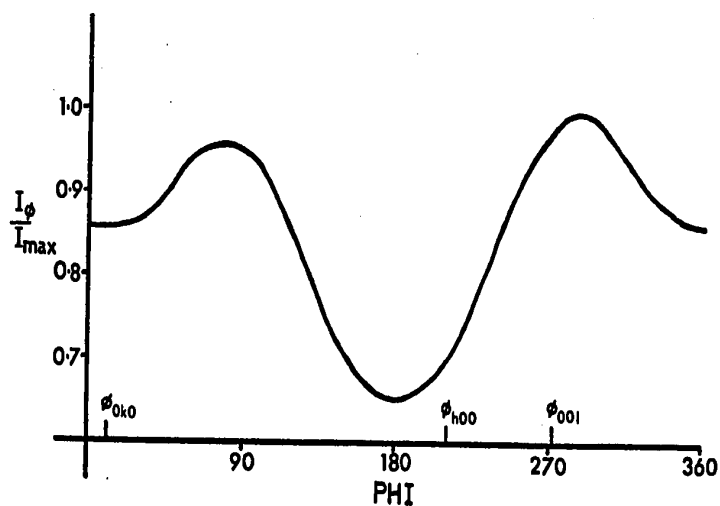


FIGURE 24

A plot of relative intensity versus ϕ for the maleic acid crystal. The ϕ value at which reflections from the principal axial rows were measured are marked.

absorption correction procedure is that of North, Phillips and Mathews⁽¹²⁷⁾.

Data reduction procedures included: (i) the calculation of observational weights according to the formula given above (page 19), (ii) interpolation of form factor curves derived from the coefficients of Cromer and Mann⁽⁴⁵⁾ for carbon and oxygen, and that of Stewart, Davidson and Simpson⁽⁷⁰⁾ for hydrogen, and (iii) application of the appropriate Lorentz and polarization corrections⁽⁴³⁾. The scattering factor tables for carbon and oxygen were corrected for the real part of the anomalous scattering effect by application of the terms $\Delta f'_C = 0.005$ electrons and $\Delta f'_O = 0.015$ electrons⁽⁵⁰⁾.

An approximate overall scale factor was derived by assuming that $|U|_{0.0.2} \doteq 0.9$ and equating Σf_s , where s is the $\sin \theta/\lambda$ value for 0.0.2, to $k|F_o|_{0.0.2}/|U|_{0.0.2}$. The 0.066 scale factor so derived differs by 41% from the value of 0.0389 in use at the end of the refinement.

Individual atom isotropic temperature factors of 3.5\AA^2 were assigned to carbon and oxygen atoms with the coordinates of Shahat and least-squares refinement initiated. Three unit-weighted block-diagonal cycles⁽⁵³⁾, with relaxation factors of 0.8, 0.9 and 0.7 respectively, followed by one unit-weighted full-matrix⁽⁴⁹⁾ least-squares calculation resulted in convergence of the isotropic model at $R = 24.8\%$. Two subsequent cycles with the reflection data weighted as before, but allowing the atoms anisotropic motion, reduced this residual to 8.7%. A difference electron density synthesis computed at this stage clearly revealed the hydrogen atoms as electron density maxima with peak heights ranging from 0.45 to 0.67 $e/\text{\AA}^3$. These atoms were assigned the final isotropic

temperature factors of the atoms to which they were bonded and included with fixed parameters in the next two refinement cycles which employed observational weights. Six reflections of exceptionally high intensity, and with small scattering angle, were considered to be effected by extinction and so were excluded from the next two, and subsequent, cycles. Two further cycles permitting the parameters of the hydrogen atoms to vary resulted in final convergence with the discrepancy indices R and R' having the values 5.04% and 7.31% respectively.

There are indications that this data set is of rather higher precision than would be implied by the above values, and it is hoped, at some future date, to further refine the present model using more sophisticated techniques^(128,129). The very low internal discrepancy index of 1.44% calculated from $R = \frac{\sum |F_{hk0}| - |F_{\bar{h}k0}|}{\sum |F_{hk0}|}$ for the 122 $hk0/\bar{h}k0$ pairs indicates that random errors of measurement are not major contributors to the final relatively high R factors. Systematic errors inherent in the individual spherical atom approach to structural analyses of molecular crystals are highlighted by Figure 25 which clearly indicates the unaccounted for electron density in the carbon-carbon bonds. This diagram and the more complete stereoscopic view given as Figure 26 have contour increments of $0.05 \text{ e}/\text{\AA}^3$ with base levels of $0.05 \text{ e}/\text{\AA}^3$ and $0.1 \text{ e}/\text{\AA}^3$ respectively. The standard error in this residual electron density map was calculated from the approximate formula of Cruickshank⁽¹³⁰⁾ (given below) to be $0.032 \text{ e}/\text{\AA}^3$.

$$\sigma_{\Delta\rho_{xyz}} = \frac{1}{V} \left[\begin{array}{ccc} +h & +k & +l \\ \Sigma & \Sigma & \Sigma \\ -h & -k & -l \end{array} (\sigma_{F_o})^2 \right]^{\frac{1}{2}}$$

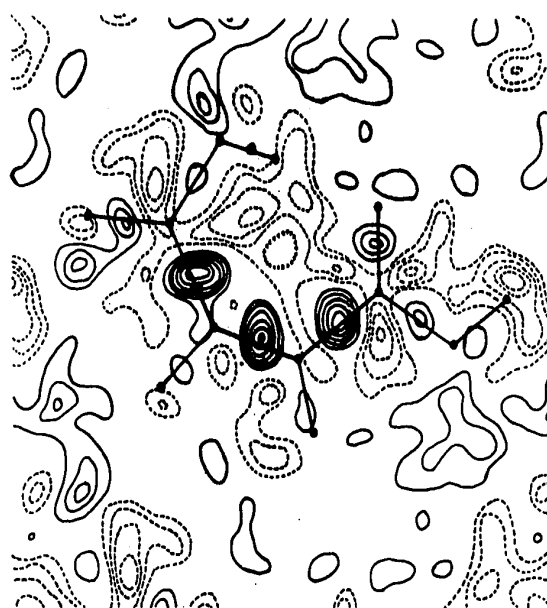


FIGURE 25

The molecular plane section of the final difference map. Reflections with $\sin \theta/\lambda$ greater than 0.9 were excluded from this calculation. Contours start at $\pm 0.05 \text{ e}/\text{\AA}^3$ and are in increments of this same amount.

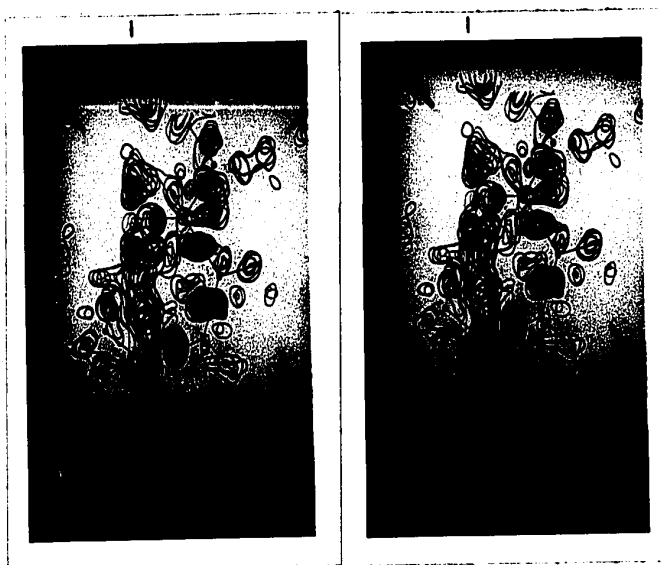


FIGURE 26

A stereoscopic pair of the final difference map. Red contours are negative and the atomic positions are shown. The base level is $0.1 \text{ e}/\text{\AA}^3$ and the increments are $0.05 \text{ e}/\text{\AA}^3$. Reflections with $\sin \theta/\lambda$ greater than 0.9 were excluded from the calculation of this map.

The set of observed structure amplitudes and the final calculated structure factors is presented as Table 29. The positional and thermal parameters used to describe the final model are given in Tables 30 and 31.

Results and Discussion

Figure 27 contains the bond distances and interbond angles for one maleic acid molecule as well as the numbering scheme used here. Estimated standard deviations in these parameters were derived by the independent atom method⁽⁵¹⁾ from the error estimates in the positional para-



FIGURE 26

A stereoscopic pair of the final difference map. Red contours are negative and the atomic positions are shown. The base level is $0.1 \text{ e}/\text{\AA}^3$ and the increments are $0.05 \text{ e}/\text{\AA}^3$. Reflections with $\sin \theta/\lambda$ greater than 0.9 were excluded from the calculation of this map.

The set of observed structure amplitudes and the final calculated structure factors is presented as Table 29. The positional and thermal parameters used to describe the final model are given in Tables 30 and 31.

Results and Discussion

Figure 27 contains the bond distances and interbond angles for one maleic acid molecule as well as the numbering scheme used here. Estimated standard deviations in these parameters were derived by the independent atom method⁽⁵¹⁾ from the error estimates in the positional para-

TABLE 29

A listing of the observed structure amplitudes and the final calculated structure factors. Excluded reflections are marked with an asterisk. These amplitudes have been multiplied by 10.

TABLE 30

Positional parameters for the atoms of one maleic acid molecule.

Atom	x/a	y/b	z/c
C(1)	0.9702(1)	0.3502(1)	0.2500(2)
C(2)	0.8087(2)	0.4346(1)	0.2492(2)
C(3)	0.6366(2)	0.3969(1)	0.2482(2)
C(4)	0.5930(2)	0.2634(1)	0.2493(2)
O(1)	0.9664(1)	0.2292(1)	0.2441(2)
O(2)	1.1199(1)	0.4191(1)	0.2551(2)
O(3)	0.3915(2)	0.2534(1)	0.2510(2)
O(4)	0.6510(1)	0.1558(1)	0.2518(2)
H(1)	1.2193(24)	0.3568(18)	0.2516(17)
H(2)	0.8375(26)	0.5322(22)	0.2602(17)
H(3)	0.5351(22)	0.4729(18)	0.2349(16)
H(4)	0.7627(27)	0.1765(21)	0.2397(21)

TABLE 31
Thermal motion parameters for the atoms of Table 30.

(a) The non-hydrogen atoms

Atom	β_{11}^*	β_{22}	β_{33}	β_{12}	β_{13}	β_{23}
C(1)	0.01729 (19)	0.00488 (7)	0.02872 (25)	-0.00030 (8)	0.01527 (19)	-0.00009 (9)
C(2)	0.01962 (20)	0.00411 (6)	0.03138 (28)	0.00022 (9)	0.01683 (21)	-0.00011 (10)
C(3)	0.01910 (20)	0.00477 (6)	0.03001 (26)	0.00114 (9)	0.01631 (20)	0.00012 (11)
C(4)	0.01762 (19)	0.00553 (7)	0.02847 (26)	0.00054 (9)	0.01566 (19)	0.00013 (10)
O(1)	0.02419 (22)	0.00471 (6)	0.04792 (33)	0.00038 (8)	0.02599 (24)	-0.00038 (10)
O(2)	0.02305 (20)	0.00593 (7)	0.04778 (33)	-0.00139 (9)	0.02535 (23)	-0.00044 (12)
O(3)	0.02403 (22)	0.00766 (8)	0.05029 (35)	-0.00006 (9)	0.02788 (25)	-0.00014 (13)
O(4)	0.02454 (20)	0.00468 (5)	0.04424 (30)	0.00004 (8)	0.02513 (22)	0.00042 (10)

(b) The hydrogen atoms

Atom	B_{iso}
H(1)	3.68 (28)
H(2)	4.65 (35)
H(3)	3.66 (29)
H(4)	5.08 (39)

* These coefficients are terms in the expression
 $\exp[-[h^2\beta_{11} + k^2\beta_{22} + l^2\beta_{33} + 2hk\beta_{12} + 2hl\beta_{13} + 2kl\beta_{23}]]$

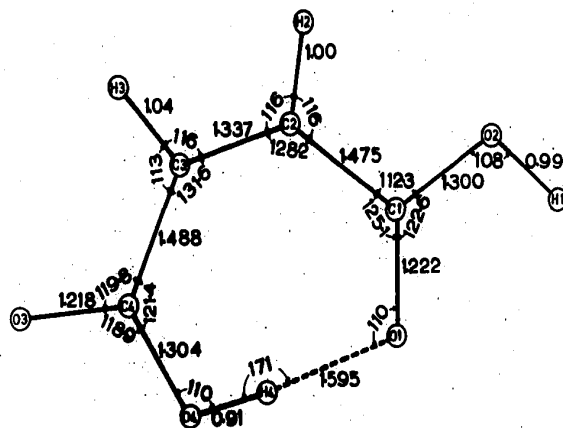


FIGURE 27

A diagram showing the numbering scheme, the bond distances and the interbond angles for maleic acid. Distances X-X and X-H have e.s.d.'s of 0.002 and 0.02Å respectively. Angles X-X-X, X-X-H and X-H-X have e.s.d.'s of 0.1, 1.0 and 1.7°.

meters. These latter error estimates were derived from the elements of the inverse matrix by the least-squares refinement program. The fact that the full matrix of normal equations was used for refinement means that the atomic position estimated standard deviations more closely approach reality than was the case for the structures refined by block-diagonal least-squares. The neglect of cross correlations in deriving the e.s.d.'s in the molecular parameters, however, means that these quantities are probably still underestimated and that they should be interpreted with caution. For this reason, only the average e.s.d.'s are given. Using X to denote a carbon or oxygen atom, then the distances X-X and X-H have average e.s.d.'s of 0.002Å and 0.02Å respectively. The angles X-X-X, X-X-H and X-H-X have associated error estimates of 0.1°,

1.0° and 1.7° respectively.

It will be noticed from Figure 27 that the results of Shahat are substantiated. In this analysis, the two carboxyl groups are not equivalent with respect to carbon-oxygen bonding pattern, and hydrogen atom H(4) is situated asymmetrically between oxygen atoms O(1) and O(4). That Donohue's postulate is also verified may be ascertained by studying the molecule packing diagram, Figure 28. The hydrogen atom utilised in the intermolecular hydrogen bond is along the line between O(2) and O(3) of molecules related by unit translation along a. This hydrogen bond has an O...O separation of 2.643(2)Å and an interbond angle at the hydrogen atom of 178(2)°. This length falls neatly between the 2.56 and 2.69Å values tabulated by Donohue for hydrogen bonds between an acidic OH as donor and an acidic O as acceptor.

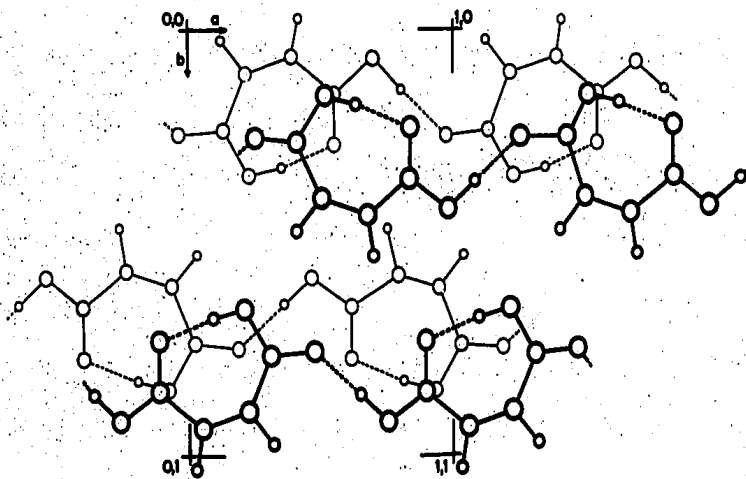


FIGURE 28

The molecular packing viewed parallel to the c^* direction.

A useful survey by Dunitz and Strickler⁽¹³¹⁾ contains the observed geometries of 17 carboxyl groups in aliphatic acids. In all of these examples one C-O bond is approximately 1.23Å in length and the other is about 1.31Å long, the exact averages being 1.229Å and 1.309Å respectively. In the present molecule, the two shorter carbon-oxygen bonds are insignificantly different from each other and average 1.220Å. The two longer bonds here are again statistically identical and their average is 1.302Å. The linkages from the ethylenic centre to the two carboxyl groups are 1.475Å and 1.488Å respectively for the donor groups in the inter- and intramolecular hydrogen bonds. The 0.013Å (ca. 6σ) difference is highly significant but bearing in mind the fact that these two quantities only differ by 3σ from their mean and that the σ's may well be in error by a factor of two, no meaningful comments relating to this difference can be made. This same conclusion was reached by Hecht-fischer et al.⁽¹¹⁸⁾ who gave their average for this distance as 1.49Å. In both of the two independent molecules of previous study, and in this work, however, the C(sp²)-C(sp²) bond to the carboxyl group bearing the intramolecularly hydrogen bonded hydrogen atom is longer (by 0.016, 0.007 and 0.013Å) than the other comparable linkage. This small difference may be indicative of some slightly preferred direction for π electron delocalization to occur, but any such speculations should be supported by evidence derived from an inspection of the C=O bond lengths. Consistent evidence for this hypothesis is not provided from these structures; thus, from the standpoint of the carbon atoms of the C=C bond, the two carboxyl groups must be regarded as being equivalent.

That little, if any, π electron delocalization from the ethylenic bond occurs may be inferred from the fact that the 1.337(2)Å found here and the 1.349(4)Å and 1.344(4)Å determined previously⁽¹¹⁸⁾ are not significantly different from the spectroscopic value of 1.335(5)Å⁽⁵⁵⁾ in simple compounds.

From the foregoing, it may be deduced that the bond distances of these strained species are not significantly different from those of similar molecules without any strain. Suitable compounds for comparison are fumaric acid (trans maleic acid)^(132,133) and acrylic acid (ethylene carboxylic acid)⁽¹³⁴⁾.

Some of the interbond angles, however, are quite different from expected values. The two C-C-OH angles are 112.3° and 121.4° at C(1) and C(4) respectively. Although slightly smaller than the 115° average for angles of this type tabulated by Dunitz and Strickler⁽¹³¹⁾, the angle C(2)-C(1)-O(2) is not greatly distorted. Angle C(3)-C(4)-O(4), on the other hand, is opened by 6.4° from the expected value. The most important difference between these angles is that the former is outside the strained ring, whereas the latter is subjected to the ring opening force imposed by the close contact (1.595Å) of H(4) and O(1). A normal non-bonded contact distance between hydrogen and oxygen atoms is ca. 2.6Å⁽⁶⁷⁾ and in hydrogen bonds of the more usual type these species are found 1.77Å apart on the average⁽⁶⁵⁾. Very similar comments can be made with respect to the two C-C=O angles. These are observed to have values of 119.8 and 125.1° respectively for the outer and inner angles of the ring. Dunitz and Strickler's values for this angle range from 119° to 126° with an average of 122.7°. The fact that the greatest

deviation from this average value is 2.6° , whereas a distortion of 6.4° was noted above for the C-C-OH angle, probably reflects the greater rigidity of the double bond. The third angle at the carboxylic carbon is that between the oxygen atoms and these have the values 122.6° and 118.9° for the carboxyl groups attached to C(2) and C(3). The expectation value for this angle is 122.3° and it can be seen from Figure 27 that the only one of these two angles which deviates significantly from this value is that involving the more easily deformable C-O single bond of the internal hydrogen bond. Severe opening of the internal C-C-C angles at C(2) and C(3) from the nominal value of 120° to ca. 130° is evident from Figure 27, but it must be pointed out that not all of this opening can be attributed to strain inherent in the cis dicarboxylic acid. Darlow⁽¹²⁰⁾ has estimated bond angles of the type C-C-COOH in unstrained molecules to be 121.5° . Values of 112.5 , 124.0 , 122.8 and 125.4° have been found for fumaric acid^(132,133) and the value for acrylic acid is 120° ⁽¹³⁴⁾. That there is some steric interference effect responsible for this, even in fumaric acid for example, is inferred from the oxygen-hydrogen contact distance of 2.4\AA which is some 0.2\AA less than the sum of their Van der Waals radii.

The non-hydrogen atoms of this molecule do not define a good plane. The best plane defined by this group as a whole has $\chi^2 = 2538.1$ and exo-planar deviations of up to 0.03\AA . The geometry of the maleic acid molecule is best described with respect to three planar segments made up from the carbon spine and those of the two carboxyl groups. Table 32 summarizes the results of several least-squares planes calculations. Only planes II, III and IV are good enough to be of importance here, and

TABLE 32

A results summary for the least-squares planes calculations of maleic acid.

(a) Distances from the planes ($\text{\AA} \times 10^4$)

Atom	I	II	III	IV	V	VI
C(1)	13*	7*	-44*	-132	-139*	-174*
C(2)	106*	-19*	14*	-139	77	-44*
C(3)	154*	19*	-248	-16*	239	102*
C(4)	23*	-9*	-776	57*	153*	76*
O(1)	332*	438	16*	361	167*	204*
O(2)	-275*	-307	12*	-539	-521	-564
O(3)	-91*	-155	-1129	-21*	151	43
O(4)	-190*	-97	-1089	-14*	-140*	-132*
H(1)	-83	-31	207	-269	-406	-390
H(2)	-549	-759	-402	-938	-581	-757
H(3)	1033	805	667	767	1194	990
H(4)	593	696	-103	723	562	585

* Atoms used to define the plane.

(b) Equations of the form $lx + my + nz - p = 0$ and χ^2 values for the planes

Plane	l	m	n	p	χ^2
I	-0.0001	0.0046	-1.0000	-1.5723	2538.1
II	0.0034	-0.0046	-1.0000	-1.5830	7.4
III	0.0179	0.0257	-0.9995	-1.3802	23.8
IV	-0.0018	-0.0097	-1.0000	-1.6191	34.9
V	-0.0094	0.0057	-0.9999	-1.6110	841.3
VI	-0.0064	-0.0002	-1.0000	-1.6097	1003.1

(c) Dihedral angles between the planes[†]

Plane	I	II	III	IV	V	VI
I	0	1.926	0.417	0.939	0.700	0.0
II		0	2.322	0.0	1.017	0.400
III			0	2.267	2.017	2.017
IV				0	0.959	0.0
V					0	0.500
VI						0

[†] Interplanar angles are measured in degrees.

from these it can be seen that the two carboxyl groups are individually planar and that the carbon spine of maleic acid also conforms to a plane. The two carboxyls, however, are not coplanar with this latter surface. In the case of the acid grouping bonded to C(2), the two oxygen atoms are on opposite sides of the plane of the carbon atoms, and the torsion angle about the O(2)-C(1)-C(2)-C(3) bond is 1.93° . The two oxygen atoms of the other carboxyl group are both displaced by small amounts towards the same side of the molecule's spine, the similar torsion angle in this case being -0.42° . These findings differ from those of Hechtfischer et al. where their molecules were both observed to have much larger torsion angles. In their study the two torsion angles equivalent to O(4)-C(4)-C(3)-C(2) of the present study had values of 5.06° and 17.7° , whereas their angles equivalent to O(1)-C(1)-C(2)-C(3) were 4.02° and 19.5° respectively. The two larger values were both from the same molecule and these authors attributed this large difference between the two molecules to different hydrogen bonding geometries of the two independent molecules.

That the thermal vibration ellipsoids have their major axes perpendicular to the molecular plane is evident from Figure 29. The sur-

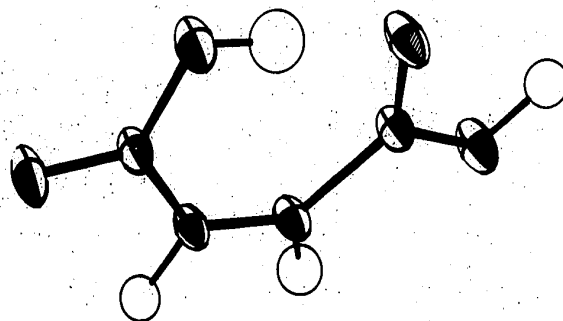


FIGURE 29

An ORTEP⁽⁶⁴⁾ drawing of one molecule.
Ellipsoid surfaces enclose 25% probability.

faces drawn enclose 25% probability that the centroid of the electron distribution is within the surface. The thermal motion ellipsoids were analyzed⁽⁶⁴⁾ with reference to an axial system coincident with that used for the calculation of the least-squares planes, i.e., a,b,c*. The various planes of the molecule were found to be very nearly parallel to (001), Table 32(b), and inspection of the direction cosines for the major axes of the ellipsoids under discussion, Table 33, reveals that the greatest deviation of a major axial direction from the normal to the molecular plane is 3.9°. The very similar sizes and shapes of these representational surfaces could well mean that the atoms of one molecule are undergoing some vibratory translation motion in concert; the predominating direction of this motion being perpendicular to the molecular plane. Further evidence for this assertion is taken from the comparatively large halos of diffuse scattering which surround the 00 λ reflections - particularly the very strong 0-0-2. This set of planes, incidentally, scatters X-radiation so efficiently that Dame Kathleen Lonsdale had cause to remark that its intensity was "very large indeed"⁽¹²⁵⁾.

That the ribbons of hydrogen bonded maleic acid molecules pack together edge-to-edge and that these sheets stack together to form a layer structure is indicated by Figure 28. Between the edges of the ribbons the attractive forces are of the normal Van der Waals type and need no special mention, but see later. The 3.144Å (twice the distance of plane l from the origin) separation of the layers, however, implies an interaction of rather greater interest. The literature pertaining to stacking interactions is, so far as the writer has been able to determine, concerned solely with aromatic molecules. The present substance is not aromatic and, as was noted above, does not even exhibit signifi-

TABLE 33

The root-mean-square displacements and direction cosines of the principal axes of the ellipsoids used to describe the thermal motion of the maleic acid atoms.

Atom	\bar{u}	i	j	k
C(1)	0.1566	-0.5833	-0.8109	-0.0476
	0.1630	-0.8091	0.5852	-0.0544
	0.2424	0.0720	0.0068	-0.9974
C(2)	0.1452	0.1182	-0.9930	-0.0015
	0.1733	-0.9908	-0.1178	-0.0668
	0.2534	0.0662	0.0094	-0.9978
C(3)	0.1488	-0.5179	0.8549	-0.0298
	0.1773	0.8540	0.5187	0.0401
	0.2476	-0.0497	0.0047	0.9988
C(4)	0.1570	-0.9085	0.4163	-0.0351
	0.1714	-0.4165	-0.9091	-0.0027
	0.2411	0.0330	-0.0122	-0.9994
O(1)	0.1528	-0.3936	0.9193	0.0006
	0.1717	0.9184	0.3932	0.0438
	0.3129	-0.0399	-0.0178	0.9990
O(2)	0.1552	0.8256	0.5614	0.0569
	0.1833	-0.5614	0.8274	-0.0173
	0.3127	-0.0568	-0.0177	0.9982
O(3)	0.1557	-0.9998	0.0037	-0.0180
	0.1989	-0.0036	-0.9999	-0.0071
	0.3204	0.0180	0.0070	-0.9998
O(4)	0.1551	-0.1502	-0.9885	0.0208
	0.1708	-0.9886	0.1503	-0.0001
	0.3005	-0.0030	-0.0205	-0.9998
H(1)	0.2161	1.0	0.0	0.0
H(2)	0.2426	1.0	0.0	0.0
H(3)	0.2154	1.0	0.0	0.0
H(4)	0.2536	1.0	0.0	0.0

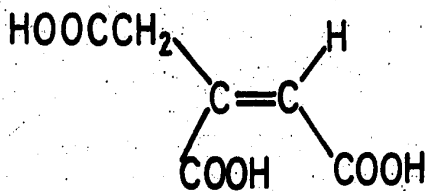
cant delocalization of the π electrons. However, the molecule is basically planar and does have three centres of π electron density, which facts may permit cautious interpretation in terms of the principles developed from other systems. Bugg et al.⁽¹³⁵⁾ have documented over 70 base stacking interactions in nucleic acid constituents and from their examination of these data determined that, (i) "the solid-state stacking apparently cannot be rationalized on the basis of permanent, molecular dipole-dipole interactions", and (ii) "...purine and pyrimidine stacking occurs with minimal ring overlap and involves interaction between a polar region of one base and the polarizable ring system of the other". This latter point particularly is closely related to an earlier observation that there seemed to be a specific interaction between carbonyl groups or other polarized multiple bonds and aromatic systems⁽¹³⁶⁾. Prout and Wallwork also suggested that there was often a competition between the tendency of molecules to maximize their π - π overlap and the interaction of polarized charge clouds with delocalized systems.

In the maleic acid structure there are no specific interactions between either non-polar C=C bonds or between a carbonyl function and the ethylenic centre. Figure 28 shows that the -CH=CH- part of the molecule is excluded from the overlap region and that the intra-ring area between the carboxyl groups has a carboxyl group [C(4), O(3), O(4)] on one side and a carbonyl group [C(1)=O(1)] on the other. These facts indicate that polar forces involving the carbon-oxygen bonds are the most important in stabilizing this crystal structure. Specific contributions to the binding energy are difficult to discern, but that between the approximately antiparallel C(4)-O(4) and C(1)-O(1) bond directions in adjacent sheets may be cited as an example, as may that between the C(4)-

O(4) and C(4)-O(3) bonds.

Within each stack of ribbons the donor \rightarrow acceptor directions for the hydrogen bonds are all approximately parallel rather than antiparallel and, with respect to the first, this common direction is reversed in moving along *b* to the next stack. This would imply an attractive force between the stacks and a repulsive force within them. This would explain the fact that it is extremely easy to cleave the crystals so as to expose a fresh (001) face or shear them perpendicular to c^* . Imperfect cleavage is observed parallel to (010) and this must be taken as evidence that dipolar forces are strengthening the Van der Waals attraction between the stacks.

In closing this section, several points may be made with respect to the final difference map. Apart from the expected finding that there is a build-up of electron density within the bonds and regions of negative density near the atoms but on the opposite sides from the bonds, Figures 25 and 26 show two interesting features. The first of these is that in all cases where significant maxima exist these are inside the cyclic structure, in just the positions where sp^2 hybridized orbitals would be expected to overlap. The angles between these maxima and the atomic positions were measured on a large scale version of this map to be close to 120° . This situation has been observed before, but not with such clarity, for the maleate mono-anion portion of dipotassium cis aconitate⁽¹³⁷⁾ (XXX).



(XXX). Cis aconitic acid

An accurate structural study of a cyclopropane derivative has provided an analogous result⁽¹³⁸⁾. The interbond angles in this latter study were 60°, but the angles between the electron density maxima, measured from the published figure, are 109°. The term "banana bonds" has been coined for this strain effect and it is tempting to apply the designation "inverted banana bonds" to the present case.

The second point of interest concerns the levels of electron density in the various bonds. The three carbon-carbon bonds have by far the greatest charge build-up with electron densities of greater than $0.25 \text{ e}/\text{\AA}^3$. Because the central bond is of order 2 and the others of single order, one might expect a greater electron density here. The fact that this is not so simply indicates that the π bond does not have significant electron density in the molecular plane. The two C=O bonds both have electron density maxima greater than those of the two C-O bonds, and all four bonds seem to have much lower residual electron density than is observed in the carbon-carbon bonds. This observation has been made before⁽¹³⁹⁾ but not discussed further at that time. A simple explanation of this effect could be that the very high electronegativity of oxygen, 3.5 on Pauling's scale⁽⁶⁷⁾, means that the electronic environment of the oxygen atoms is contracted and so this species more closely approaches a spherical atom than does a carbon atom. The observation that the electron density maxima in the C-O bonds of the present structure and in that of Hanson, Sieker and Jensen⁽¹³⁹⁾ are shifted towards the oxygen atom lends some support to this suggestion.

Maleic acid has the virtue of crystallizing in a centrosymmetric space group, and so phase angle errors are likely to be small in this or

subsequent more accurate work. Despite the twinning problem, crystals of the order of one millimeter should be obtainable and so this compound would seem to be a good candidate for a neutron diffraction study. A comparison of the results which would be obtained from such work and those obtainable from low temperature X-ray diffraction, together with those of the present room temperature study, may well prove to be of exceptional interest.

3.3 DISODIUM MALEATE

Experimental

Disodium maleate was prepared by adding an excess of NaOH pellets to a concentrated solution of maleic acid in water. On cooling and standing, the syrupy solution solidified into a mass of very tiny needles. A sample from this preparation was dissolved in DMSO with the addition of the minimum amount of water necessary. Acetone was then vapour diffused into the test tube containing the material and a great many very small crystals again resulted. Allowing firstly the acetone and then some of the water to evaporate by opening the vessel to the atmosphere, resulted in platy crystals of good quality.

An irregularly shaped specimen of maximum dimensions $0.5 \times 0.6 \times 0.08$ mm was mounted so as to rotate about an axis contained within the plate. Preliminary oscillation, Weissenberg and precession photography revealed $2/m$ diffraction symmetry and the systematic absences: $hk\ell$, $h+\ell = 2n+1$; $h0\ell$, $h = 2n+1$, $\ell = 2n+1$; $0k0$, $k = 2n+1$. These absences imply either Cc or $C2/c$ as the space group for this material. This ambiguity was resolved (see later) in favour of the centrosymmetric space group. The crystal was aligned on the diffractometer and the refined unit cell constants and orientation parameters obtained in the usual way. Table 34 contains the unit cell parameters and other data pertaining to this analysis. Graphite monochromatised Mo K radiation ($\lambda = 0.71069\text{\AA}$) was used for the data collection which utilized a $\theta/2\theta$ scan procedure over a basic peak width of 1.6° in 2θ and fixed position 10 second background counts on each side of the peak. Because it was desired to spend as little time as possible in fruitless irradiation of the crystal,

TABLE 34

A data summary for the structural analysis of disodium maleate monohydrate.

formula	$C_4H_2O_4 \cdot H_2O \cdot Na_2$
molecular weight	180.07 Daltons
crystal size	0.5 x 0.6 x 0.08 mm
space group	C2/c
a	20.979(4) Å
b	10.004(3) Å
c	6.369(1) Å
cos β	-0.1763(2)
β	100.15(1)°
V	1371.56 Å ³
Z	8
ρ_{calc}	1.744 gm/cm ³
ρ_{obs}	1.85(2) gm/cm ³
$\bar{\mu}$ (Mo. K α)	2.86 cm ⁻¹
2 θ range explored	3.5°-80°
no. unique reflections	4157
no. observed reflections	2871 (69.1% of total)
no. variable parameters	116
ratio observations/parameters	24.8
final unweighted R	3.30%
final weighted R	4.82%
mean sigma in C-C bond	0.001 Å
mean sigma in C-C-C angle	0.08°
standard deviation in difference map	0.084 e/Å ³

the B2/b rejection routine of the Picker software was modified (MNGJ) to exclude all of the systematic extinctions for space group C2/c. Data for this compound were again collected in two spherical annuli. The low θ data between $2\theta = 3.5^\circ$ and 60° were collected first and this was followed by examination of those reciprocal lattice points with scattering angle between 60° and 80° . Only insignificant intensity changes had occurred in the monitor reflections at the end of this data collection, but because 4157 data points had already been examined for this 15 atom structure, and because the majority of reflections in the outer shell were found to have low intensities, the data collection was terminated at this point. The same statistical tests as had been employed previously (page 74) were used to test the net counts of each reflection for significance. In this way, 2871 reflections were considered observed, the remainder being appropriately coded and excluded from all subsequent calculations except the generation of the normalised structure factors. Data reduction included Lorentz and polarization⁽⁴³⁾ corrections, and the calculation of observational weights according to the formula on page 19.

A three dimensional Patterson map, sharpened by the $1/L_p$ function for a zero level of reciprocal space, was computed and interpretation of this map attempted by the symmetry minimum method⁽⁶⁹⁾. Space group C2/c was assumed for this work on the basis of the correspondence between the 8-fold multiplicity for this group and the fact that the structure contains 8 molecules per unit cell. After several trial superpositions had failed to reveal the structure, the fallacious nature of the above assumption was realized and work aimed at solving the structure by direct

methods was initiated.

An approximate overall scale factor and average thermal vibration parameter were derived according to the procedure outlined above for the oxindole alkaloid (page 111) and these quantities used in the derivation of the set of normalized structure factors. The distribution statistics derived from these E's were compared with those expected from both centrosymmetric and non-centrosymmetric structures⁽¹⁰²⁾ and found to correspond more closely to the former case. These statistics and the values for comparison are listed below:

	<u>Observed</u>	<u>Centric</u> <u>(Theor.)</u>	<u>Acentric</u> <u>(Theor.)</u>
$\langle E \rangle$	0.815	0.798	0.886
$\langle E ^2 \rangle$	0.998	1.000	1.000
$\langle E ^2 - 1.0 \rangle$	0.962	0.968	0.736
Fraction with $ E > 3.0$	0.3%	0.3%	0.01%
Fraction with $ E > 2.0$	4.6%	5.0%	1.83%
Fraction with $ E > 1.0$	30.8%	32.0%	36.8%

Because of the C centering symmetry operation in this space group, half of the nominally distinct centres of symmetry become identical with the other half. This reduces the number of general reflections which may be assigned arbitrary phases from three for P cells to two. Preliminary hand phasing indicated that if the structure invariant $\phi_{8.0.0}$ ($|E| = 3.340$) could be assigned its correct phase, then assignment of origin specifying phases to the E's $\bar{5}.9.1$ ($|E| = 3.289$) and $\bar{2}4.4.3$ ($|E| = 2.807$) would probably allow the successful application of the symbolic addition procedure⁽¹⁰⁵⁾.

A sigma-one (Σ_1) relation allowed $\phi_{g.0.0}$ to be assigned the value π . This Σ_1 relation was derived by inspection from the general method given by Main⁽¹⁴⁰⁾. Starting from the general relation of Hauptman and Karle⁽¹⁴¹⁾:

$$s \{E_{2h.2k.2l}\} \approx s \{|E_{hk\bar{l}}|^2 - 1\} \quad [1]$$

where s means sign of and \approx is interpreted as probably equals, and applying the approximate relation⁽¹⁰⁵⁾:

$$\phi_{h.k.l} = \phi_{h-h'.k-k'.l-l'} + \phi_{h'.k'.l'} \quad [2]$$

to the $h0l$ zone, we can write:

$$\phi_{2h.0.2l} = \phi_{h.k.l} + \phi_{h.\bar{k}.l} \quad [3]$$

Now, for parity group 1 ($h+k = 2n, l = 2n$) of space group $C2/c$,

$$F_{(h.k.l)} = F_{(h.\bar{k}.l)} \neq F_{(\bar{h}.k.l)} \text{ and } F_{(\bar{h}.k.l)} = F_{(h.k.\bar{l})} \quad [4]$$

and for parity group 2 ($h+k = 2n, l = 2n+1$) the relations

$$F_{(h.k.l)} = -F_{(h.\bar{k}.l)} \neq F_{(\bar{h}.k.l)} \text{ and } F_{(\bar{h}.k.l)} = -F_{(h.k.\bar{l})} \quad [5]$$

hold⁽¹⁴²⁾.

From these the general relation

$$\cos(\phi_{h.\bar{k}.l}) = (-1)^l \cos(\phi_{h.k.l}) \quad [6]$$

may be verified. From equation [6] it can be seen that

$$\phi_{h.\bar{k}.l} = \phi_{h.k.l} + l\pi \quad [7]$$

but since $\phi_{h \cdot k \cdot l} = -\phi_{h \cdot k \cdot l}$ for centrosymmetric structures, equation [7] may be written

$$\phi_{h \cdot \bar{k} \cdot l} = -\phi_{h \cdot k \cdot l} + l\pi \quad [8]$$

Returning to equation [3] and substituting, we get

$$\phi_{2h \cdot 0 \cdot 2l} = l\pi \quad [9]$$

Now, since no assumptions have been made regarding the value of l , the indications obtained from equation [9] may be summed and inserted into equation [1], yielding

$$s \{E_{2h \cdot 0 \cdot 2l}\} = s \left\{ \sum_l (-1)^l (|E_{h \cdot k \cdot l}|^2 - 1) \right\} \quad [10]$$

and the appropriate probability formula is

$$P + \{E_{2h \cdot 0 \cdot 2l}\} = \frac{1}{2} + \frac{1}{2} \tan h \left\{ \frac{\sigma_3}{2\sigma_2^{3/2}} |E_{2h \cdot 0 \cdot 2l}| \sum_l (-1)^l (|E_{h \cdot k \cdot l}|^2 - 1) \right\} \dots [11]$$

In this last equation, σ_3 and σ_2 are defined by the relation

$$\sigma_n = \sum_{i=1}^N f_i^n \quad [12]$$

where f_i is the scattering factor for atom i at $\sin \theta/\lambda = 0$, and N is the number of atoms in one unit cell. For disodium maleate the quantity $\sigma_3 \cdot \sigma_2^{-3/2}$ has the value 0.1111.

Using equation [10], the reflections 8-0-0, 10-0-2 and 26-0-2 were found to have Σ_l totals of -6.51, -15.991 and -14.772 respectively. The

probability that this procedure assigned the correct phase in each case is 91.8%, 98.3% and 97.2%.

The five E's, $E_{8.0.0} = -3.340$, $E_{5.9.1} = +3.289$, $E_{24.4.3} = 2.807$, $E_{10.0.2} = -2.302$ and $E_{26.0.2} = 2.186$ were used as a starting set in the symbolic addition procedure programs of Ahmed and Hall⁽¹⁰¹⁾. All 189 reflections with $|E| > 2.0$ were correctly phased by program SAP4A⁽¹⁰¹⁾ and these large E's were then used to determine the phases of those normalized structure factors with magnitudes greater than 1.578. A Fourier synthesis using the 488 coefficients so defined clearly revealed, as the 11 largest peaks in the map, all non-hydrogen atoms of the structure.

A structure factor calculation based on the coordinates from the map in conjunction with scattering factor tables derived from the coefficients of Cromer and Mann, and assigning to each atom the overall temperature factor of the structure, returned an R factor of 21.2%. Two cycles of full-matrix and unit-weighted least-squares refinement of this isotropic model resulted in convergence at R = 10.88%. One cycle of full-matrix refinement with observationally weighted structure factors, and allowing the atomic temperature factors to assume their anisotropic form, reduced the conventional residual to 4.58%. Before least-squares refinement was continued, the model was changed in two respects:

- (i) Two small difference maps were computed around the regions where the hydrogen atoms were expected to occur. Four chemically sensible maxima of heights greater than $1.0 \text{ e}/\text{\AA}^3$ were found and these were included with the scattering factor curve of Stewart, Davidson and Simpson⁽⁷⁰⁾.

(ii) The oxygen atoms of the maleate di-anion were assigned an average $(0 + 0^{-1})/2$ scattering factor curve. The two curves which were averaged were those derived, as before, from the analytical coefficients of Cromer and Mann.

The hydrogen atoms were assigned the final isotropic temperature factor of the atom to which they were bonded and their parameters were allowed to vary during the next refinement cycle. The most dramatic parameter change (apart from that resulting from a punching error) in this cycle was in the scale factor. This quantity was observed to increase by 1.36% (13σ). That the scale factor was previously underestimated is evident from the physically unreal situation observed in the difference map where the hydrogen atoms were found to have peak heights of greater than $1 e/\text{\AA}^3$. Five reflections of high intensity and small scattering angle for which $F_o < F_c$ were removed from the data set, and least-squares refinement continued. Two further cycles on the above model resulted in final convergence. The decrease in $\Sigma w\Delta^2$ for this final cycle was 0.13%. The weighted and unweighted R factors from the final structure factor calculation over the included data are 4.82% and 3.30% respectively. A listing of the observed structure amplitudes and calculated structure factors is presented as Table 35.

The conformation of the disodium maleate di-anion found in this analysis is depicted in Figure 30 along with the numbering scheme adopted here. This diagram and the atomic parameters of Tables 36 and 37 constitute one facet of the description of the final model. In these tables and elsewhere O(5) is the water oxygen atom and its hydrogen atoms are designated OH(1) and OH(2).

TABLE 35

A listing of the observed structure amplitudes and final structure factors (absolute scale x 10) for disodium maleate monohydrate. Excluded reflections are marked with an asterisk.

Table with multiple columns containing alphanumeric codes and numerical values. The data is organized in a grid-like structure across the page.

Continued....

TABLE 36

Positional parameters for one unique portion
of the disodium maleate monohydrate structure.

Atom	x/a	y/b	z/c
Na (1)	0.06865 (2)	-0.08777 (4)	-0.05251 (6)
Na (2)	0.19473 (2)	0.24508 (4)	-0.23141 (6)
O (1)	0.04766 (3)	0.12301 (7)	0.07167 (11)
O (2)	0.08617 (3)	0.19681 (8)	-0.21138 (11)
O (3)	0.19700 (3)	0.31393 (7)	0.12467 (10)
O (4)	0.20558 (4)	0.53586 (8)	0.15176 (14)
C (1)	0.06585 (3)	0.21468 (8)	-0.04052 (12)
C (2)	0.05716 (4)	0.35364 (9)	0.03766 (15)
C (3)	0.10179 (4)	0.44445 (8)	0.11248 (15)
C (4)	0.17352 (4)	0.42990 (8)	0.13125 (12)
O (5)*	0.17796 (3)	0.13178 (8)	0.43795 (12)
OH(1)	0.2079 (9)	0.0890 (19)	0.4287 (29)
OH(2)	0.1776 (9)	0.1856 (21)	0.3370 (31)
H (2)	0.0105 (7)	0.3765 (14)	0.0346 (23)
H (3)	0.0868 (7)	0.5355 (16)	0.1625 (22)

* This is the oxygen atom of the water molecule; the two hydrogen atoms bonded to it are designated OH(1) and OH(2).

TABLE 37

The thermal vibration parameters used in the description of the final model for disodium maleate monohydrate.

Atom	(a) <u>The non-hydrogen atoms</u>					
	β_{11} *	β_{22}	β_{33}	β_{12}	β_{13}	β_{23}
Na(1)	0.00099(1)	0.00562(4)	0.01257(8)	0.00032(1)	0.00074(2)	-0.00010(4)
Na(2)	0.00087(1)	0.00535(4)	0.01281(8)	0.00004(1)	0.00060(2)	-0.00080(4)
O(1)	0.00122(1)	0.00448(6)	0.01587(15)	-0.00030(2)	0.00085(3)	0.00211(7)
O(2)	0.00113(1)	0.00758(7)	0.01263(14)	-0.00060(2)	0.00145(3)	-0.00302(8)
O(3)	0.00100(1)	0.00449(5)	0.01285(14)	0.00046(2)	0.00055(3)	-0.00007(6)
O(4)	0.00153(2)	0.00507(6)	0.02285(20)	-0.00126(2)	0.00236(4)	-0.00333(9)
C(1)	0.00062(1)	0.00369(6)	0.01034(14)	-0.00010(2)	0.00034(3)	-0.00041(7)
C(2)	0.00083(1)	0.00400(7)	0.01799(20)	0.00018(2)	0.00091(4)	-0.00128(9)
C(3)	0.00101(1)	0.00347(6)	0.01834(21)	0.0022(2)	0.00097(4)	-0.00218(9)
C(4)	0.00094(1)	0.00388(6)	0.00939(13)	-0.00213(2)	0.00073(3)	-0.00103(7)
O(5)	0.00104(1)	0.00659(7)	0.01537(16)	0.00019(2)	0.00132(3)	0.00040(8)

(b) The hydrogen atoms

Atom	Biso
OH(1)	4.45(40)
OH(2)	4.90(43)
H(2)	3.03(30)
H(3)	3.51(30)

* These coefficients are defined on page 152.

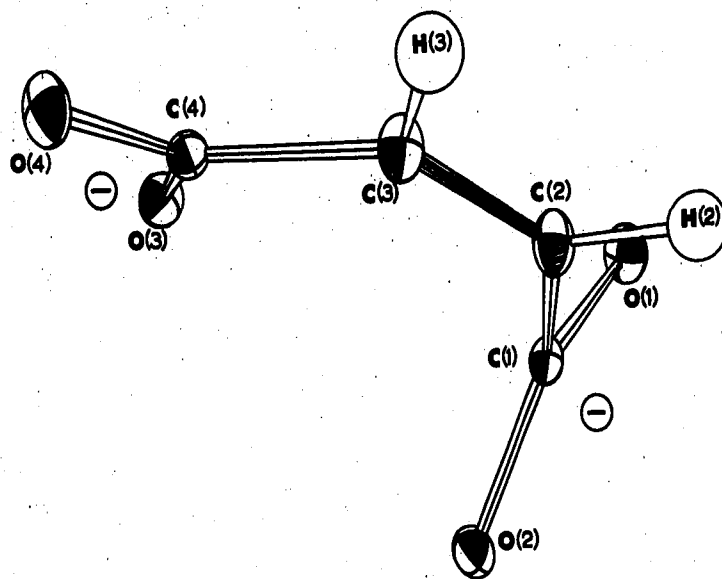


FIGURE 30

A computer produced diagram of one maleate di-anion showing the conformation assumed by the species and the numbering scheme of this analysis. The thermal ellipsoids are scaled to include 11.5% probability.

Results and Discussion

Bond distances and angles for this structure were derived as before from the atomic positional parameters; their estimated standard deviations average 0.001\AA and 0.02\AA for X-X and X-H respectively, and 0.1° and 1.0° for the angles X-X-X and X-X-H. The bond distances and angles within one maleate di-anion are given in Figure 31. The distances in the water of crystallization are $O(5)-OH(1) = 0.77(2)\text{\AA}$ and $O(5)-OH(2) = 0.86(2)\text{\AA}$ respectively, and the angle between these bonds is $100(2)^\circ$.

That the removal of the protons from the two carboxyl groups has resulted in some electronic reorganization within these groups is evident

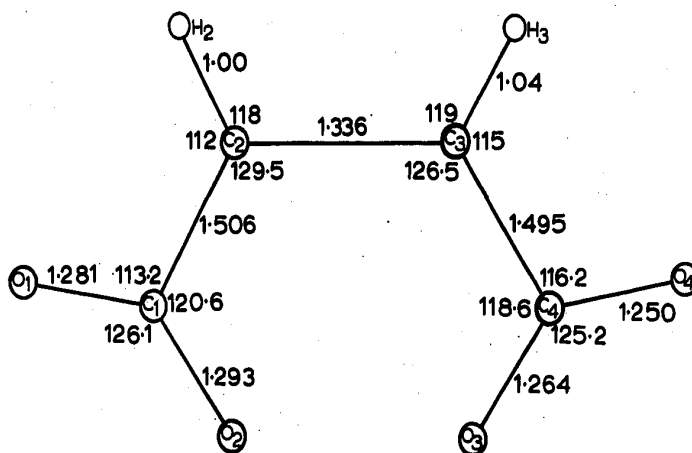


FIGURE 31

Bond distances and interbond angles for the maleate di-anion. Distances X-X and X-H have e.s.d.'s of 0.001Å and 0.02Å respectively. Error estimates for the angles X-X-X and X-X-H are 0.1° and 1.0°.

from a comparison of the carbon-oxygen bond lengths of the species presently under discussion with those obtained previously. The maleic acid molecules were found to exhibit two C=O bonds of length 1.220Å and two C-O single bonds 1.302Å long. Neither of these dimensions is exemplified here, but rather all four bonds are of intermediate length. This phenomenon of electronic redistribution upon ionization of a carboxyl group is well known and understood in terms of equal bond orders for the two carbon-oxygen linkages. In the present structure differences of 12 and 14 times the nominal 0.001Å e.s.d. in these bond distances are apparent, and a difference of 30σ is observed between the means of the C-O distances within each carboxyl group. Even allowing that the e.s.d.'s

are underestimated by 2/3 of their true value, these first differences are still significant and some explanation must be sought for them.

Figure 30 shows that when the molecule is viewed parallel to the plane of the carbon atoms and from the side which bears the hydrogen atoms, i.e., imagining the view from the top right-hand corner of the diagram, the carboxyl group O(1), C(1), O(2) is twisted with respect to the spine, and O(2) is closer to the molecular centre than is O(1).

This diagram also shows that the other carboxyl group is approximately coplanar with the carbon spine and that, from this aspect, O(4) is nearer the viewer than is O(3). With this information in hand, a careful examination of the molecular packing diagram, Figure 32, reveals several pertinent points:

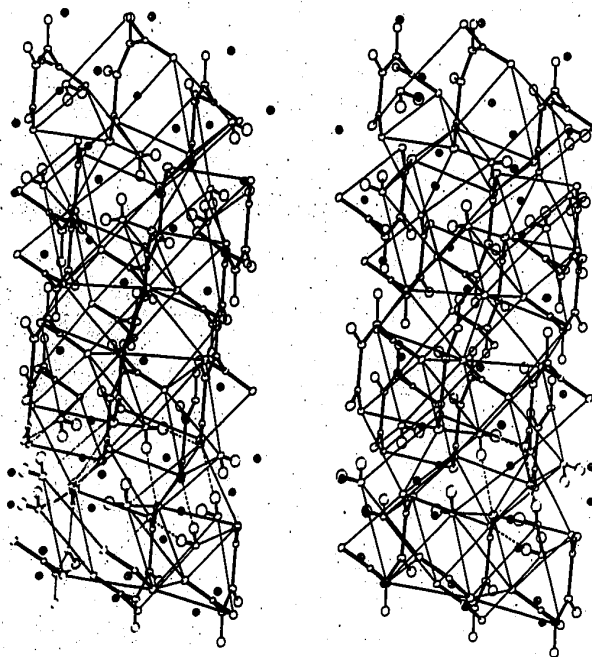


FIGURE 32

A stereoscopic pair diagram showing the crystal structure of disodium maleate monohydrate.

- (i) Oxygen atom O(1) is coordinated to three sodium ions and has approximate tetrahedral geometry.
- (ii) Oxygen atom O(2) is coordinated to two sodium ions and has approximate trigonal geometry.
- (iii) Oxygen O(3) is coordinated to two sodium ions and a water molecule and has approximate tetrahedral geometry.
- (iv) Oxygen O(4) is coordinated to one sodium ion and a water molecule and has approximate trigonal geometry.

For easy reference these facts are summarized in sketch form in Figure 33. Information derived from this analysis proves more confusing than enlightening. It would be expected that the sp^2 hybridized O(2) and O(4) atoms should exhibit the shorter of the two C-O bond lengths within their respective carboxyl groups. That this expectation is borne out only in one case is not understood at this time.

There are two major differences between the two carboxyl groups. The atoms O(3) and O(4) are both acceptor atoms in hydrogen bonds to the water molecule. These bonds surround the 2_1 screw axes parallel to (010) and link the di-anions in infinite helical chains parallel to the unique b axis. This hydrogen bonding scheme has been included in the lower right-hand group of molecules in Figure 32. The fact that these oxygen atoms accept some electron density from the water molecules would increase their bonding potential and shorten their linkages to C(4). The two hydrogen bonds are 2.785Å and 2.846Å long and have deviations from linearity of 20° and 12° respectively at the hydrogen atoms; they are therefore typical linkages of this type.

The second difference between the two carboxyl groups is that the

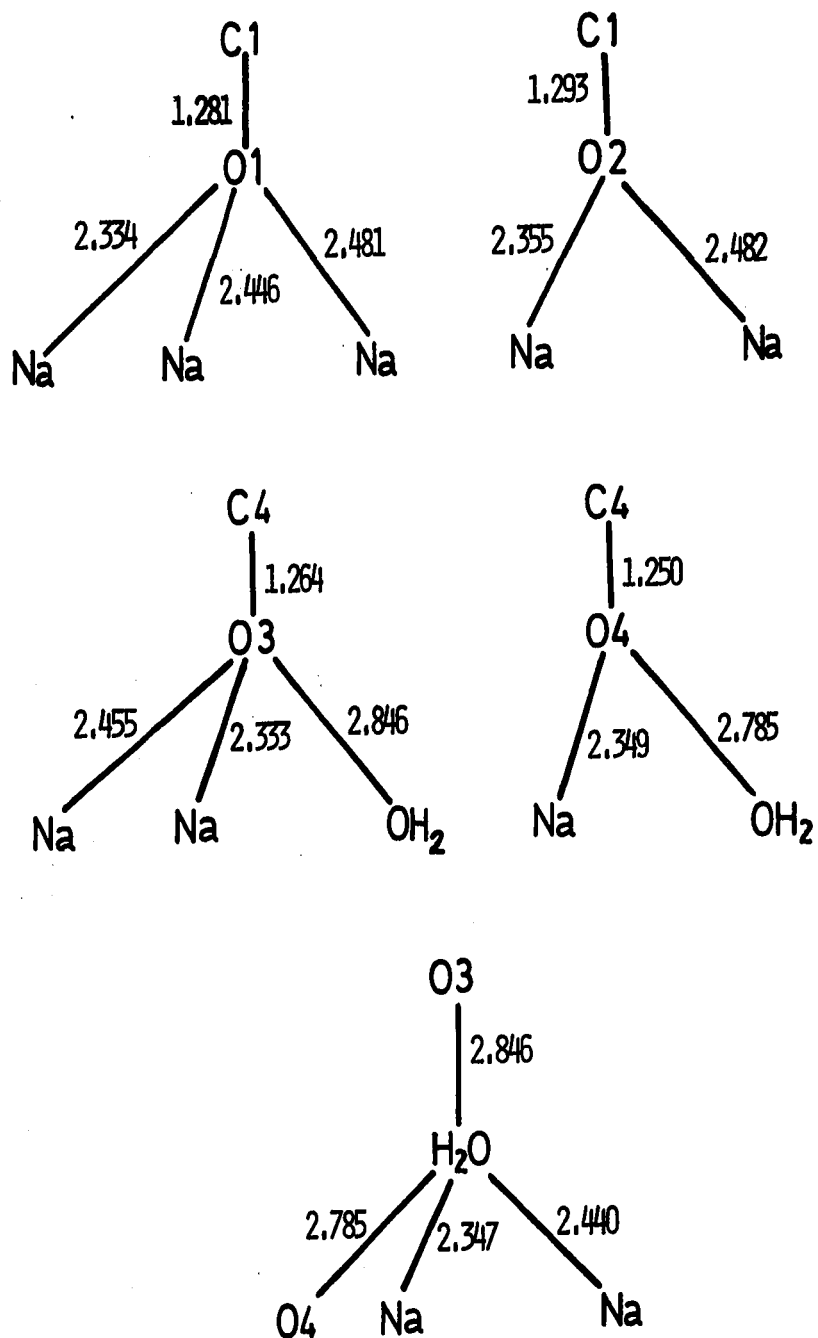


FIGURE 33

A diagrammatic representation of the environments of the five oxygen atoms of the disodium maleate monohydrate structure.

one exhibiting the shorter C-O bonds is much more nearly coplanar with the ethylenic system than is the other (see Table 38). Although this may be an important consideration, the marginal difference in C-COO distance (0.009\AA) would imply that little resonance occurs over the two π systems. The further fact that these two lengths are both slightly greater than the comparable bonds in maleic acid (1.482\AA average), where resonance was not considered important, also argues against significant π orbital interaction.

Deviations of the other molecular parameters from ideal values can, in part, be attributed to the mutual repulsion of the negatively charged centres and their attraction for the positive sodium ions. The two O-C-O angles are both significantly greater than 120° as are the angles at C(2) and C(3). The fact that the larger distortions are associated with that end of the molecule to which O(1) and O(2) are attached probably reflects the observation that these two oxygen atoms are involved in a total of five bonds to Na^+ ions, whereas O(3) and O(4) only participate in three such linkages.

Both independent sodium ions of this structure are five coordinate and reside in square pyramidal vacancies formed by oxygen atoms. Figure 34 presents the details of the coordination around Na(1) (part A) and Na(2) (part B). Coordination numbers ranging from 4 to 9 have been observed for either oxygen or fluorine bonding to Na^+ , but of the 38 citations by Shannon and Prewitt, only 7 were to compounds exhibiting coordination number 5, hexa-coordination was represented by 15 entries, and hepta-coordination was found for 7 compounds. According to the results of their survey, Shannon and Prewitt conclude that the effective

TABLE 38

A results summary for the least-squares planes for the maleate di-anion.

(a) Distances from the planes ($\text{\AA} \times 10^4$)

Atom	I	II	III
C(1)	-20*	-206*	7427
C(2)	70*	85*	3306
C(3)	-70*	-9263	5*
C(4)	22*	-22563	-13*
O(1)	-10389	64*	-639
O(2)	9988	73*	18470
O(3)	-3150	-27067	3*
O(4)	3346	-28340	5*
H(2)	-57	8584	2833
H(3)	-164	-7382	-2784

* Atoms used to define the plane.

(b) Terms in the equation $lx + my + nz - p = 0$ and χ^2 values for the planes

Plane	l	m	n	p	χ^2
I	0.1147	0.3558	-0.9275	1.1654	125.79
II	-0.8510	0.0400	-0.5236	-0.9748	1184.84
III	0.0846	0.0704	-0.9939	-0.2183	3.89

(c) Dihedral angles between the planes

Plane	I	II	III
I	0	16.9°	66.2°
II		0	63.1°
III			0

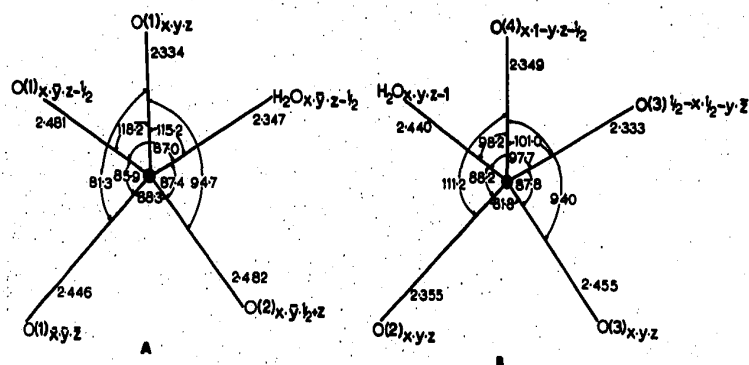


FIGURE 34

A sketch showing the distances and angles of the coordination pattern for the sodium ions. Part A refers to Na(1) and the environment of Na(2) is depicted in part B. Nominal e.s.d's for these parameters are 0.0008Å and 0.03°.

Ionic radius for penta-coordinated Na^+ is 1.00Å. Using the reference value of 1.40Å for O^{2-} (hexa-coordinated), the equilibrium Na-O distances may be expected to be about 2.40Å in length. The average of the ten Na-O distances in this structure is 2.402Å but there is a spread of $\pm 0.08\text{Å}$ about this mean value. No simple rationale has been discerned for this spread or for any one deviation from the expectation value.

That the ionic packing within this crystal structure is complex is readily appreciated from a study of Figure 32. This packing diagram is a view of the structure along a direction slightly displaced from the b axis. Using stereoscopic viewing glasses, the sodium ions (dark balls) may be seen to hang in space inside the square pyramidal volumes which their ligands define. One important bonding interaction which contri-

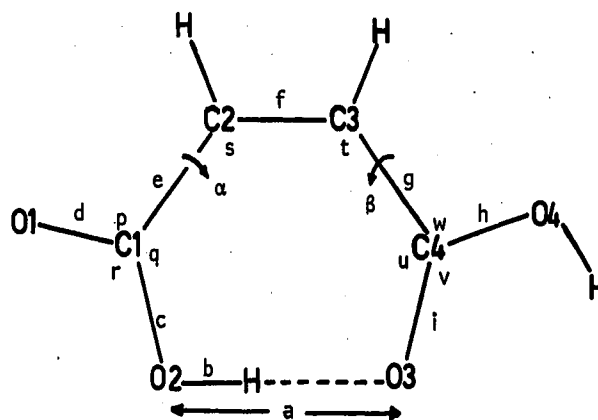
tributes to the binding energy of this structure is the hydrogen bond chain running nearly parallel to the viewer's line of sight near the bottom right-hand corner. Another, and probably more important, interaction is that between the various pyramids. Two members of a chain of alternately "up" and "down" pyramids of Na(1) coordination polyhedra sharing their O(2)-O(5) edges may be seen near the middle of the diagram and running from centre-left to top-right. That these pyramids are extensively distorted is evident from this diagram which also indicates one reason for the distortion. The face formed by the atoms O(1), O(5), O(1)' [where O(1)' is a symmetry equivalent to O(1)] of the left-most end of the chain just mentioned is seen to have O(2) overlying its centroid. This forces O(1) away from its (assumed) preferred position overlying the Na(1) ion and the centroid of the base, and accounts for the 115.2° and 118.2° angles for O(1)'-Na(1)-O(1) and O(5)-Na(1)-O(1) respectively. Other edge-to-edge contacts of the pyramids may be seen; two members of another alternating up--down--up chain, this time involving the coordination polyhedra of Na(2), may be seen running through the structure from the bottom-left corner to about 1/3 of the way up the right-hand side. The distortions of this pyramid are also fairly easily explained if it is noted that one edge of this polyhedron is formed by O(2) and O(3) from the same maleate di-anion. The fact that these two atoms are part of the same covalent structure imposes its constraints and a distorted pyramid results. No face sharing of these polyhedra exists but three pyramids do share a common vertex. Oxygen atom O(1) just slightly below the centre of symmetry in the middle of the structure is part of pyramids sharing their O(1)-O(1)' edge, and

situated one above the other (above and below here mean in the plane of the paper), as well as being at one vertex of an incomplete pyramid to the left.

A final point of interest with respect to this packing diagram is that the maleate di-anions are held together in an edge-to-edge manner by sodium ion and water molecule bridges. The water molecules and sodium ions occupy the spaces between the discontinuous sheets formed by this arrangement.

3.4 CONCLUSIONS

The structural information which is available for a total of nine maleic acid/maleate anionic species is summarized in Table 39, and the key to which these entries refer is given below in sketch (XXXI).



(XXXI) A key figure for use with reference to Table 39

The distances reported for $\text{KHC}\&\text{Ma}\&$ were corrected for the effects of thermal vibration according to the riding motion approximation⁽¹¹⁰⁾. No other entries in Table 39 were corrected for these effects.

The first three compounds in the tabulation refer to the fully protonated form of maleic acid. Remarkable constancy of the various bond distances and interbond angles for this species is evident from these entries, and indicates that the molecular environment is not, with one exception, an important factor in determining its geometry. The largest variation within the three maleic acid systems is in the torsion angle about the C-COOH bonds. The smallest value given is 0.0° for the car-

TABLE 39

A summary of the geometry of maleic acid/maleate anion structures.

(a) Distances											
Compound	a	b	c	d	e	f	g	h	i	σ_{X-X} (Å)	Ref.
H ₂ Mat	2.504	0.91	1.304	1.218	1.488	1.337	1.475	1.300	1.222	0.002	This work
tricyclic alkene acid	2.472	0.78	1.297	1.225	1.492	1.349	1.485	1.300	1.221	0.004	118
	2.512	1.03	1.305	1.219	1.503	1.344	1.487	1.310	1.225		
Brompheniramine HMat ⁻	2.417	1.08	1.292	1.209	1.497	1.329	1.481	1.230	1.265	0.006	This work
Chlorpheniramine HMat ⁻	2.444	0.87	1.280	1.209	1.489	1.331	1.486	1.236	1.266	0.006	This work
KHMat	2.437	1.22	1.284	1.235	1.498	1.348	1.498	1.235	1.284	0.004	120
KHClMat	2.411	1.207	1.284	1.230	1.524	1.349	1.512	1.244	1.288	0.002	121
cis aconitate	2.425	1.13	1.291	1.235	1.485	1.345	1.519	1.230	1.287	0.002	137
Na ₂ Mat	3.151	-	1.293	1.281	1.506	1.336	1.495	1.250	1.264	0.001	This work
mean H ₂ Mat	2.496	0.91	1.302	1.222	1.494	1.343	1.482	1.303	1.223		
mean HMat ⁻	2.427	1.10	1.286	1.223	1.499	1.340	1.499	1.235	1.278		

(b) Angles												
Compound	p	q	r	s	t	u	v	w	α	β	σ (°)	Ref.
H ₂ Mat	119.8	121.4	118.9	131.6	128.2	125.1	122.6	112.3	0.0	2.3	0.1	This work
tricyclic alkene acid	118.8	121.4	121.4	131.4	127.3	124.9	119.7	113.7	5.1	4.0	0.2	118
	119.0	120.6	122.3	130.5	127.3	124.2	120.4	113.5	17.7	19.5		
Brompheniramine HMat ⁻	118.6	119.3	122.1	131.0	130.2	119.9	123.2	116.9	8.4	6.7	0.4	This work
Chlorpheniramine HMat ⁻	118.8	120.3	120.9	131.5	129.8	120.0	123.4	116.7	1.5	7.4	0.2	This work
KHMat	117.0	120.3	122.7	130.4	130.4	120.3	122.7	117.0	0.0	0.0	0.2	120
KHClMat	118.0	118.6	123.3	130.6	129.5	120.3	122.7	117.0	8.5	9.0	0.1	121
cis aconitate	117.1	120.9	122.0	132.9	126.9	119.6	121.7	118.7	12.5	7.1	0.2	137
Na ₂ Mat	113.2	120.6	126.1	129.5	126.5	118.6	125.2	116.2	66.3	-16.9	0.1	This work
mean H ₂ Mat	119.2	121.1	120.9	131.2	127.6	124.7	120.9	113.2				
mean HMat ⁻	117.9	119.9	122.2	131.3	129.4	120.0	122.7	117.2				

boxyl group bearing the intramolecularly hydrogen bonded hydrogen atom in maleic acid; and the largest (19.5°) is for the intramolecular hydrogen bond accepting carboxyl group in one of the two independent molecules in Hechtfisher and co-workers' tricyclic alkene diacid. Other entries in the table imply that non-zero values of the same sign are to be expected for the two torsion angles and that the above two values are unusually small and large respectively. That these torsion angles are highly variable quantities is apparent from an examination of the table. The amounts by which the carboxyl groups are twisted out of the plane of the carbon spine does not seem to be correlated with the oxygen-oxygen separation across the intramolecular hydrogen bond. The suggestion of Hechtfisher and co-authors that the large difference in this parameter between their two molecules was the result of different inter- rather than intramolecular forces seems attractive, since it is difficult to explain the wide variation of these angles on intramolecular grounds. Table 32 indicates that the two oxygen atoms involved in the intramolecular hydrogen bond [O(1) and O(4) in the numbering system there] of the maleic acid molecule are not on the same side of the carbon spine. This is an unexpected result if one accepts the above generality that α and β should have the same sign. Intermolecular attractive forces arising in part from the interaction of the C(4)-O(4) single bond with other C-O bonds in another layer were postulated above, and it is thought that these interactions are probably strong enough to pull O(4) down slightly below the molecular plane, so that its equilibrium position is on the same side of this plane as is O(3). Thus, apart from the doubtful case of potassium hydrogen maleate, it is seen that the

maleic acid and the maleate mono-anion both have some of their molecular strain relieved by rotations of the carboxyl groups about their C-C bonds. It is difficult to understand why these deformations are such as to place the two oxygen atoms of the intramolecular hydrogen bond on the same side of the plane of the carbon atoms, but the general nature of this effect cannot be denied.

The tentative generality suggested above - that the two C-COO linkages of these species were not the same - seems, at first sight, to be borne out here. With the only exceptions cis aconitate and KHMa^{\ominus} , distance e is greater than its counterpart g. The last two entries in the summary table are the average values for the unionized and singly ionized forms of maleic acid. The HMa^{\ominus} entry indicates that for this species distances e and g are equivalent. The differences in these quantities for maleic acid have already been discussed (page 155) where it was concluded that supporting evidence for the existence of a preferred direction for electronic resonance to occur was not available from other bond lengths within the molecule.

A more consistent difference between molecular parameters which would be expected to be equivalent is that involving angles s and t. Table 39(b) shows that in all nine structures angle s is greater than angle t. This observation is again difficult to explain, particularly in view of the fact that in maleic acid the smaller angle (t) is at one of the two carbon atoms between two cis π electron clouds and would, on a charge repulsion basis, be expected to be larger than s where the two double bonds are trans with respect to bond e. It is worth pointing out in this context that angle s is invariant in all three species, whereas t increases by ca. 2° when the "exocyclic" proton is removed,

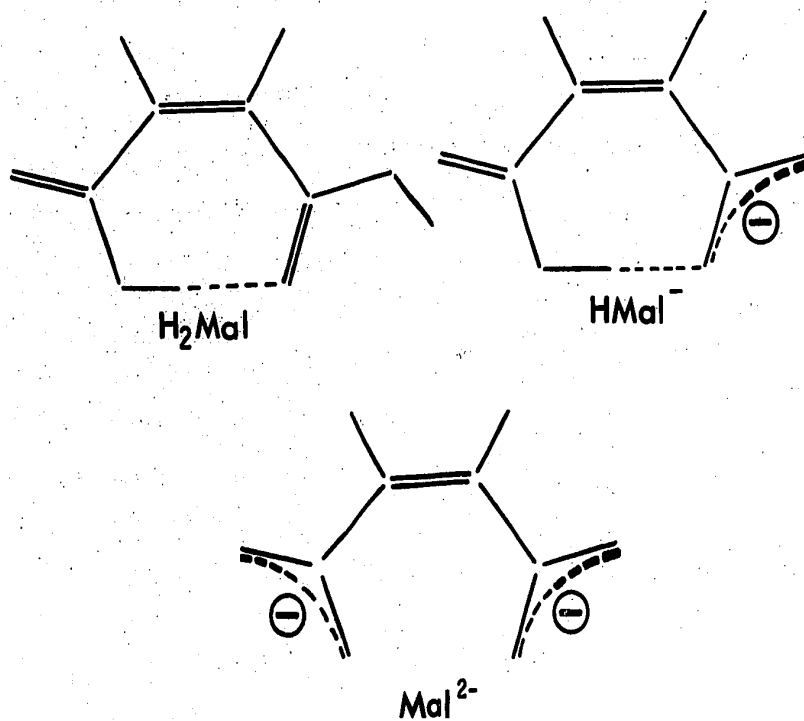
and then decreases by 3° at the second ionization step. This decrease is possibly due to the fact that bond *l* changes character considerably when the intermolecular hydrogen bonding hydrogen atom is removed.

In the average $H_2Ma\lambda$ structure, *l* is 1.223\AA in length and typifies a normal carboxylic $C=O$ bond; *h* is 1.303\AA in length and is therefore a normal C-O bond of the type found in carboxylic acids. Upon ionization it appears that *l* and *h* exchange roles - the higher bond order being now associated with *h*. This would mean that, with respect to C-O bond order, atoms O(2) and O(3) become more similar and would therefore exert more nearly equal attractions for the hydrogen atom. This would result in a moving inwards of both O(3) and C(4) with the concomitant decrease in angle *t* and a movement of the proton towards the centre of the O-O bond. The subsequent increase in angle *t* when the second base dissociable proton is removed is thought to be the result of ionic repulsive forces between the two carboxylate anions. Corroborative evidence for these assertions is provided by an examination of the O(2)-O(3) separation as a function of net charge on the species. Distance *a* is seen to decrease at the first ionization (and *b* increases) but then increase to 3.151\AA when the second proton is removed. Distance *d* changes from 1.222 in $H_2Ma\lambda$ and $HMa\lambda^-$ to 1.281 in $Ma\lambda^{2-}$, and as well as this change atom O(1) shifts its position relative to the rest of the ion, so that angle *p* decreases by ca. 6° and angle *r* increases by a like amount. Since *c* and *d* are of similar magnitude in the $Ma\lambda^{2-}$ ion, it would be expected that angles *p* and *q* would also be similar. The fact that they differ by 7° was attributed in the disodium maleate results and discussion section to their different ionic environments, and this

"explanation" is adhered to here.

Throughout all of these changes in the geometry and charge on the system, several quantities remain constant. The length of the C=C bond (f) is one such parameter which shows little variation. Another fixed geometrical parameter seems to be angle s which has values 131.2° , 131.3° and 129.5° respectively for H_2Mal , $HMal^-$ and Mal^{2-} . Angle q , which is the C-C-O angle to the single bonded oxygen atom of the hydrogen donor carboxyl group in the intramolecular hydrogen bond, also remains constant as the protons are removed.

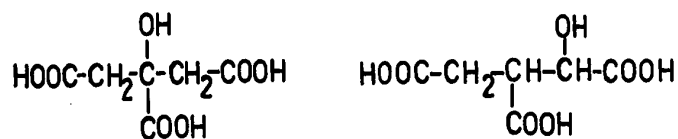
Unfortunately it cannot be said that the results herein discussed have explained the problem of the symmetric/asymmetric hydrogen bond. Apart from the facts presented in Table 39, the main result of this work is given below in sketch form wherein attempt is made to depict the most probable electronic configurations for the H_2Mal , $HMal^-$ and Mal^{2-} species.



(XXXII) Probable valence electron distributions

Future crystallographic work in this system would be valuable particularly for the HMal^- and Mal^{2-} species. It is suggested that an investigation of the effect of the cation on the structure by studying the Li_2Mal and/or the K_2Mal structures could well determine whether the conformation of the anion adopted here is an intrinsic property of the species or is forced upon it by various packing forces. A set of satisfying theoretical calculations for this system which made no assumptions regarding the symmetry of the species would also be helpful in understanding this system.

An interesting offshoot of this work is in the relationship it has to the work of Glusker et al. on the substrates of the enzyme aconitase (137,143). This protein is a metallo (Fe^{2+}) enzyme active in the tri-carboxylic acid cycle in the inter-conversions of citrate, isocitrate (XXXIII), and cis aconitate (XXX) (144).



(XXXIII) Two substrates of the enzyme aconitase

In Glusker's proposal (145) for the mechanism of aconitase activity, the citrate or isocitrate species are bound to the ferrous ion through a central and a terminal carboxylate ion. The coordinate linkages to the enzyme are assumed to be via an axial and an equatorial position at the metal ion. With these two linkages to the protein and a third via the remaining terminal carboxyl function, it is presumed that the iron atom

rotates on its axis by about 90° . This process would first expose one surface of the bound substrate to the enzyme and then the other.

Detailed arguments relating to the known stereospecificity of the substrate(s) and product(s) follow, but for the purposes of this comment it is sufficient to note that the proposed mechanism depends upon the Mg^{2+} portion of the enzyme bound intermediate (cis aconitate) being able to accommodate the suggested conformational change. The present study has shown that the maleate di-anion can adopt a non-planar conformation and so supports Glusker's contention. One minor point remains to be clarified: In Glusker's original drawings one carboxyl group was always approximately coplanar with the ethylenic bond, whereas in her most recent paper⁽¹⁴³⁾ seemingly equal torsion angles (α and β of sketch XXXI) are proposed. Because of the result found here where approximate coplanarity of one carboxyl group is retained and the other is rotated through a large angle, it is felt that the earlier drawings probably more closely represent the truth.

PART 4
Computer Programs Used

4.1 INTRODUCTION

The set of crystallographic programs of F.R. Ahmed et al. (51) of the National Research Council of Canada, Ottawa, were used throughout the course of this work. This set provided an excellent nucleus for the solution, refinement and analysis of crystal structures, but where appropriate the FORTRAN coding of other people was used as well. References to such other programs as ORFLS, ORTEP, and SUPER (P.D. Cradwick) are incorporated into the body of this thesis.

Several FORTRAN programs, useful in X-ray crystallography, and in general use in this laboratory, were written by the author and are described below. As well as these new programs, significant modifications to two of the N.R.C. programs were done by the author and these are also described below.

4.2 ALPHA

The utility of this program lies in its ability to translate the set of numbers which comprise a Fourier map (electron density, vector synthesis or difference map) into an equivalent set of single characters. By a suitable choice of map grid it is possible to obtain printed sections which are true to scale, of sufficiently fine resolution, and of manageable size.

Both the set of alphanumeric characters to be used for the compressed map and the range to which these correspond are set by the user. Also, under the control of the user are the FORMAT specifications which control the printed output.

A complete listing of the FORTRAN coding of this program is given below.

4.3 CROMERCURVE

The most recently published sets of atomic scattering factors have been made available in the form of a tabulation of analytical coefficients from which the curves may be derived. The evaluation of these curves from the coefficients is the primary purpose of this program, although several ancillary functions may be invoked as well.

The scattering power curve $[\sum n f(s)^2]$ may be calculated for the user's unit cell contents as may the quantities $\sigma_1, \sigma_2, \sigma_3, \sigma_4, \sigma_3 \cdot \sigma_2^{-3/2}$. Corrections to the curves for anomalous dispersion may be applied and the $\Delta f'$ and $\Delta f''$ terms may be made linear functions of $\sin \theta/\lambda$.

Provision has been made for punching the curves in forms suitable to be read by any or all of the programs NRC2, ORFLS and SFLS5.

A listing of the program is reproduced below.


```

C PROGRAM 'FORMCURVE' CC 10
C TO CALCULATE SCATTERING FACTOR CURVES IN HRC, OPL, L, AND MFLS FORMATS CC 20
C FROM THE MOST RELATIVISTIC HARTREE-FOCK CALCULATIONS OF DON T. CROMER CC 40
C ACTA CRYST. INT. PART. 1965 6:217-234B MAR 65 CC 60
C ***** MODIFIED TO CALCULATE SIGMAS FOR DIRECT METHOD PROBABILITY CC 80
C COMPUTATIONS AND NEW/99 S=J.F CC 90
C ***** CC 95
DIMENSION A(4,10),B(4,10),C(10),TITLE(10),ICURVE(10),F(10,10) CC 100
DIMENSION DICURVE(10),FPM(10) CC 110
DIMENSION DMAL(10),FPMAL(10),DIMAG(10),FPMAG(10) CC 120
DIMENSION F(10,10),FANOM(10) CC 130
INTEGER IANOM,IPUNCH,IPRINT CC 140
REAL*8 READ*8 CC 150
PRINT*8 CC 160
READ(READ,*)MCC,ICURVE CC 170
DO 2 I=1,MCC/2 CC 180
  READ(READ,*)TITLE(I),A(I,1),B(I,2),C(I),D(I),E(I) CC 190
  2 CONTINUE CC 200
90 FORMAT(10,*) CC 210
91 FORMAT(10,*) FANOM(1),FPM(1),FPMAL(1),DIMAG(1),FPMAG(1) CC 220
92 FORMAT(10,*) FANOM(2),FPM(2),FPMAL(2),DIMAG(2),FPMAG(2) CC 230
93 FORMAT(10,*) FANOM(3),FPM(3),FPMAL(3),DIMAG(3),FPMAG(3) CC 240
94 FORMAT(10,*) FANOM(4),FPM(4),FPMAL(4),DIMAG(4),FPMAG(4) CC 250
95 FORMAT(10,*) FANOM(5),FPM(5),FPMAL(5),DIMAG(5),FPMAG(5) CC 260
96 FORMAT(10,*) FANOM(6),FPM(6),FPMAL(6),DIMAG(6),FPMAG(6) CC 270
97 FORMAT(10,*) FANOM(7),FPM(7),FPMAL(7),DIMAG(7),FPMAG(7) CC 280
98 FORMAT(10,*) FANOM(8),FPM(8),FPMAL(8),DIMAG(8),FPMAG(8) CC 290
99 FORMAT(10,*) FANOM(9),FPM(9),FPMAL(9),DIMAG(9),FPMAG(9) CC 300
100 FORMAT(10,*) FANOM(10),FPM(10),FPMAL(10),DIMAG(10),FPMAG(10) CC 310
101 FORMAT(10,*) FANOM(11),FPM(11),FPMAL(11),DIMAG(11),FPMAG(11) CC 320
102 FORMAT(10,*) FANOM(12),FPM(12),FPMAL(12),DIMAG(12),FPMAG(12) CC 330
103 FORMAT(10,*) FANOM(13),FPM(13),FPMAL(13),DIMAG(13),FPMAG(13) CC 340
104 FORMAT(10,*) FANOM(14),FPM(14),FPMAL(14),DIMAG(14),FPMAG(14) CC 350
105 FORMAT(10,*) FANOM(15),FPM(15),FPMAL(15),DIMAG(15),FPMAG(15) CC 360
106 FORMAT(10,*) FANOM(16),FPM(16),FPMAL(16),DIMAG(16),FPMAG(16) CC 370
107 FORMAT(10,*) FANOM(17),FPM(17),FPMAL(17),DIMAG(17),FPMAG(17) CC 380
108 FORMAT(10,*) FANOM(18),FPM(18),FPMAL(18),DIMAG(18),FPMAG(18) CC 390
109 FORMAT(10,*) FANOM(19),FPM(19),FPMAL(19),DIMAG(19),FPMAG(19) CC 400
110 FORMAT(10,*) FANOM(20),FPM(20),FPMAL(20),DIMAG(20),FPMAG(20) CC 410
111 FORMAT(10,*) FANOM(21),FPM(21),FPMAL(21),DIMAG(21),FPMAG(21) CC 420
112 FORMAT(10,*) FANOM(22),FPM(22),FPMAL(22),DIMAG(22),FPMAG(22) CC 430
113 FORMAT(10,*) FANOM(23),FPM(23),FPMAL(23),DIMAG(23),FPMAG(23) CC 440
114 FORMAT(10,*) FANOM(24),FPM(24),FPMAL(24),DIMAG(24),FPMAG(24) CC 450
115 FORMAT(10,*) FANOM(25),FPM(25),FPMAL(25),DIMAG(25),FPMAG(25) CC 460
116 FORMAT(10,*) FANOM(26),FPM(26),FPMAL(26),DIMAG(26),FPMAG(26) CC 470
117 FORMAT(10,*) FANOM(27),FPM(27),FPMAL(27),DIMAG(27),FPMAG(27) CC 480
118 FORMAT(10,*) FANOM(28),FPM(28),FPMAL(28),DIMAG(28),FPMAG(28) CC 490
119 FORMAT(10,*) FANOM(29),FPM(29),FPMAL(29),DIMAG(29),FPMAG(29) CC 500
120 FORMAT(10,*) FANOM(30),FPM(30),FPMAL(30),DIMAG(30),FPMAG(30) CC 510
121 FORMAT(10,*) FANOM(31),FPM(31),FPMAL(31),DIMAG(31),FPMAG(31) CC 520
122 FORMAT(10,*) FANOM(32),FPM(32),FPMAL(32),DIMAG(32),FPMAG(32) CC 530
123 FORMAT(10,*) FANOM(33),FPM(33),FPMAL(33),DIMAG(33),FPMAG(33) CC 540
124 FORMAT(10,*) FANOM(34),FPM(34),FPMAL(34),DIMAG(34),FPMAG(34) CC 550
125 FORMAT(10,*) FANOM(35),FPM(35),FPMAL(35),DIMAG(35),FPMAG(35) CC 560
126 FORMAT(10,*) FANOM(36),FPM(36),FPMAL(36),DIMAG(36),FPMAG(36) CC 570
127 FORMAT(10,*) FANOM(37),FPM(37),FPMAL(37),DIMAG(37),FPMAG(37) CC 580
128 FORMAT(10,*) FANOM(38),FPM(38),FPMAL(38),DIMAG(38),FPMAG(38) CC 590
129 FORMAT(10,*) FANOM(39),FPM(39),FPMAL(39),DIMAG(39),FPMAG(39) CC 600
130 FORMAT(10,*) FANOM(40),FPM(40),FPMAL(40),DIMAG(40),FPMAG(40) CC 610
131 FORMAT(10,*) FANOM(41),FPM(41),FPMAL(41),DIMAG(41),FPMAG(41) CC 620
132 FORMAT(10,*) FANOM(42),FPM(42),FPMAL(42),DIMAG(42),FPMAG(42) CC 630
133 FORMAT(10,*) FANOM(43),FPM(43),FPMAL(43),DIMAG(43),FPMAG(43) CC 640
134 FORMAT(10,*) FANOM(44),FPM(44),FPMAL(44),DIMAG(44),FPMAG(44) CC 650
135 FORMAT(10,*) FANOM(45),FPM(45),FPMAL(45),DIMAG(45),FPMAG(45) CC 660
136 FORMAT(10,*) FANOM(46),FPM(46),FPMAL(46),DIMAG(46),FPMAG(46) CC 670
137 FORMAT(10,*) FANOM(47),FPM(47),FPMAL(47),DIMAG(47),FPMAG(47) CC 680
138 FORMAT(10,*) FANOM(48),FPM(48),FPMAL(48),DIMAG(48),FPMAG(48) CC 690
139 FORMAT(10,*) FANOM(49),FPM(49),FPMAL(49),DIMAG(49),FPMAG(49) CC 700
140 FORMAT(10,*) FANOM(50),FPM(50),FPMAL(50),DIMAG(50),FPMAG(50) CC 710
141 FORMAT(10,*) FANOM(51),FPM(51),FPMAL(51),DIMAG(51),FPMAG(51) CC 720
142 FORMAT(10,*) FANOM(52),FPM(52),FPMAL(52),DIMAG(52),FPMAG(52) CC 730
143 FORMAT(10,*) FANOM(53),FPM(53),FPMAL(53),DIMAG(53),FPMAG(53) CC 740
144 FORMAT(10,*) FANOM(54),FPM(54),FPMAL(54),DIMAG(54),FPMAG(54) CC 750
145 FORMAT(10,*) FANOM(55),FPM(55),FPMAL(55),DIMAG(55),FPMAG(55) CC 760
146 FORMAT(10,*) FANOM(56),FPM(56),FPMAL(56),DIMAG(56),FPMAG(56) CC 770
147 FORMAT(10,*) FANOM(57),FPM(57),FPMAL(57),DIMAG(57),FPMAG(57) CC 780
148 FORMAT(10,*) FANOM(58),FPM(58),FPMAL(58),DIMAG(58),FPMAG(58) CC 790
149 FORMAT(10,*) FANOM(59),FPM(59),FPMAL(59),DIMAG(59),FPMAG(59) CC 800
150 FORMAT(10,*) FANOM(60),FPM(60),FPMAL(60),DIMAG(60),FPMAG(60) CC 810
151 FORMAT(10,*) FANOM(61),FPM(61),FPMAL(61),DIMAG(61),FPMAG(61) CC 820
152 FORMAT(10,*) FANOM(62),FPM(62),FPMAL(62),DIMAG(62),FPMAG(62) CC 830
153 FORMAT(10,*) FANOM(63),FPM(63),FPMAL(63),DIMAG(63),FPMAG(63) CC 840
154 FORMAT(10,*) FANOM(64),FPM(64),FPMAL(64),DIMAG(64),FPMAG(64) CC 850
155 FORMAT(10,*) FANOM(65),FPM(65),FPMAL(65),DIMAG(65),FPMAG(65) CC 860
156 FORMAT(10,*) FANOM(66),FPM(66),FPMAL(66),DIMAG(66),FPMAG(66) CC 870
157 FORMAT(10,*) FANOM(67),FPM(67),FPMAL(67),DIMAG(67),FPMAG(67) CC 880
158 FORMAT(10,*) FANOM(68),FPM(68),FPMAL(68),DIMAG(68),FPMAG(68) CC 890
159 FORMAT(10,*) FANOM(69),FPM(69),FPMAL(69),DIMAG(69),FPMAG(69) CC 900
160 STOP CC 910
END CC 920

```

4.4 DATAMEND

The second stage in the data reduction process involves a format change from a direct image of the FACS-1 paper tape output to a suitable input form for program NRC2A. DATAMEND was written to accomplish this format change for the several different types of input data available. As well as this function, several useful facilities were built into the program. These include: the assignment of standard numbers, the generation of statistical percentage errors in the net counts, examination of the net:background ratio, tabulations of the numbers of reflections within certain ranges of the net counts and in ranges of percentage error. As well as these an in-sequence tabulation of the various measurements of the monitor reflections is produced.

The FORTRAN coding which accomplishes this is listed below.


```

PDEL(1)=0
4 CONTINUE
L=LINE(1)=100
PDEL(1)=0
DO 7 I=1,L
7 DELBOT(I)=0
DO 8 I=1,L
8 DELTOT(I)=0
9 CONTINUE
PDEL(1)=0
PDEL(1)=0
DELTOP=0
RETURN
C
C ENTER HERE TO ACCUMULATE BUNS
C
C FIND THE APPROPRIATE DEL/I BOX AND INCREMENT ITS TOTAL BY 1
C
8 CONTINUE
DOEL=DEL(I),
IDEL=I(I)DEL(I)
IF(I(DEL)=1) I=1
18 IDEL=IDEL(I)
DELBOX(I)=DEL(I)DEL(I)
PDEL(I)=PDEL(I)+1
GO TO 81
9 DEL=DEL(I),
IDEL=I(I)DEL(I)
IF(I(DEL)=1) I=1
19 IDEL=IDEL(I)
DELBOX(I)=DEL(I)DEL(I)
PDEL(I)=PDEL(I)+1
GO TO 81
11 IF(DEL=2) I=1,13
18 DELBOX(I)=DEL(I)DEL(I)
PDEL(I)=PDEL(I)+1
GO TO 81
12 IF(DEL=3) I=1,15
18 DELBOX(I)=DEL(I)DEL(I)
PDEL(I)=PDEL(I)+1
GO TO 81
14 DELBOX(I)=DEL(I)DEL(I)
PDEL(I)=PDEL(I)+1
GO TO 81
16 IF(DEL=4) I=1,17
18 DELBOX(I)=DEL(I)DEL(I)
PDEL(I)=PDEL(I)+1
GO TO 81
17 DELBOX(I)=DEL(I)DEL(I)
PDEL(I)=PDEL(I)+1
81 CONTINUE
C
C SORT OUT THE NETT COUNTS INTO RANGES AND ACCUMULATE DEL/I
C C TOTALS FOR THESE RANGES
C
C IF(PRO) 31,32,33
C
C FOR THE NEGATIVE NETT COUNTS
C
32 PDEL(I)=PDEL(I)+1
DELTOT(I)=DELTOT(I)+DEL
GO TO 91
33 IF(PRO) 34,35,36
34 PDEL(I)=PDEL(I)+1
DELTOT(I)=DELTOT(I)+DEL
GO TO 91
35 IF(PRO) 37,38,39
37 PDEL(I)=PDEL(I)+1
DELTOT(I)=DELTOT(I)+DEL
GO TO 91
38 IF(PRO) 40,41,42
40 PDEL(I)=PDEL(I)+1
DELTOT(I)=DELTOT(I)+DEL
GO TO 91
41 IF(PRO) 43,44,45
43 PDEL(I)=PDEL(I)+1
DELTOT(I)=DELTOT(I)+DEL
GO TO 91
44 PDEL(I)=PDEL(I)+1
DELTOT(I)=DELTOT(I)+DEL
GO TO 91
45 PDEL(I)=PDEL(I)+1
DELTOT(I)=DELTOT(I)+DEL
GO TO 91
C
C FOR THE POSITIVE NETT COUNTS
C
43 CONTINUE
43 IF(PRO) 44,45,46
44 PDEL(I)=PDEL(I)+1
DELTOT(I)=DELTOT(I)+DEL
GO TO 91
45 IF(PRO) 47,48,49
47 PDEL(I)=PDEL(I)+1
DELTOT(I)=DELTOT(I)+DEL
GO TO 91
48 PDEL(I)=PDEL(I)+1
DELTOT(I)=DELTOT(I)+DEL
GO TO 91
49 IF(PRO) 50,51,52
50 PDEL(I)=PDEL(I)+1
DELTOT(I)=DELTOT(I)+DEL
GO TO 91
51 IF(PRO) 53,54,55
53 PDEL(I)=PDEL(I)+1
DELTOT(I)=DELTOT(I)+DEL
GO TO 91
54 PDEL(I)=PDEL(I)+1
DELTOT(I)=DELTOT(I)+DEL
GO TO 91
55 PDEL(I)=PDEL(I)+1
DELTOT(I)=DELTOT(I)+DEL
GO TO 91
56 PDEL(I)=PDEL(I)+1
DELTOT(I)=DELTOT(I)+DEL
GO TO 91
57 IF(PRO) 58,59,60
58 PDEL(I)=PDEL(I)+1
DELTOT(I)=DELTOT(I)+DEL
GO TO 91
59 IF(PRO) 61,62,63
61 PDEL(I)=PDEL(I)+1
DELTOT(I)=DELTOT(I)+DEL
GO TO 91
62 PDEL(I)=PDEL(I)+1
DELTOT(I)=DELTOT(I)+DEL
GO TO 91
63 IF(PRO) 64,65,66
64 PDEL(I)=PDEL(I)+1
DELTOT(I)=DELTOT(I)+DEL
GO TO 91
65 PDEL(I)=PDEL(I)+1
DELTOT(I)=DELTOT(I)+DEL
GO TO 91
66 PDEL(I)=PDEL(I)+1
DELTOT(I)=DELTOT(I)+DEL
GO TO 91

```

```

66 IF(PRO) 67,68,69
67 PDEL(I)=PDEL(I)+1
DELTOT(I)=DELTOT(I)+DEL
GO TO 91
68 IF(PRO) 70,71,72
70 PDEL(I)=PDEL(I)+1
DELTOT(I)=DELTOT(I)+DEL
GO TO 91
71 IF(PRO) 73,74,75
73 PDEL(I)=PDEL(I)+1
DELTOT(I)=DELTOT(I)+DEL
GO TO 91
74 PDEL(I)=PDEL(I)+1
DELTOT(I)=DELTOT(I)+DEL
GO TO 91
75 IF(PRO) 76,77,78
76 PDEL(I)=PDEL(I)+1
DELTOT(I)=DELTOT(I)+DEL
GO TO 91
77 PDEL(I)=PDEL(I)+1
DELTOT(I)=DELTOT(I)+DEL
GO TO 91
78 PDEL(I)=PDEL(I)+1
DELTOT(I)=DELTOT(I)+DEL
GO TO 91
91 RETURN
C
C ENTER HERE WHEN LAST REFLECTION PROCESSED AND OUTPUT THE BUNS
C
3 CONTINUE
C
C AVERAGE THE DEL/I TOTALS IN THE NETT RANGES
C
DO 81 I=1,13
IF(DELTOT(I)) 81,81,87
87 DELTOT(I)=DELTOT(I)/FLOAT(PDEL(I))
81 CONTINUE
IF(PDEL) 88,88,89
88 DELBOT=DELTOT/PLD(I)
89 DELTOT=DELTOT/PLD(I)
92 DELTOT=DELTOT/PLD(I)
94 CONTINUE
C
C OUTPUT THE DEL/I RANGE ANALYSIS
C
WRITE(6,900)
WRITE(6,901)
DO 82 I=1,13
IF (DELTOT(I)) 100,100,101
100 AVPS=0
GO TO 103
101 AVPS=PLD(I)/DELTOT(I)
102 DELM(I)=DELTOT(I)*AVPS
103 CONTINUE
WRITE(6,902) I,DELM(I),AVPS
DM 4760
92 CONTINUE
WRITE(6,903) I,DELM(I),AVPS
DM 4770
104 AVPS=PLD(I)/DELTOT(I)
GO TO 103
105 AVPS=0
106 WRITE(6,904) I,DELM(I),AVPS
DM 4780
DM 4800
DM 4810
DM 4820
DM 4830
DM 4840
DM 4850
DM 4860
DM 4870
DM 4880
DM 4890
DM 4900
DM 4910
DM 4920
DM 4930
DM 4940
DM 4950
DM 4960
DM 4970
DM 4980
DM 4990
DM 5000
DM 5010
DM 5020
DM 5030
DM 5040
DM 5050
DM 5060
DM 5070
DM 5080
DM 5090
DM 5100
END

```

```

DM 4890
DM 4900
DM 4910
DM 4920
DM 4930
DM 4940
DM 4950
DM 4960
DM 4970
DM 4980
DM 4990
DM 5000
DM 5010
DM 5020
DM 5030
DM 5040
DM 5050
DM 5060
DM 5070
DM 5080
DM 5090
DM 5100

```

4.5 FRAME

The continuous paper tape data-stream output by the FACS-1 diffractometer must be modified in two ways before it is in useable form:

(i) The records corresponding to the data for one reflection must be "framed" and written to an interim storage device as one logical record.

(ii) The modified ASCII code eight channel, odd parity character representation of the data must be translated into its equivalent EBCDIC coding. An ASSEMBLER subroutine written by Mr. Ken May of Computing Services at this University accomplishes this.

The 80 byte magnetic tape records read by this program are written without being prefaced by any control words. Because of this fact, and the expectation by the FORTRAN Input/Output Control System (FIOCS) that these words be present, it became necessary to use a modified version of FIOCS which did not examine the first two words of each record. The modified version of FIOCS was supplied by Mr. D. Webster of Computing Services.

A listing of the FORTRAN mainline and the ASSEMBLER translation subroutine is given below.

```

C      * FRAME 1                                PR 10
C      PROGRAM TO TRANSLATE AND BLOCK THE MASCITE TAP IMAGE OF THE PR 30
C      FACIS-1 PAPER TAPE INTO A USABLE ONE RECORD PER REFLECTION FORMAT. PR 50
C      MARCVTS G.J.WILLIAMS (WITH A LITTLE HELP FROM MY FRIENDS) PR 70
C      TYPE AND SIZE SPECIFICATIONS AND INITIALIZATION PR 100
C      LOCAL(4) INDATA(80),OUTDAT(200),TESCH(4),BLANK PR 100
C      INTERIOR FAPIN(10),FLOUT(10),PRINTR,READR,POINT(1),PUT PR 110
C      INTERIOR TITLES(1) PR 120
C      DATA TESCH(4)='0',BLANK(4) '/' PR 130
C      NCHANGES PR 140
C      READPR(8) PR 150
C      PRINTPR(8) PR 160
C      LIND(8) PR 170
C      PUT(4) PR 180
C      DO 10 I=1,80 PR 181
C      10 INCH(I)=BLANK PR 182
C      DO 11 J=1,200 PR 183
C      11 OUTDAT(J)=BLANK PR 184
C      12 READR(4)=TESCH TITLE PR 200
C      000 FORM(I(80))=TESCH(4) FAPIN(FLOUT(I),PRINTR,LINCH PR 210
C      FPL(IN,EN,LE,LS) LIND(I) PR 211
C      001 FORM(I(80)) PR 220
C      002 PRINTR(8)=TESCH(4) TITLE PR 230
C      003 FORM(I(4))='00000000',EN,LS,***** PR 250
C      GET ONE DATA BLOCK FROM TAPE - AND TRANSLATE IT PR 300
C      1 READR(4)=TESCH(4) INDATA PR 300
C      CALL TRANSR(INDATA,INDATA) PR 300
C      PUT THE TRANSLATED DATA INTO 'OUTDAT' PR 300
C      DO 2 I=1,NCHANG PR 320
C      2 OUTDAT(I)=PUT(INDATA(I)) PR 340
C      PUT=PUT+NCHANG PR 360
C      IS THERE MORE IN 'OUTDAT' FOR MORE DATA ? PR 370
C      13 IF(PUT(4)=10) GO TO 1 PR 380
C      FIND A 'TEST CHARACTER' --'CARBONISE RETURN' PR 400
C      10 J=1 PR 410
C      4 IF(OUTDAT(I)=TESCH(4)) GO TO 3 PR 420
C      10 J=J+1 PR 430
C      3 POINT(J)=I PR 440
C      IF HAVE FOUND TWO TEST CHARACTERS WHICH DO NOT CORRESPOND PR 450
C      TO EITHER A DATA LINE OR A STANDARD LINE PR 460
C      WRITE OUT WHAT HAS BEEN FOUND PR 470
C      IF(J(2)=8) GO TO 10 PR 500
C      J=J+1 PR 510
C      GO TO 6 PR 520
C      10 POINT(3)=POINT(1)+1 PR 530
C      GO TO 9 PR 540
C      DOES THE PREVIOUSLY FOUND TEST CHARACTER CORRESPOND TO - PR 550
C      A DATA LINE ? PR 560
C      6 IF(OUTDAT(I+LEN(LIND)-EN,TESCH(4)) GO TO 8 PR 570
C      DOES THE PREVIOUSLY FOUND TEST CHARACTER CORRESPOND TO - PR 580
C      A STANDARD LINE ? PR 590
C      10 POINT(4)=INLEN(EN,EN,TESCH(4)) GO TO 10 PR 600
C      10 J=J+1 PR 610
C      10 POINT(5)=INLEN(LIND) PR 620
C      GO TO 6 PR 630
C      6 POINT(6)=INLEN(LIND) PR 640
C      WRITE OUT THE POULS LINE PR 710
C      0 ENR(OUT) PR 720
C      L=OUT(I) PR 730
C      WRITE(FLOUT,OUT) (OUTDAT(I),L) PR 740
C      003 FORM(I(80))=L PR 750
C      FPL(IN,EN,LE,LS) PR 760
C      0 LIND(LIND(4)) PR 770
C      PRINTR(8)=TESCH(4) LIND(LIND(4)) PR 780
C      004 FORM(I(4))='1000',LIND(4) PR 790
C      DEPOSITION EVERYTHING AT THE BEGINNING OF THE ARRAY PR 810
C      - AND CLEAR THE TOP END PR 820
C      7 MLEFT=PUT-1 PR 830
C      DO 11 J=MLEFT PR 840
C      11 OUTDAT(J)=OUTDAT(J+1) PR 850
C      MLEFT=MLEFT-1 PR 860
C      MLEFT=1 PR 870
C      DO 12 M=1,NCHANG PR 880
C      12 OUTDAT(M)=LIND PR 890
C      PUT=PUT+L PR 900
C      GO TO 13 PR 910
C      WRITE OUT THE REMAINDER AT THE FINISH PR 920
C      100 WRITE(FLOUT,OUT) CUDAT PR 930
C      ENDFILE FLOUT PR 940
C      005 FORM(I(80))=LIND PR 950
C      IF(IN,EN,LE,LS) WRITE(PRINTR,OUT) OUTDAT PR 960
C      006 FORM(I(4))='1000' PR 970
C      STOP PR 1000
C      END PR 1020

```

```

TRANS CECT
* THIS ROUTINE TRANSLATES 'MASCITE' TO 'MASCITE'
* THE FORTRAN CALLING SEQUENCE IS:
* CALL TRANSR(LENGTH)
* UNDEFINED CHARS 0
* CARBONISE RETURN 0
* LINE FEED 0
* TRAILER 0
*
R0 EQU 0
R1 EQU 1
R2 EQU 2
R3 EQU 3
R4 EQU 4
R5 EQU 5
R6 EQU 6
R7 EQU 7
R8 EQU 8
R9 EQU 9
R10 EQU 10
R11 EQU 11
R12 EQU 12
R13 EQU 13
R14 EQU 14
R15 EQU 15
R16 EQU 16
R17 EQU 17
R18 EQU 18
R19 EQU 19
R20 EQU 20
R21 EQU 21
R22 EQU 22
R23 EQU 23
R24 EQU 24
R25 EQU 25
R26 EQU 26
R27 EQU 27
R28 EQU 28
R29 EQU 29
R30 EQU 30
R31 EQU 31
R32 EQU 32
R33 EQU 33
R34 EQU 34
R35 EQU 35
R36 EQU 36
R37 EQU 37
R38 EQU 38
R39 EQU 39
R40 EQU 40
R41 EQU 41
R42 EQU 42
R43 EQU 43
R44 EQU 44
R45 EQU 45
R46 EQU 46
R47 EQU 47
R48 EQU 48
R49 EQU 49
R50 EQU 50
R51 EQU 51
R52 EQU 52
R53 EQU 53
R54 EQU 54
R55 EQU 55
R56 EQU 56
R57 EQU 57
R58 EQU 58
R59 EQU 59
R60 EQU 60
R61 EQU 61
R62 EQU 62
R63 EQU 63
R64 EQU 64
R65 EQU 65
R66 EQU 66
R67 EQU 67
R68 EQU 68
R69 EQU 69
R70 EQU 70
R71 EQU 71
R72 EQU 72
R73 EQU 73
R74 EQU 74
R75 EQU 75
R76 EQU 76
R77 EQU 77
R78 EQU 78
R79 EQU 79
R80 EQU 80
R81 EQU 81
R82 EQU 82
R83 EQU 83
R84 EQU 84
R85 EQU 85
R86 EQU 86
R87 EQU 87
R88 EQU 88
R89 EQU 89
R90 EQU 90
R91 EQU 91
R92 EQU 92
R93 EQU 93
R94 EQU 94
R95 EQU 95
R96 EQU 96
R97 EQU 97
R98 EQU 98
R99 EQU 99
R100 EQU 100

```

4.6 PARALISTER

The generation of the requisite atomic parameter tables for the publication of a structure was, prior to the introduction of this program, a tedious process fraught with the possibility of clerical error. PARALISTER will accept a card or binary file of the atomic parameters and will produce the various tables required. Options permit the user to choose between decimal or integerised parameters, inclusion or exclusion of e.s.d's, separate or integrated listings for the isotropic and anisotropic atoms, "B" or "U" thermal motion parameters, and the number of atoms to be listed per page in the case of very large tables.

Following this is a listing of the program and a sample of its output.

ATOMIC PARAMETERS FOR THE HYDROGEN ATOMS ($\times 10^4$)

ATOM	X/A	Y/B	Z/C	UISO
H(10)	8679(15)	1845(25)	910(18)	476
H(8)	7061(15)	1444(23)	1089(17)	456
H(3')	4475(17)	1975(27)	334(20)	638
H(4')	3343(17)	337(27)	664(19)	638
H(5')	3772(17)	-1365(25)	1888(20)	593
H(6')	5207(16)	-1233(25)	2655(20)	566
H(2)	7669(17)	-1327(26)	3147(20)	613
H(3)	7869(16)	-2336(27)	4632(20)	613
H(5)	5865(17)	300(27)	5682(20)	655
H(6)	5799(14)	1082(23)	4159(17)	423
H(91)	8482(17)	306(26)	2048(21)	664
H(92)	8186(15)	1632(25)	2778(18)	486
H(111)	8182(19)	3819(30)	2175(24)	838
H(112)	7874(18)	3669(28)	994(20)	674
H(121)	9075(20)	5363(33)	1278(22)	905
H(122)	9051(22)	4783(36)	609(26)	1021
H(131)	10433(24)	3629(38)	811(27)	1143
H(132)	10426(19)	4021(30)	1667(23)	807
H(141)	9741(18)	2286(28)	2457(23)	717
H(142)	9966(17)	1462(28)	1486(20)	664
H(151)	7140(19)	-1097(28)	6881(23)	803
H(152)	7544(16)	-1865(27)	6560(20)	621
H(153)	6500(20)	-2182(31)	6620(24)	896
WH(1)	9028(19)	-947(28)	380(23)	750
WH(2)	-14(23)	-1294(35)	797(26)	1058

4.7 PRECLP

The Lorentz and polarization correction terms which should be applied routinely to all sets of diffraction intensities differ according to the manner of the data collection.

In the case of photographic data obtained with the Buerger precession instrument, the combined correction term is dependent upon all three of the cylindrical reciprocal space coordinates and must be evaluated according to a complicated expression. The FORTRAN algorithm given below will compute and apply these correction terms for data originating from a crystal of any class and mounted in any rational manner.

```

C*****
C TO CALCULATE AND APPLY LORENTZ AND POLARIZATION CORRECTIONS TO
C PRECESSION FILE DATA FOR THE GENERAL TRICLINIC CASE G. J. WILLIAMS
C*****
DIMENSION TITLE(20) ,AFINT(8),LWY(8),JLAY(8),INHOM(8)
COMMON P(3,3), G(3,3), R(3,3), S(3,3)
REAL N,K,L,LPCORF
INTEGER MM
1 READ(8,900)END=1001 TITLE
900 FORMAT(20A)
2 READ(8,901)A,B,C,ALPHA,BETA,GAMMA,WAVE
901 FORMAT(8F12,3,F6,6)
C*****
C TO CALCULATE RECIPROCAL LATTICE PARAMETERS
C*****
P12=141882
RAD=3.1415926/180.
ALPHA=ALPHA/RAD
BETA=BETA/RAD
GAMMA=GAMMA/RAD
60 ALSTAR=ARCOS((COS(BETA)+COS(GAMMA)-COS(ALPHA))/(SIN(BETA)+SIN(GAMMA)
X1))
61 BSTAR=ARCOS((COS(ALPHA)+COS(GAMMA)-COS(BETA))/(SIN(ALPHA)+SIN(GAMM
X2))
62 GSTAR=ARCOS((COS(ALPHA)+COS(BETA)-COS(GAMMA))/(SIN(ALPHA)+SIN(BET
X3))
48 ASTAR=WAVE/(A+SIN(BSTAR)+SIN(GAMMA))
64 BSTAR=WAVE/(B+SIN(ALSTAR)+SIN(GAMMA))
CSTAR=WAVE/(C+SIN(ALSTAR)+SIN(BETA))
WRITE(6,900) TITLE
ALPHA=ALPHA/RAD
BETA=BETA/RAD
GAMMA=GAMMA/RAD
ALSTAR=ALSTAR/RAD
BSTAR=BSTAR/RAD
GSTAR=GSTAR/RAD
WRITE(6,900)A,B,C,ALPHA,BETA,GAMMA,ASTAR,BSTAR,CSTAR,ALSTAR,BSTAR
X1,ASTAR
ALPHA=ALPHA/RAD
BETA=BETA/RAD
GAMMA=GAMMA/RAD
ALSTAR=ALSTAR/RAD
BSTAR=BSTAR/RAD
GSTAR=GSTAR/RAD
C*****
C TO CALCULATE CYLINDRICAL COORDINATES
C*****
3 READ(8,908)END=1003U,I,J,N,DELTA,INPUT,SCALE
908 FORMAT(F8,2,F3,3,F9,3,F12,F6,3)
SCALE=SCALE/872
UMPHRAD
P(1,8)=180 TO 6
P(1,9)=180 TO 6
M(6)
S(6)
L(6)
GO TO 7
5 M(1)
S(6)
L(6)
GO TO 7
99 WRITE(6,901)
GO TO 40
4 M(6)
S(6)
L(6)
7 P(1,1)=M/A
P(1,2)=COS(GAMMA)
P(1,3)=COS(BETA)
P(2,1)=N/S
P(2,2)=S
P(2,3)=COS(ALPHA)
P(3,1)=M/C
P(3,2)=COS(ALPHA)
P(3,3)=S
O(1,1)=1
O(1,2)=M/A
O(1,3)=COS(BETA)
O(2,1)=COS(GAMMA)
O(2,2)=N/S
O(2,3)=COS(ALPHA)
O(3,1)=COS(BETA)
O(3,2)=M/C
O(3,3)=S
R(1,1)=M/A
R(1,2)=COS(GAMMA)
R(1,3)=M/A
R(2,1)=COS(GAMMA)
R(2,2)=N/S
R(2,3)=COS(BETA)
R(3,1)=COS(ALPHA)
R(3,2)=M/C
R(3,3)=S
S(1,1)=1
S(1,2)=COS(GAMMA)
S(2,1)=COS(GAMMA)
S(2,2)=S
S(2,3)=COS(ALPHA)
S(3,1)=COS(BETA)
S(3,2)=M/C
S(3,3)=S
46 ANUM=(M/A)*HOB*(P(1,1)+HOB*(O(2,1)+L/C)*HOB(T))
DEMO=HOB(T)
47 D=HOB(T)*INHOM(AUM)
DSTAR=WAVE/D
ANPLDATT(H)
ZETA=HOBSTAR
UM/L/RAD
WRITE(6,910)U,I,J,N,DELTA,SCALE
UM/RAD
910 FORMAT('ANGLE OF PRECESSION (DEGREE) IS',F9,3,' REAL AXIS PARALL
REL TO X-RAY BEAM INDICATOR IS',F8,3,' SPINDLE (RECIPROCAL) AXIS IND
XCATOR IS',F8,3,' ZETA (R.L.U.) FOR THIS SECTION IS',F10,6,' SCALE',F6
X,3)
IF INPUT=0=13 GO TO 99
WRITE(6,907)
40 ON=ARCOS(COS(U)-ZETA)
87 IF INPUT=0=13 GO TO 81
8 READ(8,903) MM,KX,LL,OBSSINT
903 FORMAT(3I0,F10,6)
GO TO 31
81 DO 80 N=1,8
AFINT(N)=0
LWY(N)=0
JLAY(N)=0
INHOM(N)=0
80 CONTINUE
30 READ(8,900)MM,KX,LL,MAX,(AFINT(N),LWY(N),JLAY(N),INHOM(N),N)=6)

```

4.8 NRC-8

The general Fourier synthesis program of the N.R.C. system was modified in two respects to increase its versatility.

The first simple modification permits the user to exclude reflections with small scattering angle from Patterson map calculations. This facility is used to give more prominent vector peaks for the heavier atoms of a structure.

In the initial stages of a structure solution, many of the phase angles may be in considerable error. To avoid the spurious peaks and general unreliability in maps calculated using coefficients with incorrect phase angles, a subroutine was written which computes and applies weighting factors appropriate to the phase angle reliability of each reflection⁽¹⁴⁶⁾. The FORTRAN coding of subroutine SIM is reproduced below.

4.9 NRC-10

Apart from the compiler limitations which forced the splitting of this program into three subroutines, by Dr. D. Hall in 1968 (then Professor of Chemistry at this University), further extensive reorganization was undertaken with several objectives in mind.

(i) To make the program capable of recycling without user intervention. The removal of all except the final tape rewinds and the introduction of a work disc used in direct access mode were instrumental in accomplishing this.

(ii) Because of the high speed and reliability of the IBM-360/67 it was felt that the intermediate dump and restart facility was unnecessary; it was accordingly removed and to further economise the generation of the results tape was made an optional facility.

(iii) The card input of the control parameters was simplified and the program's interpretation of these control parameters was printed out.

As well as the modifications implicit in the above concepts, several other improvements were made. These include:

More efficient paging of the printed output.

Provision for using individual atom matrix multipliers.

A facility to permit listing of the matrices for inspection.

The addition of a user programmable "weight" subroutine.

Optional and in-sequence card output of the thermal parameter e.s.d.'s.

Inclusion of an in-program tape mount facility.

In addition to all of the above, an extensive error analysis and agreement summary subroutine was added. This summary is provided in ranges of $\sin^2 \theta$, h , k , l , and $|F_0|$. An analysis of the agreement in

terms of an F_{thresh} curve is also provided. A listing of subroutine
ANAL is given below.

100
 101
 102
 103
 104
 105
 106
 107
 108
 109
 110
 111
 112
 113
 114
 115
 116
 117
 118
 119
 120
 121
 122
 123
 124
 125
 126
 127
 128
 129
 130
 131
 132
 133
 134
 135
 136
 137
 138
 139
 140
 141
 142
 143
 144
 145
 146
 147
 148
 149
 150
 151
 152
 153
 154
 155
 156
 157
 158
 159
 160
 161
 162
 163
 164
 165
 166
 167
 168
 169
 170
 171
 172
 173
 174
 175
 176
 177
 178
 179
 180
 181
 182
 183
 184
 185
 186
 187
 188
 189
 190
 191
 192
 193
 194
 195
 196
 197
 198
 199
 200

201
 202
 203
 204
 205
 206
 207
 208
 209
 210
 211
 212
 213
 214
 215
 216
 217
 218
 219
 220
 221
 222
 223
 224
 225
 226
 227
 228
 229
 230
 231
 232
 233
 234
 235
 236
 237
 238
 239
 240
 241
 242
 243
 244
 245
 246
 247
 248
 249
 250
 251
 252
 253
 254
 255
 256
 257
 258
 259
 260
 261
 262
 263
 264
 265
 266
 267
 268
 269
 270
 271
 272
 273
 274
 275
 276
 277
 278
 279
 280
 281
 282
 283
 284
 285
 286
 287
 288
 289
 290
 291
 292
 293
 294
 295
 296
 297
 298
 299
 300

301
 302
 303
 304
 305
 306
 307
 308
 309
 310
 311
 312
 313
 314
 315
 316
 317
 318
 319
 320
 321
 322
 323
 324
 325
 326
 327
 328
 329
 330
 331
 332
 333
 334
 335
 336
 337
 338
 339
 340
 341
 342
 343
 344
 345
 346
 347
 348
 349
 350
 351
 352
 353
 354
 355
 356
 357
 358
 359
 360
 361
 362
 363
 364
 365
 366
 367
 368
 369
 370
 371
 372
 373
 374
 375
 376
 377
 378
 379
 380
 381
 382
 383
 384
 385
 386
 387
 388
 389
 390
 391
 392
 393
 394
 395
 396
 397
 398
 399
 400

REFERENCES

1. J.N. Langley, *J. Physiol. (London)*, 1, 339 (1878).
2. Erlich Centennial Symposium, *Ann. N.Y. Acad. Sci.*, 59, 141 (1964).
3. B.M. Bloom, Chapter 8 in Vol. 1 of "Medicinal Chemistry", 3rd ed., A. Burger Ed., Wiley-Interscience, New York, 1970.
4. D. Nachmansohn, "Chemical and Molecular Basis of Nerve Activity", Academic Press, New York, 1959.
5. D.E. Koshland and K.E. Neet, "Annual Reviews of Biochemistry", 37, p. 359 (1968).
6. B.M. Bloom and I.M. Goldman, *Adv. Drug Res.*, 3, 121 (1966).
7. (a) P.B. Marshall, *Brit. J. Pharmacol.*, 10, 270 (1955).
(b) C. Botré, M. Marchetti, C. Del Vecchio, G. Lionetti and A. Memoli, *J. Med. Chem.*, 12, 832 (1969).
8. R.B. Barlow, "Introduction to Chemical Pharmacology", 2nd ed., Methuen, London, 1964.
9. J.W. Black, W.A.M. Duncan, C.J. Durant, C.R. Ganellin and E.M. Parsons, *Nature*, 236, 385 (1972).
10. Reference (8), p. 349.
11. R.G. Jones, in "Handbook of Experimental Pharmacology", O. Eichler and A. Farah Eds., Vol. XVIII, Part I, Springer, New York, 1966, p. 1.
12. C. Niemann and J.T. Hays, *J.A.C.S.*, 64, 2288 (1942).
13. A. Lukton, *Nature*, 192, 422 (1961).
14. T.B. Paiva, M. Tominga and C.M. Paiva, *J. Med. Chem.*, 13, 689 (1970).
15. L.B. Kier, *J. Med. Chem.*, 11, 441 (1968).
16. R. Pepinsky, J. Rathlev and J.W. Turley, *Acta Cryst.*, 11, 295 (1958).
17. D.W. Adamson, P.A. Barrett, J.W. Billingham and T.S.G. Jones, *J. Chem. Soc.*, 2315 (1957).
18. A.F. Casy, R.R. Ison and N.S. Ham, *Chem. Comm.*, 343 (1970).

19. M.V. Veidis, G.J. Palenik, R. Schaffrin and J. Trotter, *J.C.S. B*, 2659 (1969).
20. J-L. Coubeils, P. Courrière and B. Pullman, *C.R. Acad. Sc., Paris*, 272, 1813 (1971).
21. S. Diner, J.P. Malrieu, F. Jordan and M. Gilbert, *Theoret. Chim. Acta*, 15, 100 (1969).
22. D.T. Witiak, Chapter 65 in Vol. II of "Medicinal Chemistry", 3rd ed., A. Burger Ed., Wiley-Interscience, New York, 1970.
23. A.F. Casy and A.P. Parulkar, *Can. J. Chem.*, 47, 423 (1969).
24. A.F. Casy and R.R. Ison, *J. Pharm. Pharmac.*, 22, 270 (1970).
25. R.R. Ison, Doctoral Dissertation, the University of Alberta, 1970.
26. R.T. Brittain, P.F. D'Arcy and J.H. Hunt, *Nature*, 183, 734 (1959).
27. F.E. Roth and N.M. Govier, *J. Pharmacol. Exptl. Therap.*, 124, 347 (1958).
28. D.T. Witiak, Z. Muhi-Eldeen, N. Mahishi, O.P. Sethi and M.C. Gerald, *J. Med. Chem.*, 14, 24 (1971).
29. R.S. Cahn, C.K. Ingold and V. Prelog, *Angew. Chem. Internat. Ed.*, 5, 385 (1960).
30. Reference (8), p. 357.
31. Reference (8), p. 373.
32. G. Hite and A. Shafi'ee, *J. Pharm. Sci.*, 56, 1041 (1967).
33. A. Shafi'ee and G. Hite, *J. Med. Chem.*, 12, 266 (1969).
34. I. Weisz and A. Dudás, *Monats. Chem.*, 91, 840 (1960); *Chem. Abs.*, 57, 11154d (1962).
35. L. Panizzon, *Helv. Chim. Acta*, 27, 1748 (1944); *Chem. Abs.*, 40, 3117⁴ (1946).
36. R. Rometsch, *Brit. Pat.* 788226, December 23, 1957; *U.S. Pat.* 2838519 (1958); *Chem. Abs.*, 52, 11959d (1958).
37. See for example M.P. Cava and E. Moroz, *J.A.C.S.*, 84, 115 (1962).
38. W.R. Busing and H.A. Levy, *Acta Cryst.*, 22, 457 (1967).
39. The Merck Index, 8th Ed., Merck and Co. Inc., Rahway, N.J., 1968, p. 782.

40. G.H. Stout and L.H. Jensen, "X-ray Structure Determination", Macmillan, New York, N.Y., 1968, p. 245.
41. Reference (40), p. 407.
42. U.W. Arndt and B.T.M. Willis, "Single Crystal Diffractometry", Cambridge University Press, Cambridge, U.K., 1966, pp. 173-174.
43. Reference (42), p. 277.
44. S.W. Peterson and H.A. Levy, Acta Cryst., 10, 70 (1957).
45. D.T. Cromer and J.B. Mann, Acta Cryst., A24, 321 (1968).
46. R. Mason and G.B. Robertson, "Advances in Structure Research by Diffraction Methods", Vol. 2, R. Brill and R. Mason Eds., Interscience, New York, N.Y., 1966, p. 57.
47. W.R. Busing and H.A. Levy, Acta Cryst., 10, 180 (1957).
48. Reference (40), pp. 272-274.
49. W.R. Busing, K.O. Martin and H.A. Levy, "ORFLS", Report ORNL-TM-305, Oak Ridge National Laboratory, Oak Ridge, Tennessee, 1962.
50. D.T. Cromer and D. Libermann, results distributed at the 8th International Congress of Crystallography, S.U.N.Y. at Stony Brook, N.Y., 1969.
51. F.R. Ahmed, S.R. Hall, M.E. Pippy and C.P. Huber, N.R.C. Crystallographic Programs for the IBM/360 System, World List of Crystallographic Computer Programs, 2nd ed., Appendix P. 52, program NRC-12.
52. Reference (39), p. 405.
53. (a) The local version of program NRC-10 [see reference (51)] was used.
(b) This work, p. 215.
54. L.I. Hodgson and J.S. Rollet, Acta Cryst., 16, 329 (1963).
55. L.E. Sutton, "Tables of Interatomic Distances and Configuration in Molecules and Ions", The Chemical Society, London, U.K., Special Publication No. 18, 1965.
56. J. Karle, I.L. Karle and D. Mitchell, Acta Cryst., B25, 866 (1969).
57. T. Ashida, S. Hirokawa and Y. Okawa, Acta Cryst., 21, 506 (1966).
58. T. Ashida, S. Hirokawa and Y. Okawa, Acta Cryst., 18, 122 (1965).

59. K. Seff and K.N. Trueblood, *Acta Cryst.*, B24, 1406 (1968).
60. S. Hirokawa and T. Ashida, *Acta Cryst.*, 14, 774 (1961).
61. D.L. Smith and E.K. Barrett, *Acta Cryst.*, B27, 419 (1971).
62. B. Bak, L. Hansen-Nygaard and J. Rastrup-Anderson, *J. Mol. Spect.*, 2, 361 (1958).
63. P.J. Wheatley, *Acta Cryst.*, 6, 369 (1953).
64. C.K. Johnson, "ORTEP", Report ORNL-3794, Oak Ridge National Laboratory, Oak Ridge, Tennessee, 1965.
65. J. Donohue, in "Structural Chemistry and Molecular Biology", A. Rich and N. Davidson eds., W.H. Freeman and Co., San Francisco, 1968.
66. R.B. Heslop and P.L. Robinson, "Inorganic Chemistry", Elsevier, Amsterdam, 1963, pages 82 and 116.
67. L. Pauling, "The Nature of the Chemical Bond", 3rd ed., Cornell University Press, Ithaca, N.Y., 1960.
68. J.G. Topliss, Associate Director of Chemical Research, Schering Corporation, personal communication to M. James.
69. (a) P.G. Simpson, R.D. Dobrott and W.N. Lipscomb, *Acta Cryst.*, 18, 169 (1965).
(b) P.D. Cradwick, Ph.D. Dissertation, the University of Alberta, Edmonton, 1969.
70. R.F. Stewart, E.R. Davidson and W.T. Simpson, *J. Chem. Phys.*, 42, 3175 (1965).
71. Y. Okawa, in "Crystallographic Computing", F.R. Ahmed Ed., Munksgaard, Copenhagen, 1970, p. 127.
72. H. Lipson and W. Cochran, "The Determination of Crystal Structures", Vol. III in "The Crystalline State", L. Bragg Ed., Cornell University Press, Ithaca, N.Y., 1966, p. 305.
73. W.C. Hamilton, *Acta Cryst.*, 18, 502 (1965).
74. Table 5.3.5B in "International Tables for X-ray Crystallography", Vol. II, J.S. Kasper and K. Lonsdale Eds., 2nd ed., The Kynoch Press, England, 1967, p. 295.
75. R. Rudman, *Acta Cryst.*, B27, 262 (1971).
76. J.J.H. McDowell, *Acta Cryst.*, B25, 2175 (1969).

77. G.J. Palenik, J. Donohue and K.N. Trueblood, *Acta Cryst.*, B24, 1139 (1968).
78. Reference (72), p. 355.
79. R. Srinivasan, *Acta Cryst.*, 14, 1163 (1961).
80. R. Parthasarathy, J.G. Sime and R.C. Speakman, *Acta Cryst.*, B25, 1201 (1969).
81. A.I.M. Rae and E.N. Maslen, *Acta Cryst.*, 16, 703 (1963).
82. Reference (39), p. 1081.
83. Reference (51), program NRC-2A.
84. P.D. Cradwick, Ph.D. Dissertation, the University of Alberta, Edmonton, 1969.
85. C.J. Fritchie and J.L. Wells, *Chem. Comm.*, 917 (1968).
86. British Carbohydrate Nomenclature Committee, Proposed Rules for Conformation Nomenclature for Five- and Six-Membered Rings in Carbohydrates, revised 1968.
87. R.D. Shannon and C.T. Prewitt, *Acta Cryst.*, B25, 925 (1969).
88. G.R. Clark and G.J. Palenik, *J.A.C.S.*, 94, 4005 (1972).
89. M.N.G. James and G.J.B. Williams, *J. Med. Chem.*, 14, 670 (1971).
90. N.S. Ham, *J. Pharm. Sci.*, 60, 1764 (1971).
91. Reference (8), p. 357.
92. M. Rocha e Silva, *Chemotherapia*, 3, 544 (1961).
93. W. Th. Nauta, R.F. Rekker and A.F. Harms, in "Physico-Chemical Aspects of Drug Action", E.J. Ariëns Ed., Vol. 7, Pergamon Press, U.K., 1968.
94. (a) J.J. Birkof, D.M. Blow, R. Henderson and J.A. Steitz, *Phil. Trans. Roy. Soc. Lond.*, B257, 67 (1970).
(b) T.A. Steitz, R. Henderson and D.M. Blow, *J. Mol. Biol.*, 46, 337 (1969).
95. S.N. Timasheff, *Acct. Chem. Res.*, 3, 62 (1970).
96. D.M. Blow, J.J. Birkof and B.S. Hartley, *Nature*, 221, 337 (1969).

97. D.M. Shotton and H.C. Watson, *Nature*, 229, 811 (1970).
98. Reference (8), p. 350.
99. G.W.A. Slywka, Ph.D. Dissertation, the University of Alberta, Edmonton, 1969.
100. D. Rogers, Chapter 16 in "Computing Methods in Crystallography", J.S. Rollet Ed., Pergamon Press, Oxford, 1965.
101. S.R. Hall, program NRC-4 from "A Set of Crystallographic Programs for the IBM/360", F.R. Ahmed et al., National Research Council of Canada, Ottawa, 1968.
102. I.L. Karle, K.S. Dragonette and S.A. Brenner, *Acta Cryst.*, 19, 713 (1965).
103. J. Karle, paper A1 in "Crystallographic Computing", F.R. Ahmed Ed., Munksgaard, Copenhagen, 1970.
104. D. Sayre, *Acta Cryst.*, 5, 60 (1952).
105. J. Karle and I.L. Karle, *Acta Cryst.*, 21, 849 (1966).
106. L.M. Browne, M.Sc. Thesis, the University of Alberta, Edmonton, 1968.
107. I.L. Karle and J. Karle, *Acta Cryst.*, 17, 1356 (1964).
108. J.A. Wunderlich, *Acta Cryst.*, B25, 1436 (1969).
109. D.W.J. Cruickshank, *Acta Cryst.*, 9, 757 (1956).
110. W.R. Busing and H.A. Levy, *Acta Cryst.*, 17, 142 (1964).
111. R.E. Dickerson and I. Geis, "The Structure and Action of Proteins", Harper and Row, New York, 1969, p. 12.
112. W.C. Hamilton and J. Ibers, "Hydrogen Bonding in Solids", Benjamin, New York, 1968, p. 16.
113. G.H. Goldschmidt and F.J. Llewellyn, *Acta Cryst.*, 3, 294 (1950).
114. Jean M. Karle and P.W. Le Quesne, *J.C.S. Chem. Comm.*, 417 (1972).
115. "Handbook of Chemistry and Physics", R.C. Weast Ed., 49th ed., The Chemical Rubber Co., Cleveland, 1968, p. D90.
116. H.M.E. Cardwell, J.D. Dunitz and L.E. Orgel, *J.C.S.*, 3740 (1953).

117. M. Shahat, *Acta Cryst.*, 5, 763 (1952).
118. Von S. Hechtfisher, W. Steigemann and W. Hoppe, *Acta Cryst.*, B26, 1713 (1970).
119. S.F. Darlow and W. Cochran, *Acta Cryst.*, 14, 1250 (1961).
120. S.F. Darlow, *Acta Cryst.*, 14, 1257 (1961).
121. R.D. Ellison and H.A. Levy, *Acta Cryst.*, 19, 260 (1965).
122. C.A. Coulson, "Valence", 2nd ed., Oxford University Press, London, 1961, p. 349.
123. A.S.N. Murthy, S.N. Bhat and C.N.R. Rao, *J.C.S. A*, 1251 (1970).
124. P.A. Kollman and L.C. Allen, *J.A.C.S.*, 92, 6101 (1970).
125. K. Yardley, *J.C.S.*, 127, 2207 (1925).
126. K. Lonsdale, *Proc. Roy. Soc. A*, 171, 541 (1939).
127. A.C.T. North, D.C. Phillips and F.S. Mathews, *Acta Cryst.*, A24, 351 (1968).
128. P. Coppens, T.V. Willoughby and L.N. Csonka, *Acta Cryst.*, A27, 248 (1971).
129. F.L. Hirshfeld, *Acta Cryst.*, B27, 769 (1971).
130. D.W.J. Cruickshank, in "International Tables for Crystallography", J.S. Kasper and K. Lonsdale Eds., The Kynoch Press, Birmingham, England, Vol. 11, 1967, p. 331.
131. J.D. Dunitz and P. Strickler, in "Structural Chemistry and Molecular Biology", A. Rich and N. Davidson Eds., W.H. Freeman and Co., San Francisco, 1968, p. 595.
132. C.J. Brown, *Acta Cryst.*, 21, 1 (1966).
133. A.L. Bednowitz and B. Post, *Acta Cryst.*, 21, 566 (1966).
134. M.A. Higgs and R.L. Sass, *Acta Cryst.*, 16, 659 (1963).
135. C.E. Bugg, J.M. Thomas, M. Sundaralingam and S.T. Rao, *Biopolymers*, 10, 175 (1971).
136. C.K. Prout and S.C. Wallwork, *Acta Cryst.*, 21, 449 (1966).
137. J.P. Glusker, W. Orehowsky, Jr., C.A. Casciato and H.L. Carrell, *Acta Cryst.*, B28, 419 (1972).

138. A. Hartman and F.L. Hirshfeld, *Acta Cryst.*, 20, 80 (1966).
139. J.C. Hanson, L.C. Sieker and L.H. Jensen, *Trans. Amer. Cryst. Assn.*, 8, 139 (1972).
140. P. Main, in *Lecture Notes from N.A.T.O. Advanced Study Institute, Direct and Patterson Methods of Solving Crystal Structures*, York University, England, 1971.
141. H. Hauptman and J. Karle, "Solution of the Phase Problem: I. The Centrosymmetric Crystal", *American Crystallographic Association Monograph No. 3*, 1953.
142. Reference (74), Vol. I, p. 384.
143. J. Dargay, H. Berman, H.L. Carrell and J.P. Glusker, *Acta Cryst.*, B28, 1533 (1972).
144. H.R. Mahler and E.H. Cordes, "Biological Chemistry", Harper and Row, N.Y., 1966.
145. J.P. Glusker, *J. Mol. Biol.*, 38, 149 (1968).
146. G.A. Sim, Paper 24 in "Computing Methods and the Phase Problem in X-Ray Crystal Analysis", R. Pepinsky, J.M. Robertson and J.C. Speakman Eds., Pergamon Press, 1961, and references therein.